ERDA-JPL-954458-77/2
Distribution Category UC-63

INTERIM REPORT ON ACCELERATED/ABBREVIATED TEST METHODS STUDY 4 TASK 3 (ENCAPSULATION) OF THE LOW-COST SILICON SOLAR ARRAY PROJECT FOR THE PERIOD APRIL 1, 1976 THROUGH OCTOBER 24, 1977

October 24, 1977

JPL Contract No. 954458

This work was performed for the Jet Propulsion Laboratory, California Institute of Technology, under NASA Contract NAS7-100 for the U.S. Energy Research and Development Administration, Division of Solar Energy.

The JPL Low-Cost Silicon Solar Array Project is funded by ERDA and forms part of the ERDA Photovoltaic Conversion Program to initiate a major effort toward the development of low-cost solar arrays.

Prepared by

J. M. Kolyer, Principal Investigator

N. R. Mann, Statistician

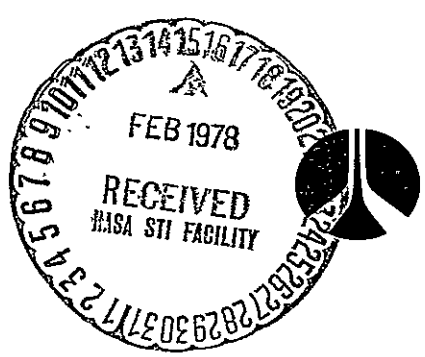

Rockwell International

Autonetics Group
3370 Miraloma Avenue
P.O Box 3105
Anaheim, California 92803

ERDA-JPL-954458-77/2
Distribution Category UC-63

INTERIM REPORT ON ACCELERATED/ABBREVIATED TEST METHODS STUDY 4 TASK 3 (ENCAPSULATION) OF THE LOW-COST SILICON SOLAR ARRAY PROJECT FOR THE PERIOD APRIL 1, 1976 THROUGH OCTOBER 24, 1977

October 24, 1977

JPL Contract No. 954458

This work was performed for the Jet Propulsion Laboratory, California Institute of Technology, under NASA Contract NAS7-100 for the U.S. Energy Research and Development Administration, Division of Solar Energy.

The JPL Low-Cost Silicon Solar Array Project is funded by ERDA and forms part of the ERDA Photovoltaic Conversion Program to initiate a major effort toward the development of low-cost solar arrays.

Prepared by

J. M. Kolyer, Principal Investigator

N. R. Mann, Statistician

Rockwell International

Autonetics Group
3370 Miraloma Avenue
P.O. Box 3105
Anaheim, California 92803

This report contains information prepared by Rockwell International Corporation under JPL subcontract. Its content is not necessarily endorsed by the Jet Propulsion Laboratory, California Institute of Technology, or the National Aeronautics and Space Administration.

ACKNOWLEDGMENTS

Significant contributions are acknowledged from members of the Jet Propulsion Laboratory, including W. F. Carroll (LSSA Project Encapsulation Task Manager), and Dr. J. Moacanin (Contract Monitor for this study).

Several technical persons at Autonetics made helpful suggestions and contributions. Desert Sunshine Exposure Tests, Inc., supplied the EMMAQUA photograph.

ABSTRACT

In this study, methods of accelerated and abbreviated testing were developed and applied to solar cell encapsulants. These encapsulants must provide protection for as long as 20 years outdoors at different locations within the U.S. Consequently, encapsulants were exposed for increasing periods of time to the inherent climatic variables of temperature, humidity, and solar flux. Property changes in the encapsulants were observed. The goal was to predict long-term behavior of encapsulants based upon experimental data obtained over relatively short test periods.

To simplify the experimental design, weather conditions throughout the U.S. were categorized into arbitrary "environmental cells." Each cell covered a distinct interval of temperature, humidity, and solar intensity. The idea was to obtain, in accelerated exposure, the values for constants in a generalized rate equation for encapsulant degradation in each cell. Then it should be an easy matter to sum the extents of degradation as the weather passes from cell to cell and so arrive at a prediction for cumulative degradation. Comparison of such predictions with actual values obtained under outdoor exposure in a specific locale should verify the mathematical model and prediction methodology.

The first attempts to accelerate degradation under fixed conditions in the laboratory have been made. Changes in encapsulant properties were observed and correlated with these artificial conditions. For example, increase in chromophore concentration in the encapsulant (yellowing) was found to be directly proportional to the cumulative ultraviolet radiation both outdoors and in accelerated exposure. Such data have proved useful in establishing mathematical models for degradation processes such as the Weibull and lognormal distributions.

Another innovation was to expose encapsulants "in situ," ie, applied directly onto miniature solar cell arrays. In this manner, interactions between the encapsulant and the array components can be identified immediately. Thus, the electrical output of solar cells is measured and directly correlated with property changes in the encapsulant.

SUMMARY

A.. OBJECTIVE AND APPROACH

Physical properties of materials change upon exposure to the weather, sunlight being a major factor. Hence, there is concern that solar cell encapsulants may not provide sufficient protection for 20 years of outdoor exposure. Our objective is to predict how long and how well encapsulants can perform.

To make predictions for a given property, eg, solar cell power output, it is necessary to develop a curve of property vs exposure time. The mathematical model for this curve should simulate the controlling physical/chemical process, thus giving greater confidence than does an empirical relationship. In principle, by inserting measured values for degradation rate constants into a suitable equation, any encapsulant characteristic, eg, transparency, can be predicted as a function of time.

A considerable part of the degradation vs time curve must be known to define its shape and identify the mathematical model. Therefore, acceleration of the weathering process is necessary. For example, samples can be exposed to the artificial sunlight provided by a xenon lamp. This light remains always at noontime intensity, thus providing "time-compression." It accelerates degradation rates by a factor of about 8. Thus, eight years of outdoor exposure would be simulated by one year of such accelerated weathering. Some other procedures claim acceleration factors much higher than 8.

In practice, there are considerable difficulties in making "paper predictions" based on accelerated data alone. One reason is that xenon lamps, or other artificial sources, give imperfect solar simulation over the important UV range of the spectrum. In fortunate cases, the specific UV wavelength causing degradation can be identified and set at a natural level for accelerated exposure. However, a problem remains. The outdoor level of this critical wavelength must be known, and UV intensity varies greatly with season and time of day. Reliable data are not now available, though they will be recorded in the near future for at least one

test site. Another problem is that property levels must be measured with high precision to distinguish among possible mathematical models and to allow meaningful extrapolation. Most property data have been too scattered for this purpose, though advances are being made with new analytical techniques. Yet another problem is that erratic/dynamic factors such as temperature cycling, air pollution, soil accumulation, or windblown sand may shift encapsulant lifetime below predicted values. Such factors may be the most important. At present, little factual data are available.

The experimental work falls into three parts as follows:

(1) Our present program to develop prediction methodology is based on the principle of measuring degradation rates under 24 accelerated conditions which can be used to define artificial "weather cells" whose dimensions are insolation, relative humidity, and temperature. Study 2 of the LSSA Program by Battelle (ref 1) has analyzed real weather at various locations and placed it into such "cells". Thus, accelerated exposures were conducted to obtain such rates as well as to disclose failure modes and to clarify the relative importance and interactions of light, humidity, and temperature.

(2) Abbreviated exposures were initiated and tests are continuing. These are natural exposures on racks for periods of up to two years. Test sites are Phoenix, AZ and Miami, FL.

(3) Samples at Phoenix also are being exposed on devices which concentrate sunlight eight times by means of mirrors: EMMA (dry) and EMMAQUA (with water spray). This approach circumvents the solar simulation problem by using natural sunlight. It is, so to speak, a hybrid accelerated/natural exposure condition.

Some preliminary predictions have been made, but extensive predictions will be made only after a full year's abbreviated data have been received. These data

will be obtained on samples whose exposure began both in midwinter and in mid-summer as explained below.

Two type of samples were exposed. One type of sample was unsupported film: Lexan, Tedlar, or polystyrene. The latter plastic was included because it degrades rapidly and will provide extensive mathematical modeling data.

The other type was a "Universal Test Specimen." This specimen comprised three pairs of solar cells and three FET (field effect transistor) chips (A4T4391) bonded to a 1.0 mm (0.040 in) thick alumina substrate. Ceramic was chosen to minimize any possible effect that substrate degradation products can have on the P/N junctions of the devices. If an epoxy board had been chosen, it might yield ionic contaminants. We want to be confident that we are testing encapsulants and not substrate materials. To eliminate corrosion problems, the circuitry is thin-film molybdenum-manganese overplated with nickel and then gold.

The entire board - front, back, and edges - was encapsulated with Sylgard 184 transparent silicone rubber. Since the rubber is soft and tends to collect dirt rapidly, a transparent "dust cover" completed the encapsulant system. The cover was one of two thermoplastic films: Lexan (bisphenol-A polycarbonate, without UV stabilizer), or Tedlar [poly(vinyl fluoride)].

B. RESULTS TO DATE

Optical transmittance measurements on the films have provided sufficiently precise data to allow the trial of mathematical models. Other properties studied include tensile properties and surface carbonyl group formation. Such properties often follow dissimilar models. However, if the functional relationship is known, it should be possible to correlate precisely-measured secondary properties with critical properties which are measured with difficulty. If this is so, then the latter can be predicted indirectly.

Abbreviated test procedures have been refined to include initiation of exposures both in midsummer and midwinter. It is essential to obtain seasonal

values for model equation parameters because degradation rates are commonly three to five times higher in summer than in winter. Models which best fit the data are the Weibull, a special case of which is the exponential, and the log-normal. An exponential model is often assumed for failure rates of semiconductor devices. In the case of yellowing of Lexan or polystyrene, this model would represent a photochemical reaction in which chromophore formed is directly proportional to photons received (in the reaction-inducing wavelength region).

In the accelerated exposures, Lexan degraded extremely rapidly. Preliminary mathematical modeling indicated a change in mechanism of degradation attributed to abnormal light-stressing; ie, there was a mismatch between the xenon light and sunlight at the critical UV wavelength of Lexan degradation. Such difficulities are not unusual in accelerated testing. Tedlar film was negligibly affected by any exposure except by those accelerated conditions in which the T_g (glass transition temperature) was exceeded. Above its T_g, a plastic typically becomes rubbery, highly oxygen-permeable, and subject to rapid chemical reactions. A danger in stressing (raising) temperature of plastic materials is that the T_g or some reaction energy barrier will be exceeded. Then degradation, such as oxidation, could proceed rapidly. On the other hand, negligible degradation might occur in 20 years of outdoor exposure at natural temperatures.

Unlike outdoor exposures for limited time, accelerated exposure proved valuable in disclosing failure modes. For example, solar cells continued to operate satisfactorily in all the outdoor exposures. However, high-humidity conditions in the accelerated program caused moisture-related failures. It was found that conductive grids, or contacts, deteriorated and lifted from the surface of the solar cells.

CONTENTS

CONTENTS (continued)

ILLUSTRATIONS

TABLES

TABLES (continued)

GLOSSARY AND DEFINITIONS

Term	Definition
A_{360}	Absorbance of UV light at 360 or 600 nm, which is $\log_{10} (\frac{1}{T})$ where T is the transmittance
Abbreviated Exposure	Outdoor (natural) exposure for considerably less than 20 years
Accelerated Exposure	Indoor exposure to light from a xenon lamp, filtered through Pyrex and water to attenuate short wavelength UV and infrared. All equipment was contained in a cabinet.
ATR-IR	Attenuated Total Reflectance of IR (analytical method)
cm	centimeters
Contact	Collector, grid, or "finger" of titanium-silver on the upper surface of the solar cell
CUV	Cumulative UV light energy received by a sample
Desert Sunshine	Desert Sunshine Exposure Tests, Inc., Box 185 Black Canyon Stage, Phoenix AZ
Drierite	Anhydrous calcium sulfate (desiccant)
DSC	Differential Scanning Calorimetry (analytical method)
EMMA	Equatorial Mount with Mirrors for Acceleration, used at Desert Sunshine for exposure of samples
EMMAQUA	EMMA with intermittent water spraying of samples
EMMA(QUA)	Both EMMA and EMMAQUA
ESCA	Electron Spectroscopy for Chemical Analysis (analytical method)
FET	Field Effect Transistor (A4T4391)
45^{o} S	Abbreviated exposure outdoors on racks tilted 45^{o} from vertical and facing south

Term	Definition
IR	Infrared radiation, above 700 nm
ISWPR	International Symposium on the Weathering of Plastics and Rubber, June 8 and 9, 1976, Institution of Electrical Engineers, London WC2R OBL
IV Curve	A plot of current vs voltage for an operating solar cell
JPL	Jet Propulsion Laboratory
Lexan	Lexan No. 8740 polycarbonate film, not UV-stabilized, nominally 127 μm (5 mils) thick, from General Electric
mm	millimeter
mW	milliwatts
Miami or Phoenix	Exposure to the weather on racks tilted at 45° and facing south in Miami FL, or Phoenix, AZ
nm	nanometers
OCLI	Optical Coating Laboratory, Inc., City of Industry, CA
Outdoor Exposure	Miami, Phoenix, or EMMA(QUA) exposure
pct	percent
P	Property, specifically fraction of original transmittance at 360 nm in our mathematical modeling
Polystyrene	Biaxially-oriented clear polystyrene film, nominally 127 μm (5 mils) thick, from Catalina Plastics, Glendale, CA
psi	pounds per square inch
Solar Cell	N120CG-9, by OCLI. Responds to light from approximately 0.4 to 1.2 μ

Term	Definition
Sylgard 184	Transparent silicone rubber, produced by Dow Corning Corp.
Tedlar	Tedlar 100BG30 TR [poly(vinyl fluoride)] film, treated on both sides to improve adhesion, nominally 25 μm (1 mil) thick, from du Pont
Tg	Glass transition temperature
TGA	Thermogravimetric Analysis (analytical method)
TMA	Thermomechanical Analysis (analytical method)
UTS	Universal Test Specimen (described in text)
UV	Ultraviolet radiation, 295-400 nm for sunlight at sea level
V	Volts
Weathered	Subjected to either natural or artificial weathering
Weathering	Exposure to either natural or artificial weather conditions

I. INTRODUCTION

This study is one of several dealing with the encapsulation of solar cells. These studies are being conducted for the Jet Propulsion Laboratory. Encapsulation is necessary to protect solar cells from natural hazards which can reduce power output. It is important to identify these hazards and to determine how rapidly they degrade solar cell performance. What actually constitutes a failure or an unacceptable level of degradation remains to be defined. However, the overall goal of the encapsulation task can be summarized as follows:

> "To select or develop a cost-effective encapsulation system which protects solar cell arrays for 20 years of outdoor exposure."

The Rockwell contract has the specific goal:

> "To develop a methodology for predicting the performance of solar cell encapsulants for periods of up to 20 years."

Consequently, this report describes the equipment, exposure modes, analytical procedures, and mathematical models which have been used during the past year to develop prediction methodology. A Summary section and Discussion of Results are presented in the body of the report. However, all details of how the work was done have been placed in the Appendix. To avoid unnecessary repetition and to conserve space, certain items have been abbreviated. It is important to note that expressions such as "Miami," "accelerated exposure," or "EMMA" have a specific meaning in the content of this report. Therefore, these abbreviations are defined in the Glossary.

Weathering studies described in the literature are summarized in ref 1. In general, the preceding studies are only qualitative and certainly are not suitable for prediction purposes. To the best of our knowledge, the present study represents the first systematic attempt to obtain precise data on the degradation rates of materials under several outdoor exposure conditions as well as in multi-condition accelerated exposure in which weather factors are closely controlled at

fixed levels. There is no question that a scientific study of weathering is very complex. For this reason, the studies described herein have been limited to the "inherent" weather factors of light intensity, temperature, and humidity. These stresses are common to exposure sites all over the United States and the world. The results represent baseline weather-resistance of encapsulants. Therefore, predictions for failure rates of solar cell arrays will tend to be optimistic. When other factors such as air pollution are superimposed on the inherent factors, the predicted failure rates will necessarily be higher and the life expectancy shorter.

II. EXPERIMENTAL DESIGN

A. GENERAL DESCRIPTION

Our design includes both abbreviated and accelerated testing.

Abbreviated tests involve truncated outdoor exposure coupled with the use of sensitive analytical procedures for the detection of incipient degradation.

In accelerated tests, time is compressed by stressing one or more of the exposure parameters. For plastics, the single most important weathering influence is the ultraviolet portion of sunlight. Accelerated test procedures have stressed this parameter three ways: (1) by using a mercury vapor lamp whose spectrum is rich in UV including wavelengths below 295 nm (the lower limit for sunlight at sea level), (2) by maintaining simulated noon sunlight continuously vs some few hours/day in nature, and (3) concentrating natural sunlight by mirrors to give an approximately 8-fold increase in intensity. Commercial instruments representing the three procedures are, respectively: (1) the QUV Cyclic Ultraviolet Weathering Tester (Q-Panel Co.), (2) the xenon-arc Weather-Ometer (Atlas Electric Devices Co.), and (3) the EMMA or EMMAQUA (Desert Sunshine Exposure Tests, Inc.). In our judgment, the first procedure is not appropriate because high-energy light of wavelengths below 295 nm may cause extraneous photochemical reactions. The other two procedures are possibilities, but they must be evaluated critically. The problem with procedure (2) is imperfect simulation of the spectrum of sunlight. The wavelength region causing degradation must be known by this case. The problem with procedure (3) is that unnaturally-elevated light intensities may create new reaction paths and change the course of degradation.

Our test plan encompassed both techniques (2) and (3). Test specimens were placed in twenty-four individual cells ("miniature Weather-Ometers"), each of which had a different combination of light intensity, temperature, and humidity. In addition, specimens were exposed under accelerated conditions using Desert Sunshine's sunlight-concentrating devices.

The conventional approach to artificial weathering has been to simulate a given site, often South Florida, with a single set of conditions in a Weather-Ometer. Usually water is introduced in the form of a spray cycle. If the accelerated degradation vs time curve has some resemblance to the outdoor curve, successful correlation is assumed and an "acceleration factor" (typically on the order of 8) is assigned to the test. The disadvantages of this straightforward procedure are: (1) it is quite specific (limited to one site and one manner of exposure), and (2) it gives no knowledge of the relative effect of the variables (light, water, and temperature). Often, in fact, this attempt to imitate erratic weather conditions does not give an "outdoor-like" degradation vs time curve. Frequently it gives a different ranking of samples, eg, material A weathers faster than B outdoors but more slowly than B in the Weather-Ometer. In contrast, our procedure involved 24 sets of conditions to give a clear indication of the relative importance of the variables as well as considerable knowledge of their interactions. This design leads to an understanding of the effect of the basic weathering factors and is applicable to any site.

The basis of this approach is to concentrate on the "baseline" or inherent weathering factors and to exclude secondary factors from the current study. These baseline factors are (1) light striking the material, (2) temperature of the material, and (3) moisture in the material. Any sample placed at any location will always be subject to these influences, and their cumulative effect provides a measure of inherent weatherability in the form of a baseline curve of degradation vs time. Baseline factors may be averaged for a given microclimate over a long period of time so that an accelerated test can hope to give a fair simulation of them. On the other hand, secondary factors are specific, erratic, and even unforeseeable. The secondary factors include mechanical stresses caused by wind or sudden temperature changes, rain and/or dew cycles, frost, sandstorms, hailstorms, air pollutants, and various biological agents such as fungus, birds, or vandals.

B. CONDITIONS FOR ACCELERATED TEST

Three levels of UV light were used, plus an alternating (on-off) condition, and also three levels of relative humidity. The temperature was intended to be at either a high or low level; actually several temperatures resulted in practice. Actual conditions were as follows:

Condition No.	UV Intensity Relative to Noon Summer Sunlight	Air Temperature, °C	Relative Humidity, (pct)
1	1.00	26.1	0
2			50
3			100
4		60.3	0
5			50
6			100
7	0.66	18.3	0
8			50
9			100
10		55.3	0
11			50
12			100
13	0	40	0
14			50
15			100
16		80	0
17			50
18			100
19	0⟷1.00	6.7⟷26.1	0
20	(alternating)	(alternating)	50
21			100
22		43.9⟷60.3	0
23		(alternating)	50
24			100

Somewhat lower temperatures were desired at the low end to cover the extreme range in Miami and Phoenix, but experimental exigencies determined the levels achieved (see Appendix). Rate equation parameters will be extrapolated as required.

C. BASIS OF EXPERIMENTAL DESIGN

Battelle have conducted a detailed analysis of environmental variables in Study 2 of the Encapsulation Task of the LSSA project (ref 1). Statistics were computed to obtain frequencies, durations, and transitions for the simultaneous occurrence of various combinations of environmental variables. It was demonstrated that the simultaneous occurrence of specific levels of air temperature, relative humidity, and insolation could be represented as an "environmental cell", shown graphically as a geometric cube:

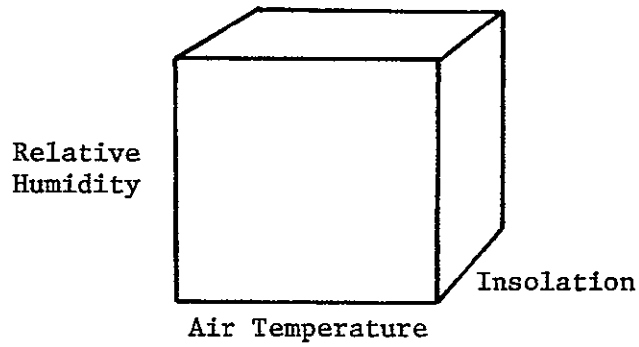

At any given time, the values of a particular combination of temperature, relative humidity, and insolation are defined by the coordinates of a point which lies in exactly one of the environmental cells. When values of the environmental variables change with time, the point moves from cell-to-cell. Three-hourly measurements for a given geographic location were used to obtain the list of successive cell code numbers, 29,216 in number, which can be computerized and analyzed. Aggregated information is used to provide frequency and duration histograms.

Environmental cell statistics are used to generate 20-year forecasts of the expected number of exposure hours, E, for each cell:

$$E = \frac{NKT}{H}$$

where N = observed number of occurrences of a cell in a historical time period H,

K = 3 hr

T = forecast time period

Thus, if Autonetics can establish for each cell the generalized rate constants of encapsulant degradation, then the total degradation can be computed for 20 yr of exposure. The changes in encapsulant properties with time in our accelerated test can be related in "environmental cells" in the same manner.

Our plan assumes the basic hypothesis that degradation rates are a unique function of temperature (T), relative humidity (RH), and ultraviolet light deposited (UV). Therefore, rates will be determined for the 24 static experimental conditions and then used to calculate the generalized rate constants for any (T, RH, and UV) condition, ie, for any arbitrary set of environmental cells. The rate constant K_i for condition i (or cell i) is $K_i = f\ (T_i, RH_i, \text{and } UV_i)$.

The procedure then is to make a prediction of P vs t for the outdoor exposure by a process of summation of increments of degradation:

$$P = \Delta P_1 + \Delta P_2 + \ldots \Delta P_n.$$

Assuming a Weibull model, three assumptions are made:

(1) A differential process is assumed: $dP/dt = f\ (P, \lambda, \beta, \alpha)$ for some f not an explicit function of time. P is a property, and λ, β, and α are parameters in the Weibull model equation:

$$P = \frac{e^{-\lambda t^{\beta}} + \alpha}{1 + \alpha}$$

(2) The physical/chemical state of the material at any property level P_i is independent of the material's history (that is, of the values of λ and β of the curves of the cells 1 through i through which the weather has passed). In other words, the sample does not know how it has reached any given level of P. This means that we start on each successive P vs t curve at the value of P at which we ended on the preceding curve.

(3) All cells have the same α so that data can be adjusted to the scale whereby P = 1 at t = 0 and P approaches 0 as t becomes infinite.

To check assumption (1), film samples have been put on outdoor exposure starting in winter as well as summer.

Mathematical models are discussed in Section V, below.

III. DISCUSSION OF RESULTS

Since this report covers only the activities and accomplishments of a 12-month study and data collection is incomplete, it is premature to make sweeping statements. Indeed, the exposure data still being gathered may substantially alter current interpretations.

This discussion is divided into two sections. One deals with behavior of UTS's under abbreviated and accelerated exposures. The other deals with the behavior of unsupported plastic films. It will be seen that the presence of an array system affects the performance of the encapsulant or element thereof. For example, in EMMAQUA exposure the Sylgard pottant reached higher-than-ambient temperatures and caused the Lexan film cover on UTS's to degrade faster than unsupported Lexan film.

A. UNIVERSAL TEST SPECIMENS

1. Substrate and Circuitry

The circuit boards comprise gold circuitry on a ceramic substrate and were visibly unaffected by weathering. Thus, degradation effects were confined to the encapsulation system. This result was exactly as planned and demonstrates an effective design.

2. Solar Cells

After 150 days of outdoor (abbreviated) exposure, including EMMA and EMMAQUA, the short circuit current and maximum power points of the solar cells were measured. These electrical performances were essentially unchanged. Only one random failure occurred. Some degradation was noted after 300 days.

After 72 days of accelerated (xenon lamp) exposure, the short circuit current fell to 47-76 pct of the original value for 10 cells, and the maximum power fell to 31-76 pct of the original value for 19 cells. Twenty-four UTS's, bearing a total of 144 cells, had been exposed. The performance losses were moisture-related, since relative humidity was 100 pct in nearly all those combinations of light, temperature, and moisture which induced failure. The plastic covers had no significant effect.

Failure analysis indicated damage to the contacts (grids) on the upper surface of the cell. The deterioration of Ti - Ag contacts by moisture is well known (ref 2). The two metals form an electrolytic cell.

3. Field Effect Transistors

The FET's showed small, moisture-related increases in leakage current. The absence of large increases indicated that the pottant, Sylgard 184, had generated essentially no ions as a result of exposure.

4. Pottant

Sylgard 184 was visibly unaffected by any of the exposures. However, this polymer is not a good moisture barrier, and it permitted the moisture related solar cell failures mentioned above.

5. Transparent Cover (Lexan or Tedlar)

Lexan yellowed slowly outdoors, and moisture-related loss of gloss occurred after 90 or more days on the EMMAQUA. Rapid yellowing of Lexan occurred in the accelerated exposures, with embrittlement and moisture-related loss of gloss under the more severe conditions.

Tedlar showed no significant color change. It was embrittled only in those accelerated conditions in which the T_g was exceeded. Such high temperatures are not normally reached in natural exposures. A plastic tends to degrade at high rates above its T_g. As a surfacing film for polyester panels, 25 μm (1 mil) Tedlar film is claimed to give a "service life of several decades" (ref 3).

Adhesion of covers to the underlying Sylgard 184 was unaffected by 90 days of outdoor weathering, including EMMA and EMMAQUA, or 72 days of accelerated exposure.

B. UNSUPPORTED FILMS

1. Lexan

Gradual yellowing proceeded at a rate which decreased in the order: accelerated test >> EMMAQUA > EMMA > Phoenix ≈ Miami. This color change

involved transmission loss only at the violet end of the visible spectrum, where the solar cells respond negligibly. Therefore, yellowing did not affect electrical performance.

In the accelerated exposures, light intensity and temperatures were major factors determining the rate of yellowing. Moisture was a minor factor.

The wavelength region of sunlight which causes yellowing is about 295-305 nm. This region is greatly variable with cloud cover, time of day, and season. In the accelerated test, high light intensity at about 300 nm caused rates of yellowing over an order of magnitude above outdoor rates. The form of the absorbance vs time curve was somewhat changed, suggesting some change in the mechanism (cf ref 4). The "fix" is to avoid over-stressing by the use of light filters.

On the other hand, the rate of chain-scission was not nearly so high as that of yellowing in accelerated exposure. For example, tensile strength fell by 50 pct after about 85 days on the EMMAQUA vs 35 days of accelerated exposure under comparable conditions. The damaging wavelength for chain-scission was about 330 nm. Seasonal variation in UV intensity can explain why the degradation rate was higher in accelerated exposure than on the EMMAQUA. The "sunlight" used in accelerated exposure has a UV intensity corresponding to summer; however, EMMAQUA exposure took place in late fall and winter.

As far as polymer degradation during exposure is concerned, chain-scission was indicated by a loss in tensile strength and by decreased values of T_g.

A moisture-related loss of gloss was observed but only under accelerated conditions. Unsupported films on EMMAQUA remained glossy, whereas the cover film on the UTS became hotter and lost gloss. Like yellowing, the loss of gloss did not affect electrical performance of solar cells. The explanation is that light is scattered but still reaches the silicon surface at about the incident intensity (less reflection).

Intensely weathered films were brittle, indicating that extensive chemical reactions, eg., chain-scission, had taken place. ATR-IR measurements showed that

oxidation had occurred. That is, the carbonyl region of the spectrum changed significantly after exposure. No hydroxyl band appeared, indicating that hydrolysis is not a significant degradation mechanism for Lexan exposed to the weather.

2. Tedlar

No significant property changes occurred. Unsupported Tedlar is extremely weather-resistant (ref 5).

3. Polystyrene

Samples were exposed at Miami only. The rate of yellowing was similar to that for Lexan. Prior studies on polystyrene have attributed yellowing to the formation of conjugated bonds in the polymer chain (ref 6).

For polystyrene, the UV wavelength region causing yellowing is said to be in the vicinity of 319 nm (ref 5). In this region, the intensity of the filtered xenon light used in accelerated exposure matched that of summer sunlight. Therefore, the acceleration factor was of the expected magnitude, and the degradation mechanism seems unchanged by the accelerated conditions.

Like Lexan, polystyrene embrittled under the more intense accelerated conditions.

IV. PREDICTION METHODOLOGY

In principle, it should be possible to (1) quantitatively establish the effects of weather factors in an accelerated test, (2) analyze the weather at a given site in terms of these factors, and (3) predict weathering behavior at the given site by means of mathematical models (ref 7). This is an ultimate goal of our program. However, there are four practical problems in this approach of using accelerated data alone. These are stated below, along with the solutions which will be available in the future.

Problems

1. Detailed outdoor UV data are lacking presently. These data are essential because UV is an important weather factor.
2. Precise property data are needed. Imprecise data give large errors on extrapolation. Most property measurements are too scattered to be useful, as mentioned in ref 8.
3. Solar simulators are imperfect in completely matching the UV spectrum of sunlight. Also, the visible region cannot always be ignored because visible light assists in degrading some plastics (ref 8).
4. Xenon lamps, the favorite solar simulators, show spectral changes with age.

Solutions

1. Spectroradiometric data will become routine in the future. Desert Sunshine is pioneering in this development.
2. New analytical methods are being applied, eg, T_g by DSC or TMA and surface carbonyl by ATR-IR. Data from these will give more alternatives for mathematical modeling and prediction.

3. EMMA and EMMAQUA avoid the solar simulation problem. Alternatively, knowledge of the most damaging wavelengths for a material enables a match of light source and sunlight to be made at only these wavelengths.

   To illustrate this point, examples can be cited from the present study. Polystyrene was found to yellow at a predictably faster rate in artificial light than in sunlight. The yellowing reaction for polystyrene requires light at 319 nm, a wavelength at which the xenon lamp and sunlight have matched intensities. On the other hand, the yellowing reaction of Lexan occurs at about 300 nm where the xenon lamp is much more intense than sunlight. Consequently, Lexan yellows much faster under xenon lamps than in sunlight even though their intensities are matched for most other wavelengths in the UV-visible spectrum. It is recommended for the future that xenon light be attenuated at 300 nm for Lexan yellowing studies.

   At longer wavelengths than 300 nm, light promotes a loss in tensile strength of Lexan. Since the intensity of xenon lamps and sunlight are matched at these wavelengths, chain-scission occurs at approximately the same rate.

4. Solarization effects can be measured and the degradation data appropriately corrected. Alternatively, lamp power can be gradually increased to compensate for solarization. The intensity of the UV wavelength of interest would be continuously monitored. Instrumentation for this continuous adjustment is available from Atlas Electric Devices Co. for installation on their Weather-Ometers.

For the present, it is expected that abbreviated testing will be required as well as accelerated testing. It is expected that prediction of weathering rates will utilize a combination of:

(1) Normal exposure outdoors for periods of 2 years or less (abbreviated test).

(2) Accelerated exposure in a light-stressed or time-compressed test.

Examples of the foregoing are sunlight concentrators and xenon lamps, respectively.

V. MATHEMATICAL MODELS

A. INTRODUCTION AND SUMMARY

The property that provided the most useful set of degradation data is UV light transmittance at 360 nm. The transmittance measurements have a small coefficient of variation (ratio of standard deviation to mean) for any given set of measurements. Also, any two data sets obtained under similar conditions tend to follow the same general distribution pattern. Only Lexan and polystyrene data were modeled since Tedlar showed very little change in any of the exposures.

Empirical longevity functions have been proposed by Langshaw (ref 9) and by Moder and Stucky (ref 10). Our initial approach resembled the predictive methodology of Clark (ref 11 and 12) which uses the Weibull model. However, it was subsequently conjectured through an analysis of the abbreviated exposure data for Lexan that the degradation data might be asymptotically lognormally distributed with time. This conjecture appears to be true for EMMA and EMMAQUA exposure of Lexan, which began in September 1976. It is possibly true for all autumn-initiated exposures. It also appears to hold for both transmittance and percent weight retention (TGA) data on polystyrene from accelerated exposure. Accelerated exposure data for Lexan represented a mechanism whose rate was inordinately high in the early stages of the test and subsequently fell off more rapidly than anticipated from outdoor tests. That is, slightly different mechanisms appeared to be operating for Lexan exposed outdoors and under accelerated conditions. For two of the four cases in which a 64-day data point was available, however, the lognormal model seems appropriate.

Polystyrene behavior outdoors and in accelerated exposure correlated well and gave relatively precise results. Therefore, it is recommended that polystyrene be included in future tests.

Though UV light intensity was the most critical factor in degradation in our tests, humidity also had an effect.

The lognormal and Weibull models currently seem promising, but judgment must await more data, including that for exposures begun on both summer and winter solstices.

B. PRECISION OF THE TRANSMITTANCE DATA

Tedlar has shown small and erratic changes to date, but degradation of transmittance in Lexan and polystyrene has been continuous and precisely measurable under all test conditions. The measurements are quite internally consistent, with sample standard deviation for any set of 5 or 10 replicates usually less than 1 pct of the mean. This ratio for tensile strength and elongation measurements is 5 to 30 times as great.

The effect of precision on ability to predict is discussed in ref 13. Clearly, a prediction model cannot be formulated and validated on the basis of a few measurements if test data are extremely scattered.

C. MATHEMATICAL MODEL TYPES

The following paragraphs describe the mathematical model types which are possible.

1. The Simple Exponential Model

The equation in this case is:

$$\ln\left(\frac{1}{P}\right) = \lambda t, \text{ where } P = \text{a property, } t = \text{exposure time.}$$

It is a special case of the Weibull model. If the P vs t curve for all "weather cells" (see Section II) were of this form, cell i would have associated with it a λ_i or first-order reaction rate constant. The sequence with which weather passes from one cell to another is not significant, and we can use the summation process:

$$\ln\left(\frac{1}{P}_{\text{outdoor}}\right) = \lambda_1 t_1 + \lambda_2 t_2 + \ldots \lambda_n t_n$$

where there is a total of n cells and $t_1 + t_2 + \ldots t_n$ = total exposure time.

2. The Weibull Model

a. β Constant

The equation in this case is

$$P = e^{-\lambda t^{\beta}} \text{ or } \ln\left[\ln\left(\frac{1}{P}\right)\right] = \ln\lambda + \beta \ln t,$$

with β constant at some number greater than 1.

Again, by our assumptions, the order in which weather passes from one cell to another is not significant, and we can use the summation process:

$$\ln\left(\frac{1}{P_{outdoor}}\right) = (\lambda_1^{1/\beta} t_1 + \lambda_2^{1/\beta} t_2 + \ldots \lambda_n^{1/\beta} t_n)^{\beta}$$

where there is a total of n cells and $t_1 + t_2 + \ldots t_n$ = total exposure time.

b. β Not Constant

The equation $P = e^{-\lambda t^{\beta}}$ again applies, but this time β can vary. In this case, the order of weather passing from cell to cell must be significant.

Note that for either $P = e^{-\lambda t}$ or $e^{-\lambda t^{\beta}}$ (where β is fixed) the curves for various values of λ fall into families, and, by our assumptions, the order of moving from curve to curve makes no difference. However, when β varies we get a mixture of curve forms so that the proper sequence must be followed.

This procedure of taking the cells in sequence can be handled by a computer program.

c. α Not Constant

If α is estimated to be the same for all cells the equation $\ln\left(\frac{1}{P}\right) = \lambda t^{\beta}$ is applied. This is the case for all the above treatments. However, if α varies, increments of degradation may be calculated by computer from the equation:

$$P = \frac{e^{-\lambda t^{\beta}} + \alpha}{1 + \alpha} \text{ or } \ln\left[\frac{1}{P(1 + \alpha) - \alpha}\right] = \lambda t^{\beta}$$

As t becomes infinite, P approaches $\frac{\alpha}{1 + \alpha}$, so values of P below this limit will give unreal solutions. Therefore, in the summing of increments, cells giving unreal solutions (no possible further degradation) are passed over.

d. With an Induction Period

In this case, we can sum across the induction period by adding up the times spent in each cell ($t_1 + t_2 + t_3 + \ldots t_i$) until the induction period for the next cell considered ($i + 1$) is less than or equal to the time summed through cell i. At this point we switch to one of the above procedures, as discussed. This involves the same assumption that the physical/chemical state is dependent only on P level and independent of curve form.

3. The Lognormal Model

This model has been used for crack growth propagation. Straight lines are obtained by plotting property vs log of exposure time on probability paper.

4. Mixed Models

The possibility exists that some cells may show, for example, a straight-line degradation curve P = kt while others follow a Weibull or other model. As in the case of the Weibull model with β not constant, the cells must be taken in order using a computer program.

D. MODELING OF ABSORBANCE (360 nm) DATA

Weibull plots of data for Lexan exposed in Phoenix, 45°S are shown in Fig 1. The A_{600} value is subtracted from the A_{360} value to correct for losses due to reflection and light-scattering. When the $(A_{360} - A_{600})$ for a control is subtracted, the result is the increase or ΔA_{360} due to yellowing. This quantity = $\log_{10} (\frac{1}{P})$ where P = property = fraction of original transmittance. That is, when $\Delta A_{360} = 0$, for the unweathered material, $\log_{10} (\frac{1}{P}) = 0$, $\frac{1}{P} = 1$, and P = 1. As ΔA_{360} becomes very large, P approaches 0. For Lexan, $A_{360} - A_{600}$ for control = 0.0309.

Note that the plots of $A_{360} - A_{600} - 0.0309$ in Fig 1 and 2 are approximately straight lines of slope = 1. This represents the exponential model, $P = e^{-\lambda(CUV)}$

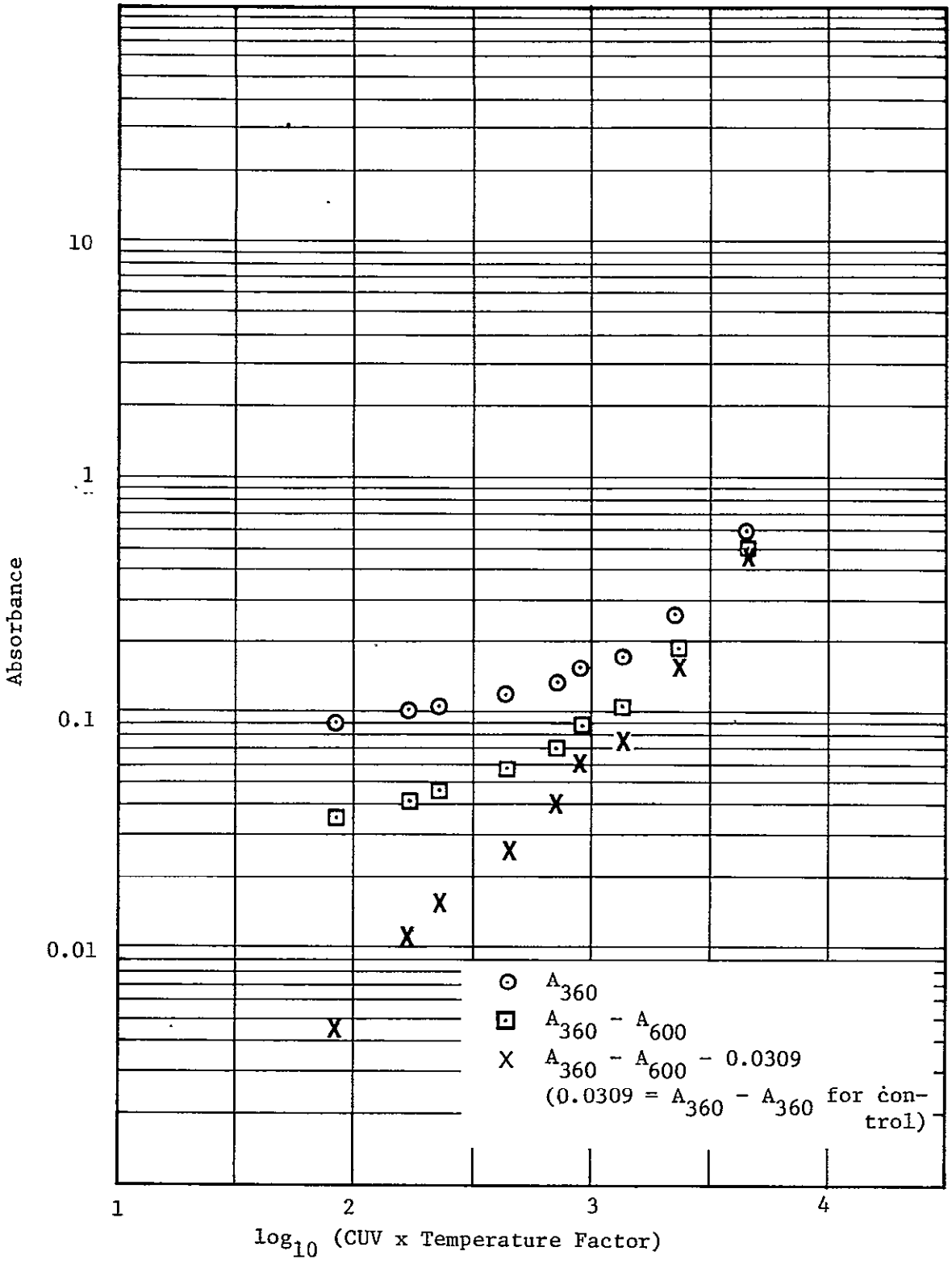

Fig 1. Phoenix A_{360} Data Plotted By Different Methods

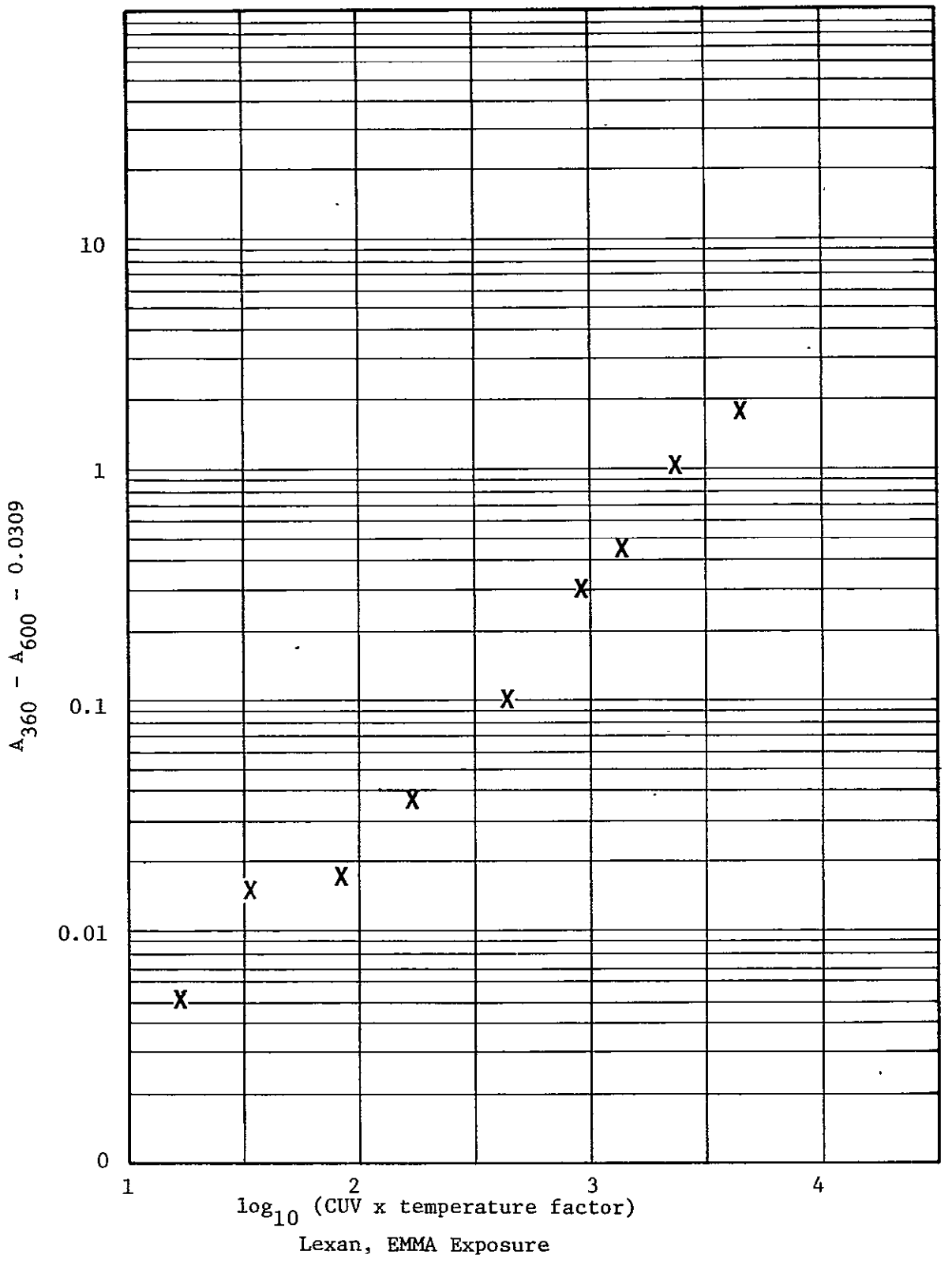

Fig. 2 EMMA A_{360} Data

where P = fraction of original transmittance, λ is the intercept on the ordinate and CUV is cumulative UV radiation. Rewriting the equation,

$$\ln \left(\frac{1}{P}\right) = \lambda(CUV)$$
$$\text{or } 2.3 \log_{10} \left(\frac{1}{P}\right) = \lambda(CUV)$$

That is, the concentration of chromophore, which is directly proportional to $\log_{10} \left(\frac{1}{P}\right)$, is directly proportional to the amount of UV deposited. In other words, this is a zero-order reaction in which the concentration of chromophore is equal approximately to the number of photons received. Relative UV at 300 nm is based on seasonal data from Desert Sunshine Exposure Tests, Inc. A small temperature correction was applied based on accelerated test results and temperature data from the Phoenix (Desert Sunshine) test site (see Table 1).

Table 1. Cumulative UV at 300 nm Deposited In Phoenix, Corrected For Seasonal Temperature Effect On Lexan Yellowing Rate (Relative Numbers)

(Start September 12)		
Time, Days	Cumulative UV x Temperature Factor	Common Log of Last Column
1	17	1.23
2	34	1.53
5	85	1.93
10	169	2.23
15	235	2.37
30	446	2.65
60	718	2.86
90	905	2.96
150	1380	3.14
210	2358	3.37
300	4579	3.66
420	6619	3.82
540	7660	3.88

If calendar time is used, the curves swing upward in spring as the UV intensity of sunlight increases (see Fig 3).

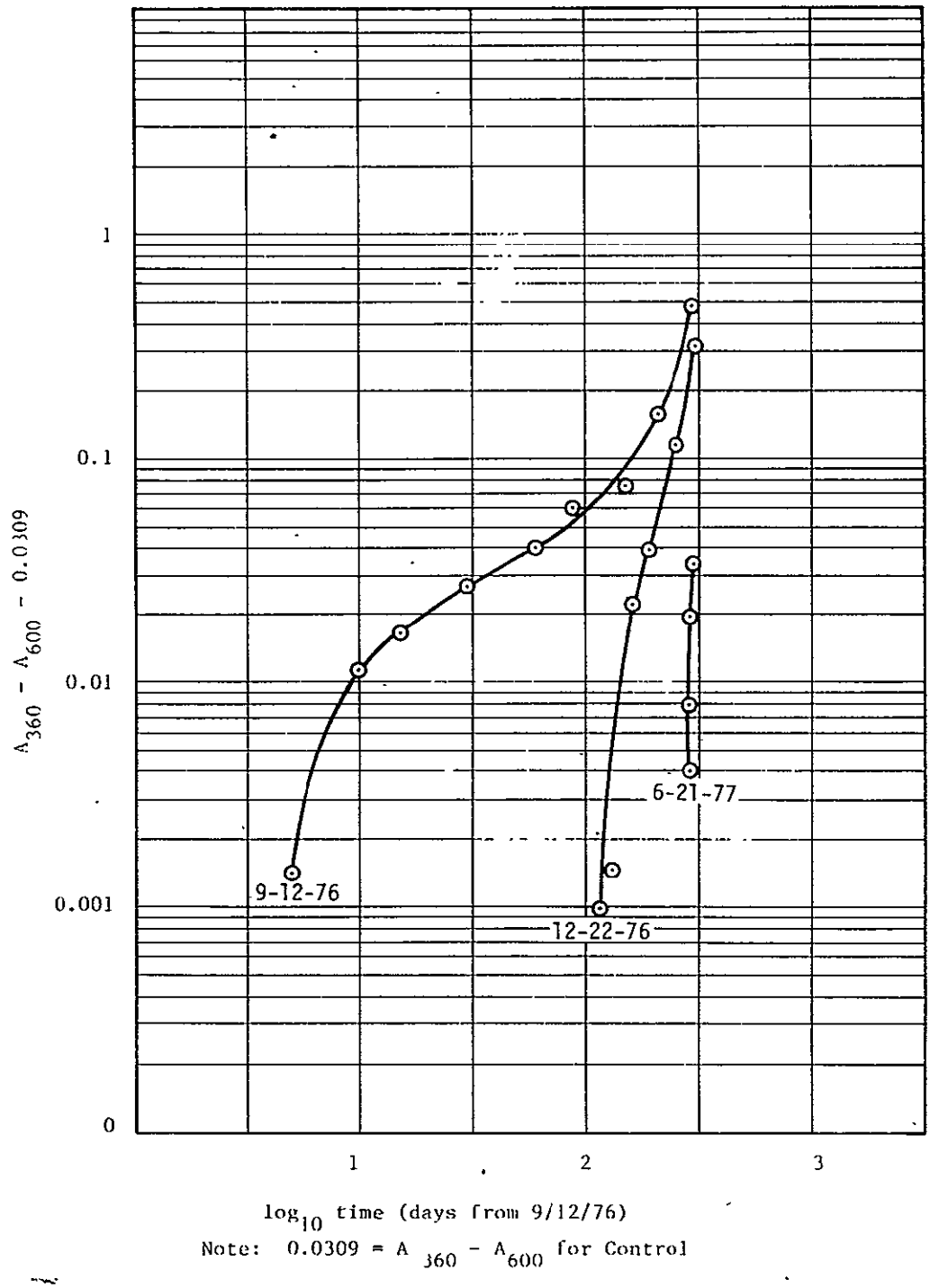

Fig 3. Absorbance Data for Lexan (Phoenix, 45°S)

Figure 4 shows typical plots for polystyrene from the accelerated test. The points approximate a line of slope 0.9, nearly the exponential model.

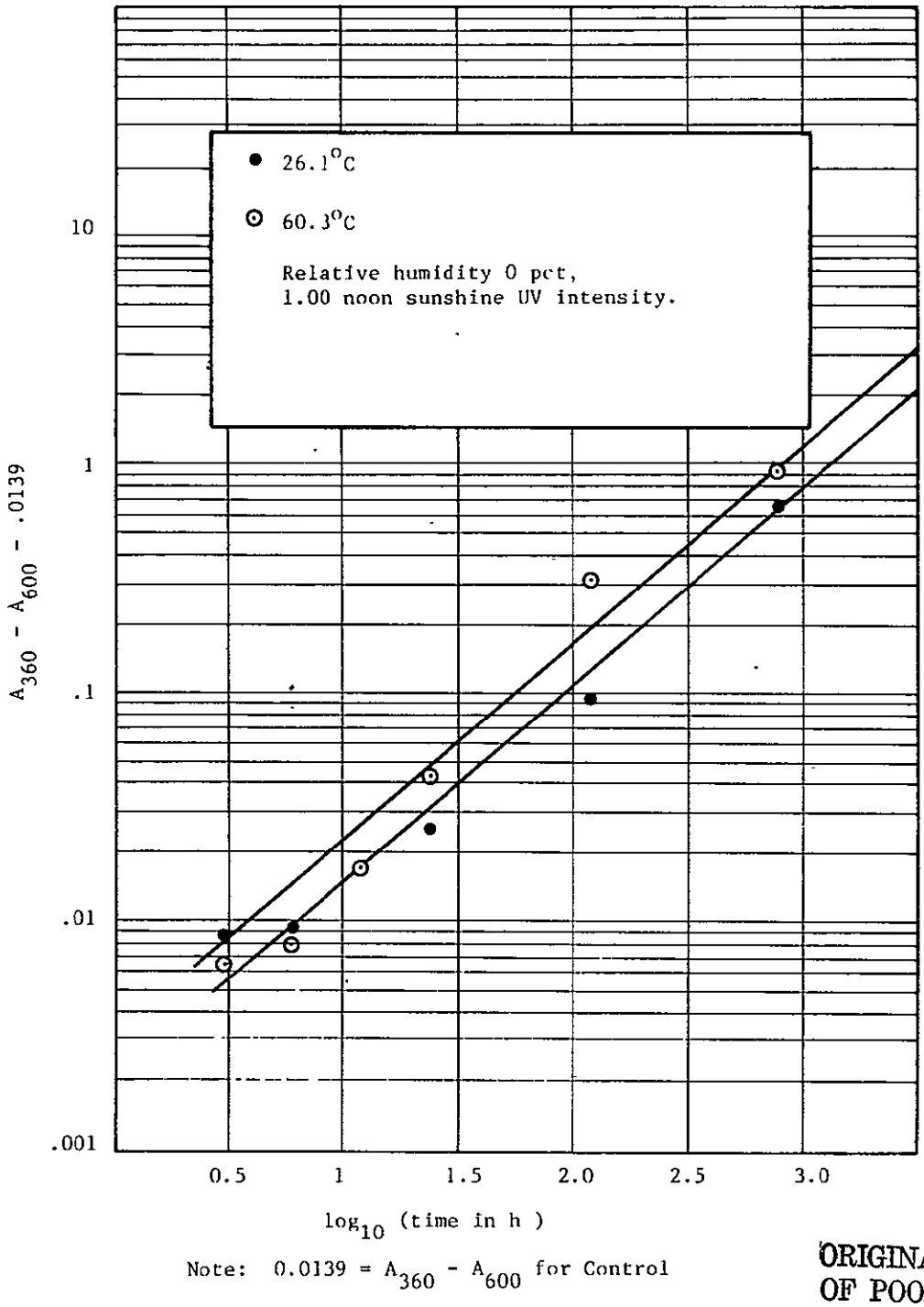

Fig 4. Absorbance Data for Polystyrene, Accelerated Test

In many other cases, the lognormal model gave a better fit. Modeling of the absorbance data requires much further work, and this subject will be treated exhaustively in the Final Report. Tensile data also were modeled successfully.

E. T_g DATA (by TMA)

The T_g data for the accelerated exposure of Lexan (see Appendix, Table A24) fitted neither a Weibull nor lognormal model. Other models must be tried.

F. LOGNORMAL PLOT OF TGA DATA

Another property giving measurements stable enough to indicate a trend was cumulative weight loss of polystyrene as measured by TGA. See the Appendix for data. Lognormal plots are shown in Fig 5. This is the first indication that a property other then transmittance appears to follow the asymptotic lognormal model.

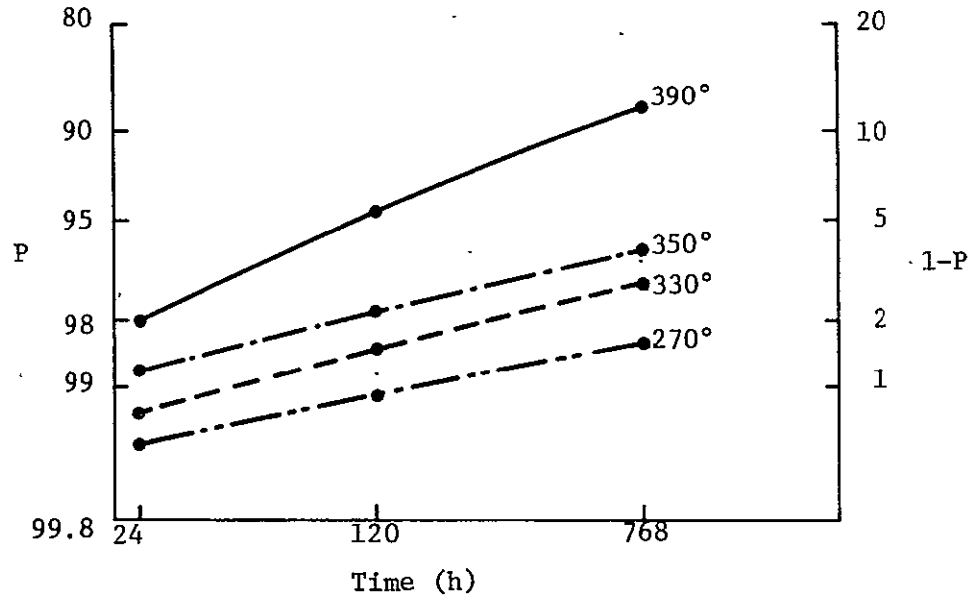

Fig 5. Weight Loss by TGA of Polystyrene, Lognormal Plot of Accelerated Data

VI. CONCLUSIONS AND FUTURE PLANS

The conclusions and future plans are as follows:

(1) Our original plan was to expose samples in 24 "miniature Weather-Ometers" each having a different combination of insolation, temperature, and humidity. Each combination represents a "weather cell" in the Battelle sense (ref 1). By relating the accelerated degradation rate data to an outdoor site via the frequency of occurrence of "weather cells" at that site (procedure developed by Battelle), it should be possible to predict outdoor degradation rates. A principal difficulty at present is scarcity of data for the UV intensity of sunlight, which is critical for the property (yellowing) we measured most closely. However, the multicondition accelerated exposure did disclose the relative importance of weather factors alone and in interaction. For example, moisture-related solar cell failure was shown to be accelerated not by light but by heat. The yellowing of Lexan proved to be hyperaccelerated in xenon lamp exposure and sometimes followed a different mathematical model than it did outdoors. The reason was imperfect solar simulation in the UV wavelength range responsible for the photochemical yellowing reaction. Optical filtering of the xenon arc light could correct this problem. The yellowing of polystyrene, on the other hand, followed a single mathematical model in both accelerated and outdoor exposure. In this case, the accelerated test should fulfill its function by predicting the shape of the degradation vs time curve for many years beyond the practical limit, perhaps 2 years, of abbreviated testing. Knowledge of the shape of the curve is necessary for confidence in a 20-year extrapolation. This extrapolation is the goal of our developing methodology. Using available UV data, we will implement our original "weather cell" prediction plan using "cells" of one month.

(2) The design of a Universal Test Specimen (UTS) proved successful. The ceramic substrate and gold circuitry so far have been inert to weathering, thus concentrating degradation effects in the encapsulant as intended. Electrical measurements on all nine elements (six solar cells and three FET's) can be made conveniently on UTS's previously exposed to weather by plugging their edge contacts into a connector wired to the test equipment. Alternatively, "in situ" readings can be taken during accelerated exposure via a tape cable.

(3) The level of sophistication for abbreviated exposures was raised. The use of multisite exposure provides insight into degradation mechanisms, eg, by showing the role of moisture when a wet and a dry site are included. Also, tests are initiated both in midsummer and in midwinter to obtain seasonal values for degradation model equation parameters. The sunlight-concentrators EMMA and EMMAQUA have given much useful data. These devices have the advantage of avoiding imperfect simulation of the solar spectrum.

(4) Mathematical modeling has been especially successful with the UV light transmittance property of our encapsulants. The big advantage is that data are relatively precise. A decrease in transmittance at 360 nm represents visible yellowing, which is readily measured and has been found useful in monitoring the degradation of plastics (ref 14). There was one case of hyperacceleration by light-stressing. However, in general, the abbreviated and accelerated test data for 360 nm transmittance tended to follow either a Weibull or lognormal failure model. Interestingly, the quite different property of thermal stability, which was determined by TGA measurements, could be graphed similarly into a straight line with a lognormal model. Firm conclusions on models must await accumulation of more data and completion of the outdoor exposure program.

(5) It appears that prediction methodology should involve three modes of exposure:

(a) Multicondition accelerated exposure with a solar simulator such as a xenon lamp or fluorescent sun lamp-black lamp combination (ref 15).

(b) EMMA(QUA) exposure

(c) Natural outdoor exposure, eg, on tilted racks facing south.

Note that the angle of the rack can greatly influence the results (ref 4). Hence samples should be positioned in the manner expected for actual arrays. It must be emphasized that only the inherent weatherability is being evaluated in our present accelerated exposures. Erratic/dynamic factors such as thermal cycling or air pollution have yet to be imposed.

(6) In the next phase of the program, the objective is to extend our prediction methodology for inherent weatherability to total array systems including circuitry and substrate. Earlier work has concentrated on degradation of one component, the encapsulant. One must also consider the effects of the possible erratic/dynamic factors such as temperature cycling, abrasion, and air pollutants. These effects, as applicable for any given site, must be superimposed upon the effects of the basic weather factors (insolation, temperature, and moisture) common to all outdoor exposures. Details of future plans are given in the Amended Test Program Plan for Add-On Contract 954458 recently submitted to JPL.

REFERENCES

1. Thomas, R. E. and Carmichael, C. D., "Final Report on Terrestrial Service Environments for Selected Geographic Location," ERDA/JPL-954328-76/5, JPL Contract No. 954328, Battelle Columbus Laboratories, June 24, 1976.

2. Fisher, H. and Gareth, R., "New Aspects for the Choice of Contact Materials for Silicon Solar Cells," 7th Photovoltaic Specialists Conference, sponsored by IEEE, Pasadena, CA, November 19-21, 1968, pp 70.

3. Anonymous, "The Score on Weatherability," Modern Plastics, May 1967, pp 91 and 162.

4. J.-Ch. Marechal and Ph. Eurin, "The Prediction of PVC Weathering," ISWPR, pp D 7.1 - D 7.10.

5. Kolyer, J. M., "Stability of Materials Under Worldwide Climatic Conditions," Conference on Aerospace Transparent Materials and Enclosures, Atlanta, GA, November 18-21, 1975, Technical Report AFML-TR-76-54, pp 405-432.

6. Grassie, N., and Weir, N. A., Journal of Applied Polymer Science, Volume 9, 1965, p 999.

7. Kamal, M. R., and Saxon, R., Applied Polymer Symposia, Volume 4, 1967, pp 1-28.

8. Davis, A., and Head, B. C., "Future Prospects for Accelerated Weathering of Polymeric Materials," ISWPR, pp C 1.1 - C 1.7.

9. Langshaw, H. J. M., Plastics, Volume 25, No. 267, London, 1960, p 50.

10. Moder, J. M., and Stucky, C., WADC Technical Report 57-711, ASTIA Document, No. 15427, April 1958.

11. Clark, J. E., "Weathering," Encyclopedia of Polymer Science and Technology, Volume 14, 1971, pp 790-795.

12. Clark, J. E., and Slater, J. A., "Outdoor Performance of Plastics III, Statistical Model for Predicting Weatherability," National Bureau of Standards Report 10 116, October 30, 1969.

13. Carmichael, D. C., "Studies of Encapsulation Materials for Terrestrial Photovoltaic Arrays," Fifth Quarterly Progress Report, ERDA/JPL-954328-76/5, by Battelle, Columbus Laboratories, December 27, 1976.

14. 1974 Annual Book of ASTM Standards, published by American Society for Testing and Materials, p 611.

15. Patel, J., and Troth, H. G., "Stabilization of Polyolefins with ZnO Synergistic Combinations," ISWPR, pp E 3.1 - E 3.10.

APPENDIX. MATERIALS, METHODS, AND DATA

A. UNIVERSAL TEST SPECIMENS

1. Introduction

The Universal Test Specimens (UTS's) were designed so that encapsulants can be environmentally tested in their use configuration, ie, in contact with solar cells. Thus, thermal, mechanical, and chemical stresses affect UTS components as if they were part of solar arrays because UTS's are, in fact, miniature arrays.

There are several possibilities for failure to occur:

(1) Corrosion or short circuits caused by ions produced by degradation of the encapsulants. Moisture permeation may contribute.

(2) Loss of light transmittance by delamination of encapsulants from the solar cell and substrate.

(3) Entrapment of moisture close to the solar cell.

(4) Reduction in mechanical strength leading to eventual cracking or other loss of integrity.

Thus UTS's can test both interfacial and bulk properties of materials. Also, UTS's can disclose interactions or incompatibilities between encapsulants and substrate, circuitry, or metallization of the solar cells.

Selection of the substrate materials was based on world experience in outdoor testing of solar cell arrays and materials in general. Many failure mechanisms have been reported, and it would be impossible to quantify degradation rates if several mechanisms operated simultaneously. Therefore, a decision was made to concentrate failure in the encapsulant by using substrates and circuitry having maximum resistance to weathering. Before UTS's were sent to Miami and Phoenix for exposure testing, they were subjected to "torture" tests as discussed subsequently. Thus there was reasonable assurance that UTS's would not fail suddenly in the outdoor environment. Data from gradual degradation processes are necessary for mathematical modeling.

The transparent silicone pottant was known to be weather-resistant, but plastic films used to surface it were expected to show changes. To ensure that degradation would occur, UV-unstablized Lexan was chosen as one cover film. For this first series of tests, the choice of material proved to be well founded. The other cover film was Tedlar fluorocarbon, which degrades much more slowly.

These films were specifically:

(1) Lexan 8740, 0.13 mm (5 mils), non-UV-stabilized, which degrades relatively rapidly and provides workable data, and

(2) Tedlar 100 BG 30 TR poly(vinyl fluoride), 0.025 mm (1 mil), a weather-resistant film which is a serious candidate for solar cell encapsulation. This grade is treated by the manufacturer on both sides to promote adhesion.

2. Fabrication of UTS's

As explained, the object of our UTS design was to encourage failure of the cover film, not the pottant, substrate, or circuitry. Accordingly, the substrate chosen was 96 pct alumina because it is chemically inert and not subject to warpage. Its dimensions were 28.6 x 101.6 x 1.02 mm. The circuitry was thin-film, fire-metallized molybdenum/manganese overplated with nickel and then gold by Ceradyne, Inc. This substrate and circuitry are highly resistant to corrosion or other deterioration.

Three pairs of solar cells (see Fig A1) and three FET's were bonded to each substrate. (Figures and tables of this appendix are placed at the end of the text.) The solar cells were N/P, shallow-diffused, space cells with cosmetic defects. The electrically conducting grid (collectors or "fingers") and bus bar were vacuum-deposited titanium-silver. The back of the cell was also covered with titanium-silver. The cell was coated with a silicon monoxide antireflection coating. Cells were bonded to the substrate with a 0.2 mm layer of Dow Corning RTV 3140 silicone adhesive. The bus bar was wire-bonded using Sn62 solder, and

contact to the back of the cell was made via a gold-plated Kovar tab, also soldered. The FET's were bonded to the circuitry with silver-filled, electrically conductive epoxy. This connected the gate. Source and drain were ultrasonically wire-bonded to pass a 2-g nondestructive pull test on the 25-μm gold wires.

The board was then completely encapsulated with Sylgard 184 transparent silicone rubber after priming with Sylgard primer. Vertical glass molds were used. Lexan and Tedlar film covers, 29 x 29 mm, were also primed with Sylgard primer and cemented onto the cured Sylgard surface. The Sylgard was abraded with Norton Tufbak Durite silicon carbide paper No 120-C to give excellent adhesion of the "cement," which was a thin layer of freshly-mixed Sylgard. Note that the Lexan film had to be abraded with No 320-A carbide paper to promote adhesion. Adhesion of films was good, as discussed elsewhere.

Figure A2 diagrams a UTS; Fig A3 shows a photograph of a UTS, and Fig A4 sketches a UTS in its rectangular tube ready for exposure in the accelerated test. Note the Teflon-covered tape cables which led through the top of the weathering chamber for "in situ" electrical readings.

It was desired that continued weathering, and not merely short-term stress from thermal cycling or moisture-caused warpage, would be necessary for degradation to occur. Therefore, three prototype UTS's were "torture-tested" with 50 thermal cycles. One cycle was 15 min at 100°C, 10 min at room temperature, 15 min at -40°C, and 10 min at room temperature. There was no change in the voltage/current output of the solar cells at an arbitrary point (0.52 V, 17mA). The leakage current of the FET's was unchanged.

Two of the UTS's then were suspended in steam for 7 days. Again there was no change in solar cell performance, while the leakage current of the FET's increased slightly. FET leakage current was observed to be greater in humid vs dry air. and Sylgard is permeable to water and retains about 0.1 pct when immersed at room temperature. The Lexan cover developed fine cracks during steam exposure, but adhesion of films was unaffected.

On completing the "torture tests," 85 UTS's were fabricated. All were tested individually and found to be electrically acceptable.

3. Temperatures of UTS's During Exposure

Temperature, along with insulation and moisture, is a major factor in degradation due to weathering. It is especially important to measure encapsulant temperatures for correlating outdoor and accelerated exposures as discussed below.

a. Outdoor Exposure

A UTS with two embedded Type J (iron-constantan) thermocouples and one protruding thermocouple, for air temperature, was exposed at Desert Sunshine. The three thermocouple beads (1 mm diameter) were shaded by strips of aluminum foil elevated from the UTS surface. Typical data are given in Table A1. With ambient air at about 20°C, UTS temperatures were about 12°C higher on the EMMA than on a rack at 45° S. This would be expected because the EMMA samples receive about eight times the IR energy received by samples at 45° S. An air blast is directed over the EMMA samples but cannot remove all the extra heat.

b. Accelerated Exposure

The same thermocouple-instrumented UTS as used at Desert Sunshine (above) was installed in the accelerated weathering chamber. Readings were taken after reaching thermal equilibrium. Relative humidity had negligible effect. Data are given in Table A2. The UV intensity is given to identify the exposure conditions. Heating is due largely to IR radiation, of course. The IR content of the xenon lamp is discussed elsewhere in this report.

Subsequently, a UTS with fine-wire (0.13 mm) thermocouples was prepared (see Fig A5). The shaded results (see Table A3) agree well with the previous results (Table A2) using thermocouples with a large (1 mm) bead. Temperatures were similar to those observed in commercial arrays in JPL work (ref A1). Temperature uniformity was high throughout the cross section. There was some experimental error; the value of 45.0°C in Table A3 seems obviously low.

B. ACCELERATED EXPOSURE EQUIPMENT AND PROCEDURES

1. Accelerated Weathering Chamber

a. Chamber Construction

The accelerated weathering system is shown in Fig A6. The power supply is shown in the foreground, the control panel is above it, and the weathering chamber is the white box. An exhaust blower and exit duct on the top remove hot air. The material of construction of the chamber was 0.75 inch (1.91 cm) exterior-type plywood, painted with white fire-resistant paint. The inside dimensions were 1.06 m wide, 0.57 m shelf to roof, and 0.61 m deep. Fig A7 shows the chamber interior with a detail of the 2500-W, ozone-free, xenon lamp (Type 975C2980, Canrad-Hanovia, Inc.). Efficient cooling is required, especially of the large upper electrode (anode). Consequently, the inlet ducts from a second blower behind the chamber direct air down onto the lamp as well as across its lower part. The igniter produces a 20,000-V surge to ignite the lamp; it can be seen on the lower right under the shelf on which the quartz tanks were placed. As a precaution against overheating, a thermostat was placed inside the chamber set to turn off the lamp at 66°C (150°F). Similarly, a pressure sensor in the duct turned off the lamp in the event of blower failure.

Thermal control of UTS's was achieved by circulating deionized water on all sides of the rectangular cross section Pyrex 7740 tube (15 x 35 mm I.D., 27 cm high, 1.8 mm wall) containing each UTS to absorb infrared radiation. The tubes were prepared from R-1535 rectangular tubing from Vitro Dynamics, Inc. Three of the Pyrex tubes were contained in each of six quartz tanks as diagrammed in Fig A8 (top view) and sketched in Fig A9. The tank wall was 3.2 mm thick. Figure A10 shows the tanks in place in the chamber, with water hoses (0.75 inch and 1 inch, or 1.91 and 2.54 cm, I.D. Tygon) attached. The instrumented UTS (with fine-wire thermocouples) is included in this photograph. Water entered the bottom of each tank through the 0.75-inch tubing and exited near the top through the 1-inch tubing.

The three tanks on the left were cooled with water at 2 to 3°C (refrigerated by means of a Blue M Model PCC-24SSA-3 Portable Cooling Unit). The three tanks on the left were cooled with water at 40 ± 1°C from a reservoir whose temperature was balanced by passing tap water through a submerged heat exchanger and applying heat with a Blue M Model TH-2004 (300 W) thermostated immersion heater. Tops of the tanks were sealed with cast silicone rubber.

The shutter, visible in Fig A10, shaded the middle two tanks when lowered. It was raised and lowered by a linear actuator to provide 12-h periods of alternate light and shade.

b. Lamp Characterization

The xenon lamp was characterized by means of an EG&G Model 580 Spectroradiometer which had been calibrated, for both spectral and total irradiance, against a 1000-W standard quartz-iodine lamp supplied by an NBS-designated agency. The slit width was 2.5 nm. The Eppley 12-couple thermopile, used for total irradiance measurements, was calibrated in the same way. These instruments are shown in Fig A11.

The thermopile data follow. Lamp distances are from arc to thermopile.

Source	Total Incidence (mW/cm^2)
Sun, 6/30/76, 1:15 p.m., 32°C (90°F), relative humidity 20 pct, Anaheim	103.0
Xenon Lamp at 25.4 cm (10 inches)	249.4
Same at 50.8 cm (20 inches)	78.6
Same at 76.2 cm (30 inches)	
Xenon Lamp, light passed through a water-filled cell (3.2 mm quartz, 14 mm deionized water, and 2.0 mm Pyrex 7740)	
Lamp at 26.0 cm (10-1/4 inches)	129.2
Same at 50.8 cm (20 inches)	44.3
Same at 76.2 cm (30 inches)	21.3

The value of 129 mW/cm^2 is exactly that given by Atlas Electric Devices Co. (ref A2) at 25 cm from a similar lamp with a quartz or Pyrex water-jacket. Obviously, considerable infrared radiation was absorbed by the water-filled cell. Data obtained using the cell are shown in Fig A12. By this graph, the distance from the lamp corresponding to our measured value for the sun (103 mW/cm^2) is determined to be about 30.5 cm (12 inches). However, we wish to match the integrated incident UV energy of the sun, not the total incident radiation.

Spectra in the UV-visible range for the sun, the xenon lamp, and the xenon lamp screened with a water-filled cell (quartz and Pyrex, as above) are shown in Fig A13 and A14). The supplier's data (ref A3) indicates that the ozone-free lamp has the same spectrum as the standard lamp down to 300 nm. Below this, the ozone-free lamp's irradiance decreases rapidly.

Integrated energies over the 300-400 nm (UV) range were determined by making rectilinear plots of incidence vs wavelength (as in Fig A14) and comparing relative areas. Results are as follows:

Source	Relative Area of 300-400 nm Trace	Incidence (mW/cm^2)
Sun	1.000	6.07
Xenon Lamp at 25.4 cm (10 inches)	1.181	7.17
Xenon Lamp with water-filled cell (as above) at 25.4 cm	1.103	6.70

Since the total incidence at 25.4 cm is 133 mW/cm^2 (Fig A12) and the UV incidence is 6.70 mW/cm^2, the desired total incidence for a UV incidence of 6.07 mW/cm^2 is 120 mW/cm^2. From Fig A12, the appropriate distance from lamp to sample is 27.5 cm (10.8 inches).

Two of the tanks were placed at 36.0 cm (14.2 inches) from the lamp and received 79 mW/cm^2. The purpose was to study the relative effects of two levels of light intensity.

The spectrum of the lamp changed as the lamp aged.

After 35 days of continuous operation, the spectrum of the lamp through the same water-filled cell (representing the light reaching the samples) was checked again. The integrated UV intensity (see Fig A15) was similar: 7.74 mW/cm^2 for the 300-400 nm range at 25.4 cm from the lamp vs 6.70 found when the lamp was new.

At the short-wavelength end of the spectrum, the results were:

Wavelength (nm)	Incident Energy, $mW/cm^2/nm$	
	Lamp, New	Lamp Operated 35 days
300	4.0×10^{-3}	0
306	3.9×10^{-3}	1.8×10^{-3}
310	3.8×10^{-3}	5.4×10^{-3}
320	1.8×10^{-2}	4.0×10^{-2}
330	4.5×10^{-2}	4.8×10^{-2}

The cut-off for the used lamp was 304 nm.

These data suggest that Lexan degradation should be less rapid with the aged lamp, because intensity below about 310 nm has decreased because of solarization of the lamp envelope (ref A2 and A4). This proved to be the case, as discussed

below. The most damaging wavelength for polystyrene has been found to be 319 nm (ref A5); and, according to the data, the lamp output has not decreased at this wavelength.

See the description of results on film transmittance at 360 nm for data on the effects of lamp aging on degradation efficiency.

2. Accelerated Exposure Procedure

The midpoints of the UTS's were positioned in the rectangular tubes at the height of the xenon arc. Samples of the three plastic films (1.6 x 7.5 cm for Lexan and Tedlar, 1.8 x 6.3 cm for polystyrene) were attached to the UTS with Teflon tape. The Lexan and Tedlar films hung at the bottom of the UTS, and the polystyrene film was attached just above the upper pair of solar cells (see Fig A4).

Humidity control was achieved with 2 cm of blue (indicating) Drierite in the bottom of the tube for 0 pct relative humidity, a glycerol-water solution of refractive index 1.444 (with 0.1 pct $CuSO_4$ to prevent microbiological growth) for 50 pct relative humidity (ref A6), or deionized water for 100 pct relative humidity.

The shutter provided 12 h of "day" and "night" alternately. Exposure periods were 6, 24, 120, and 768 h. Each exposure began with fresh films. A few of the 768-h films were exposed an additional 768 h, for a total of 1536 h. During the 6-h exposure, the shutter was raised for the first 3 h, then lowered for 3 h. This procedure provided samples, from the two tanks behind the shutter, exposed to light for 3 h. Similarly, the samples behind the shutter in the 24-h exposure were given 12 h of light.

Samples in darkness were thermally controlled by immersion of the Pyrex tubes in agitated baths at 40°C (water bath) and 80°C (silicone oil).

C. OUTDOOR WEATHERING EQUIPMENT AND PROCEDURES

For each of the items shown in column 1 below, 14 samples were exposed under three conditions, at two locations, and with different start dates, as follows:

Items Exposed	Location	Conditions	Exposure Started
UTS's, Lexan film, Tedlar film	Phoenix	45° S	September 12, 1976
Lexan film	Phoenix	45° S	December 22, 1976
Lexan film	Phoenix	45° S	June 21, 1977
UTS's, Lexan film, Tedlar film	Phoenix	EMMA	September 12, 1976
UTS's, Lexan film, Tedlar film	Phoenix	EMMAQUA	September 12, 1976
UTS's, Lexan film, Tedlar film	Miami	45° S	September 1, 1976
Lexan film	Miami	45° S	December 22, 1976
Lexan film	Miami	45° S	June 21, 1977
Polystyrene film	Miami	45° S	October 20, 1976

Sizes of the film samples were 10 x 14 cm for Lexan and Tedlar, and 20 x 25 cm for polystyrene.

Samples were returned according to the following schedules:

Cumulative Exposure Time (days)	
45° S	EMMA, EMMAQUA
5	1
10	2
15	5
30	10
60	30
90	90
150	150
210	210

The Miami site was South Florida Test Service Inc., 9200 N.W. 58th Street, Miami, FL 33178. The Phoenix site was Desert Sunshine Exposure Tests, Inc., Box 185, Black Canyon Stage, Phoenix, AZ 85020. Both services provide extensive weather data.

Ultraviolet sun hours have been reported for some test sites. An "ultraviolet sun hour" is a total of 60 min when the solar radiation intensity exceeds 0.823 Langleys/min. (Note: One Langley is 1 g calorie/cm^2). This light intensity has been used as a rule-of-thumb value above which degradation of plastics occurs. It is reported that UV sun hours correlate better with degradation than does exposure time (see ref A7). However, recent opinion is that UV sun hours show "general non-relevance to weathering" (ref A8). Desert Sunshine has ceased to report UV sun hour data because more sophisticated UV intensity criteria are being developed. Satisfactory mathematical modeling requires that

(1) The most damaging UV wavelength region be known for a particular material

(2) The intensity of this specific region be known daily or even hourly.

The EMMA and EMMAQUA are "dry" and "wet" sunlight-concentrators, respectively. The EMMAQUA has nozzles (visible in Fig A16). These are used to spray distilled water on test samples for 8 min every hour in the standard cycle, as we used. The 10 aluminized mirrors reflect 70 to 80 pct of UV radiation down to the cut-off point of about 295 nm for terrestrial sunlight. Thus, total UV radiation is seven or eight times that on an equatorial mount without mirrors. Samples are cooled by air flow; the blower is seen at the upper right of the device in Fig A16. The machine has a solar-energized guidance system which keeps the mirrors at 90° to the sun throughout the day. The samples, facing downward, are exposed on a 13 x 140 cm target area. In general, data obtained on the EMMA correlates with that obtained in dry desert climates. On the other hand, the EMMAQUA gives more or less successful correlations with Miami and European locations.

In the 45° S exposures, the samples were mounted on racks with noncorrosive fittings and without backing. The racks were tilted 45° and faced south. Although this is the conventional arrangement for natural weathering, diffuse UV from the sky constitutes up to 70 pct of total UV radiation. UV radiation from the direction of the sun contributes down to 30 pct of the total incident UV (ref A9).

D. ANALYTICAL METHODS

1. Applied to Films

a. Optical Transmittance

A Cary 16 Spectrophotometer was used for measuring optical changes in the films. The absorbance was read at 360 nm (slit width 0.63 nm) and at 600 nm (slit width 0.07 mm), using the tungsten-halogen light source.

It is assumed that A_{600} represents light lost by reflection and scattering. To check this assumption, a Lexan control which gave $A_{360} = 0.0824$ and $A_{600} = 0.0580$ was abraded with carbide paper. The new readings (also means of 5 replicates) were $A_{360} = 0.7902$ and $A_{600} = 0.6370$. The value $A_{360} - A_{600}$ was 0.0244 before abrasion and 0.1532 after abrasion. The sample then was abraded further to give $A_{360} = 1.266$ and $A_{600} = 1.142$, so that $A_{360} - A_{600} = 0.122$.

It appears that abrasion caused greater light-scattering at 360 nm than at 600 nm but in an erratic ratio. Clouding and/or surface-dulling of samples may have the same effect, making it impossible to know precisely the A_{360} due to yellowing. However, this uncertainty does not change the general trend of data plots. In fact, A_{600} is low and approximately constant except for very severly-weathered samples.

The photometric accuracy of the Cary 16 is specified to be 0.00024 absorbance units near absorbance = 0 and 0.001 units near absorbance = 1.

The accelerated data from 1536 hours accelerated exposure (Table A4) include typical examples of replicates. The standard deviation was approximately 1 or 2 pct of the mean.

The values in the tables are means of 10 replicates for outdoor exposure samples (including EMMA and EMMAQUA) and of 5 replicates for accelerated exposure samples.

b. Attenuated Total Reflectance Infrared Spectroscopy (ATR-IR)

The instrument was a Beckman IR 4240 Spectrophotometer. A KRS-5 crystal (approximately 2 x 5 cm) was clamped against the film with beam entry at 45°. To improve contact of film and crystal, a rubber spacer was placed under the film before clamping. Weak spectra had been obtained before using the rubber spacer. The depth of penetration of the IR radiation into the sample is on the order of 3 to 50 μm (ref A10). This analytical method was one of the few found useful for following the degradation of weathered polyvinyl chloride (ref A11).

c. Tensile Tests

Using a paper cutter, the Lexan and Tedlar films from outdoor exposures were sliced into 0.20 x 5 inch (0.5 x 13 cm) strips. These were pulled on an Instron testing machine at a crosshead speed of 2 inches/min (5 cm/min). Clamp separation was 3 inches (7.6 cm). The average thickness of the films was 1.1 mils (0.028 mm) for Tedlar and 5.3 mils (0.13 mm) for Lexan. Percent elongation was determined by dividing the absolute elongation by only that portion of the strip which elongated. The number of replicates was 8 to 10. For Lexan, controls (unweathered samples) were run at the beginning and end of the test series and then averaged. The final control showed 98 pct of the breaking stress and 101 pct of the ultimate elongation of the initial control.

For accelerated test specimens, only three replicates could be cut because the film strips were only 16 mm wide. Lexan and Tedlar were pulled at 2 inches/min (5 cm/min) crosshead speed; polystyrene was pulled at 0.2 inch/min (0.5 cm/min). Clamp separation was 0.5 inch (1.3 cm) in all cases. Controls (5 replicates) were run before and after the weathered samples. The means were close: 9691 and 9764 psi breaking stress for Lexan and 11,554 and 11,318 for polystyrene.

d, Thermogravimetric Analysis (TGA)

A Perkin-Elmer TGS-1 Thermobalance was used in conjunction with the DSC-2 unit for temperature programming. The heat-up rate was 10°C/min, with the sample under nitrogen.

e. Thermomechanical Analysis (TMA)

The instrument used was a Perkin-Elmer Thermomechanical Analyzer TMS-1, with quartz penetration probe Part No. 219-0209. The heat-up rate was either 5 or 10°C/min and the penetration force was varied from 12 to 20 g to give the sharpest transition on the recorder plot. Two plies of the Tedlar film were used because of its thinness (25 μm, 1 mil).

f. Differential Scanning Calorimetry (DSC)

A Perkin-Elmer DSC-2 Differential Scanning Calorimeter was used. This was calibrated with indium (transition point 156.6°C) and K_2CRO_4 (transition point 670.5°C). The heat-up rate was 40°C/min, with a recorder chart speed of 4 cm/min and a sensitivity of 5 mcal/sec.

g. Electron Spectroscopy for Chemical Analysis (ESCA)

The Lexan film exposed for 30 days on the EMMAQUA was examined by Electron Surface Chemical Analysis (ESCA). The weathered sample showed two new carbon lines and at least two new oxygen lines, with a much higher oxygen signal. This represents a marked change, but interpretation was difficult.

ESCA analysis of polystyrene films from accelerated exposures will be reported later. The data are in percent oxygen and follow a Weibull or lognormal model. ESCA has been useful in plastics weathering studies, eg, for carbonyl formation in epoxy resin (ref A12).

2. Applied to UTS's

a. Electrical Properties

IV curves for the solar cells were determined by OCLI using standard illumination (tungsten lamp, 2800°K, 100 mW/cm^2). The short circuit current is

the amperage at 0 V. The maximum power, or power point, was determined by OCLI. This is the point on the IV curve where the product of current and potential is at a maximum. In the course of failure analysis, IV curves were also plotted in our own laboratory using an arbitrary tungsten lamp source. "In situ" readings were taken with no applied resistance on the 18 UTS's placed in the accelerated weathering chamber. The current was in the 50-120 mA range, and the voltage was in the 50-150 mV range. On the IV curve, these values are on the short circuit current "plateau" at low voltage, so the measured current is considered approximately the short circuit current. Readings were normalized by means of a "standard cell" encapsulated with glass and a heavy layer of Sylgard 184. See Table A5 for results.

The leakage current is that which flows into the connected drain and source and out the gate of an FET chip when a potential of 20 V is applied.

b. Peel Strength of Cover Films

The plastic covers were scored with a razor blade and five strips 5 mm wide were peeled off. With the UTS clamped in the horizontal position, each strip was peeled at 90° by pulling upward at 2 inches/min (5 cm/min) with an Instron testing machine. The strip was held in a small clamp and pulled with a nylon tie-cord, ie, a flexible connection. The chart speed was 1 inch/min (2.5 cm/min). Tension varied somewhat during pulling, and an average value was estimated visually from the graph.

E. EXPERIMENTAL DATA

1. Films

a. Absorbance

(1) Outdoor Exposure - Data for A_{360} and A_{600} are given in Tables A6 through A10.

Tedlar showed only small changes (Table A10). There was no yellowness detectable by eye. Greater light scattering at 360 nm than at 600 nm could explain all of the observed increase in $A_{360} - A_{600}$ on weathering.

For Lexan, abrasion gave an $A_{360} - A_{600}$ of 0.15 vs 0.02 for a control, and the largest value of $A_{360} - A_{600}$ for weathered Tedlar was 0.09 vs 0.04 for a control.

Increase in yellowness due to "dark reaction" after the end of outdoor (or accelerated) exposure was checked on samples which had been stored in the dark. Table A11 shows increases of 8 to 12 pct in A_{360} after 15 weeks storage. This result indicates only minor error introduction if samples are measured promptly, as they were, when mailed back from the exposure sites.

(2) Accelerated Exposure - Data for A_{360} and A_{600} are given in Tables A12 through A15. Data at 600 nm, where absorbance became significantly large only for exposures longer than 24 h, are given in Tables A16 and A17.

Figure A17 shows complete UV spectra for unweathered Lexan and polystyrene vs samples exposed at the high light intensity, 60.3°C air temperature, and 100 pct relative humidity for 5 days. At 360 nm, we are measuring on the side of a broad UV absorption, which is shifting toward the visible as the sample degrades. Tedlar showed little spectral change.

The rate of spectral change is higher for accelerated weathering than for outdoor exposure. The explanation is that light near 300 nm degrades Lexan fastest. General Electric's data give 295 and 330 nm as the most damaging wavelengths for Lexan. Although the filtered xenon lamp light and sunlight are very similar in intensity over nearly all of the 300 to 400 nm region, they do differ at 300 nm by a factor of 43 for the new lamp. Our determination of noon sunlight gave 8.0×10^{-5} $mW/cm^2/nm$ vs 3.4×10^{-3} at 300 nm for the xenon light as it reaches the sample. A $\log (\frac{1}{p}) \times 10^4$ value of 278 Lexan was attained in 30 days outdoors in Phoenix. However, this value was reached in 2.3 h in the accelerated test, equivalent to an acceleration factor of 313. This result can be explained by multiplying 43 by the time-compression factor of about 8 to give 344. The assumption that light in the

300 nm vicinity is responsible for degradation was supported by a separate experiment. The spectral change of Lexan was twice as rapid behind quartz (90 pct transparent over the 300 to 400 nm region) as behind Pyrex 7740 (1.0 mm thick). The latter transmits about 40 pct at 300 nm vs 80 pct at 330 nm.

Incidentally, the decrease in transmittance at 360 nm for Lexan proceeded at about the same rate under argon as under air. Yellowing of polystyrene is reported to proceed under nitrogen (ref A13).

In interpreting the data, it is important to note that solarization of the lamp envelope and/or Pyrex tubes caused decreased UV intensity below about 310 nm as discussed above. To check the efficiency of the lamp in degrading Lexan (in terms of transmittance at 360 nm), Lexan samples were exposed for 24 or 16 h when the lamp had operated for 0, 40, and 69 days.

Results are given in Table A18. In terms of ΔA_{360} (the increase in the value of $A_{360} - A_{600}$ over that of a control), the efficiency of the lamp in yellowing Lexan had fallen to 27 pct after 69 days of operation.

In contrast, lamp aging had little effect on the rate of polystyrene yellowing (Table A19). An explanation is that polystyrene is degraded by UV wavelengths higher than the wavelength range which is affected by solarization. Polystyrene degrades especially at 319 nm according to the literature (see ref A5).

b. ATR-IR

Changes in the carbonyl region occurred with Lexan in the form of ambiguous band broadening. There was no evidence of hydroxyl groups. This suggest oxidation without hydrolysis.

The Tedlar film exposed for 30 days on th EMMAQUA was examined by Fourier transform ATR-IR by Digilab Inc. (Cambridge, MA). An absorbance subtraction plot of the weathered film vs a control indicated that chemical changes had occurred due to weathering. However, there was no carbonyl peak (region of 5.9 μ or 1700 cm^{-1}).

ATR on polystyrene films from accelerated exposure clearly showed development of a carbonyl band at 5.9 μ (see Table A20.) An aromatic peak at 6.7 μ was used as the internal standard. The control result of 4 pct was subtracted from all the experimental values to give the percent data in the table. The carbonyl concentration was 22 times higher on the side facing the xenon lamp than on the reverse side in a 768-h sample (see Table A20).

The polystyrene films were very brittle after 768 h exposure.

c. Tensile Tests

Data are given in Tables A21, A22, and A23 for outdoor exposure and Tables A24 through A26 for accelerated exposure. Some of the data are plotted in Fig A22 and A24. A loss of 50 pct in tensile properties often is considered failure (see ref A14).

c. TGA, TMA, DSC

Data are presented in Tables A27 through A29. Note that the experimental values for the T_g of Tedlar were 50°C by TMA and 57°C by DSC. A literature value is 40°C (ref A15).

The T_g of Lexan fell progressively with accelerated exposure (Table A29). A similar progressive decrease was found for the T_g of epoxy resin during weathering (ref A12).

2. UTS's

a. Electrical Properties

Short circuit current data are given in Tables A5, A30, and A31. Short circuit current is a measure of encapsulant light transmittance (ref A16). Maximum power data are given in Tables A32 and A33. See the section on failure analysis below.

FET leakage current data are given in Tables A34 and A35. The higher values in accelerated exposure (Table A35) seem associated with moisture because they did not occur under the 0 pct relative humidity conditions.

b. Peel Strength of Cover Films

Data are given in Table A36.

c. Surface Deterioration of Cover Films

With no cover, Sylgard 184 picked up some fine dust in the accelerated test, more on EMMAQUA, and larger particles on EMMA (see Fig A20). Presumably, the lack of washing by water-spraying allowed retention of larger particles in the EMMA case.

Tedlar accumulated a little dust on EMMA and EMMAQUA (see Fig A21a). In the accelerated test, only the highest UTS temperature (71.1°C), measured just under the film cover, was associated with wrinkling (Fig A21b), presumably due to contraction. Embrittlement also was observed.

The Lexan cover showed no deterioration at 400X after 150 days EMMA exposure, but the corresponding EMMAQUA exposure gave a dull surface with a vermiculated appearance when magnified (Fig A21c and A21d). The 90-day EMMAQUA sample also showed severe loss of gloss.

For accelerated exposure, the effects of temperature and moisture on gloss, and on other properties, are summarized in Table A37.

d. Failure Analysis on Solar Cells

In world experience with various solar cell array systems, moisture permeation has been a major factor in failure by causing corrosion of metallization, contacts, and leads. Degradation in properties by UV light has been less of a problem than expected, though exposure times have been only up to 4 years at present (ref A17).

Five of six solar cells on a UTS exposed to 100 pct relative humidity at 80°C in the dark showed 42-53 pct power loss (see Fig A22 and A23, in which the numbered curves are for the individual cells). The five low-power cells were examined after peeling off the Sylgard pottant. The contacts were visibly deteriorated when viewed under magnification. Deterioration of contacts was responsible for reduced electrical performance, as clearly demonstrated by coating the contacts with conductive paint and restoring power output of the cell (Fig A24).

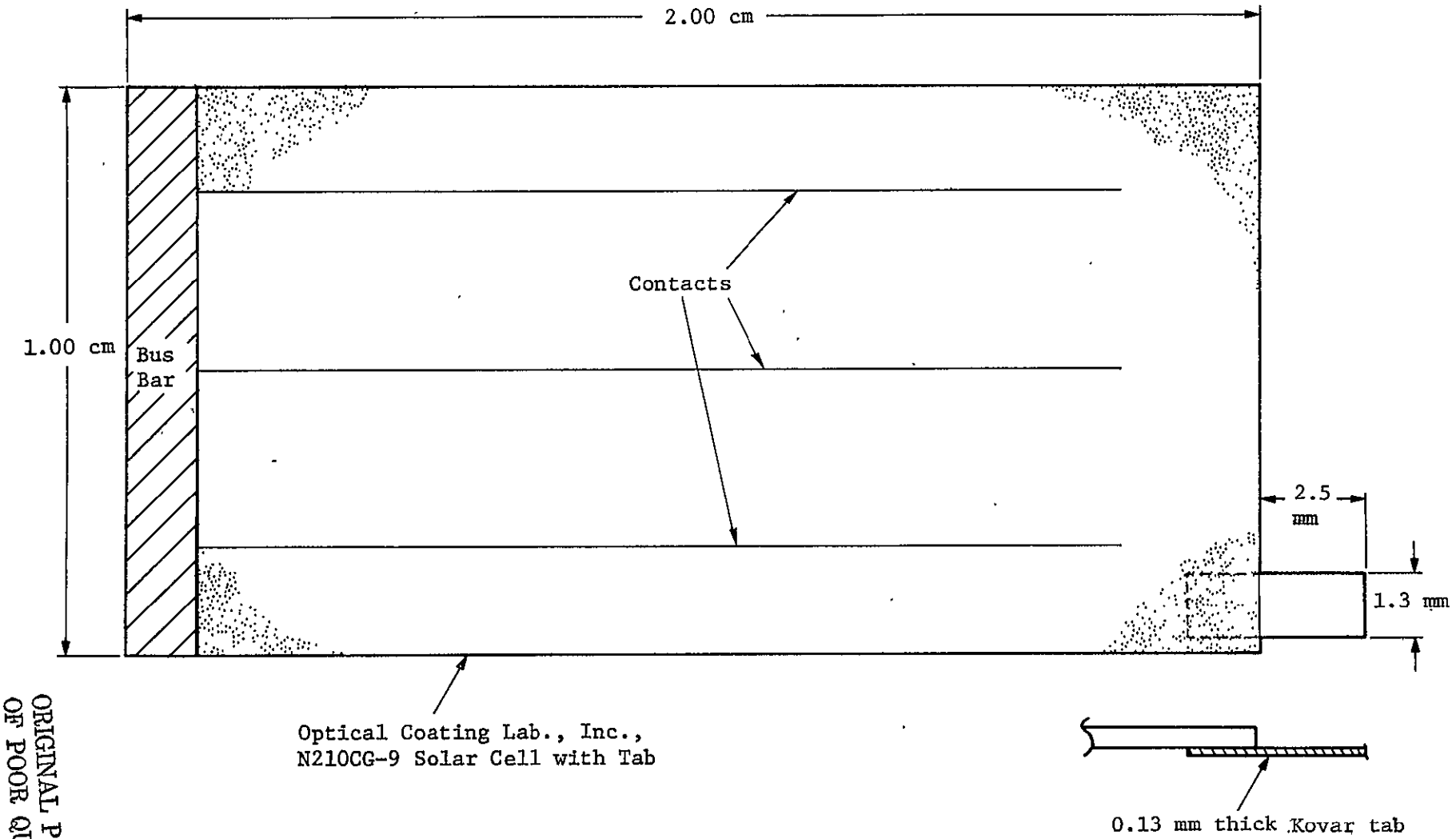

Fig A1. Diagram of Solar Cell.

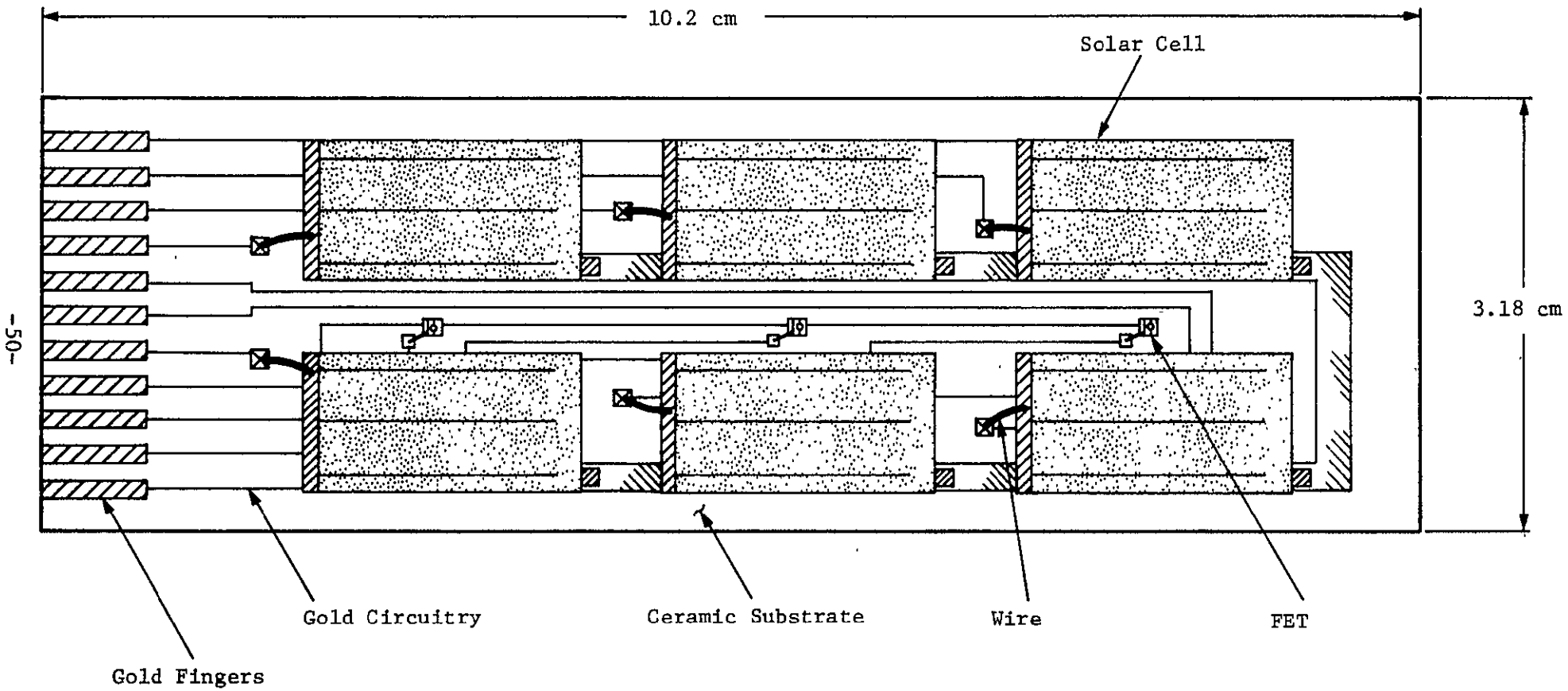

Fig A2. Diagram of Universal Test Specimen, Top View

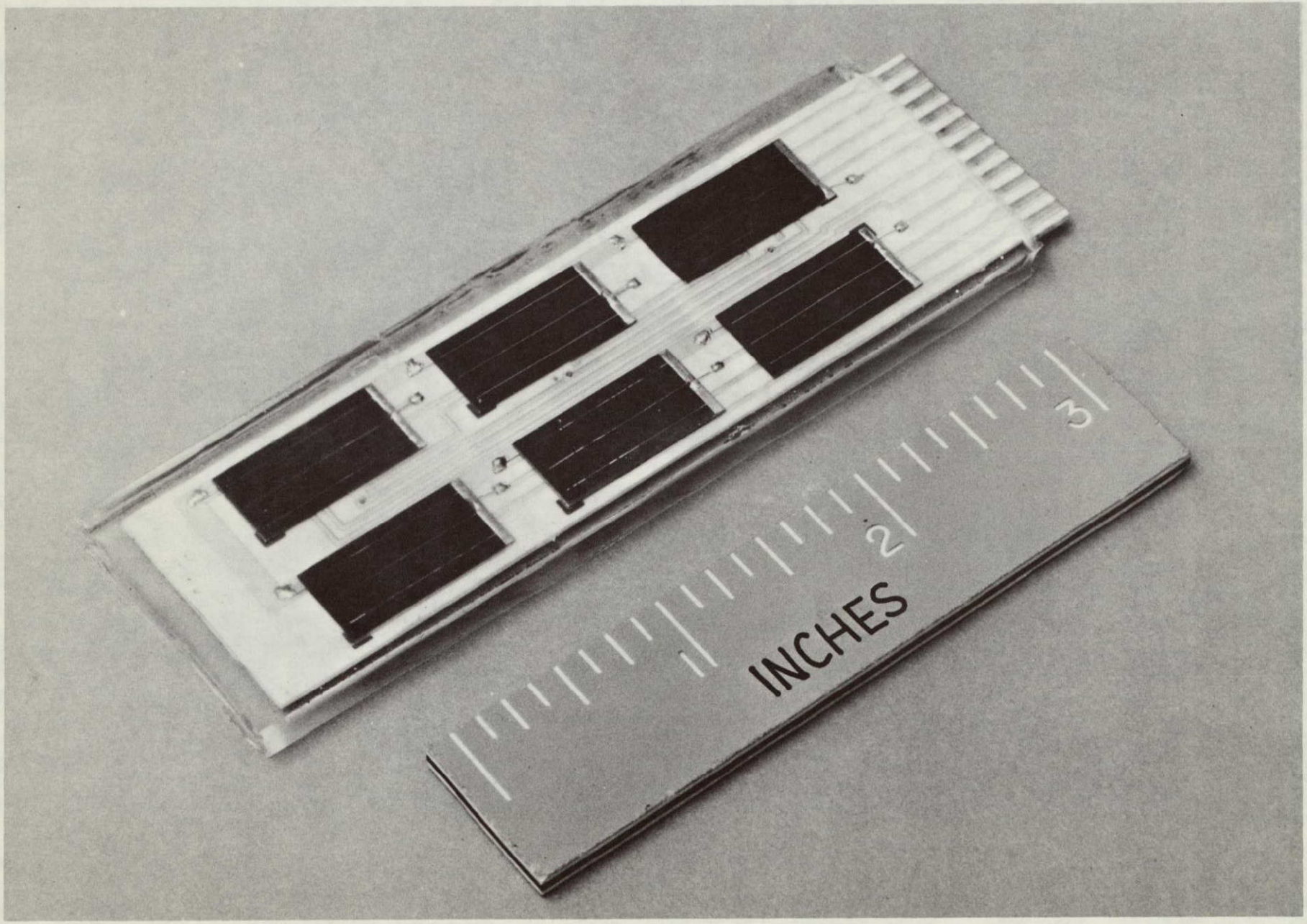

Fig A3. Universal Test Specimen (UTS)

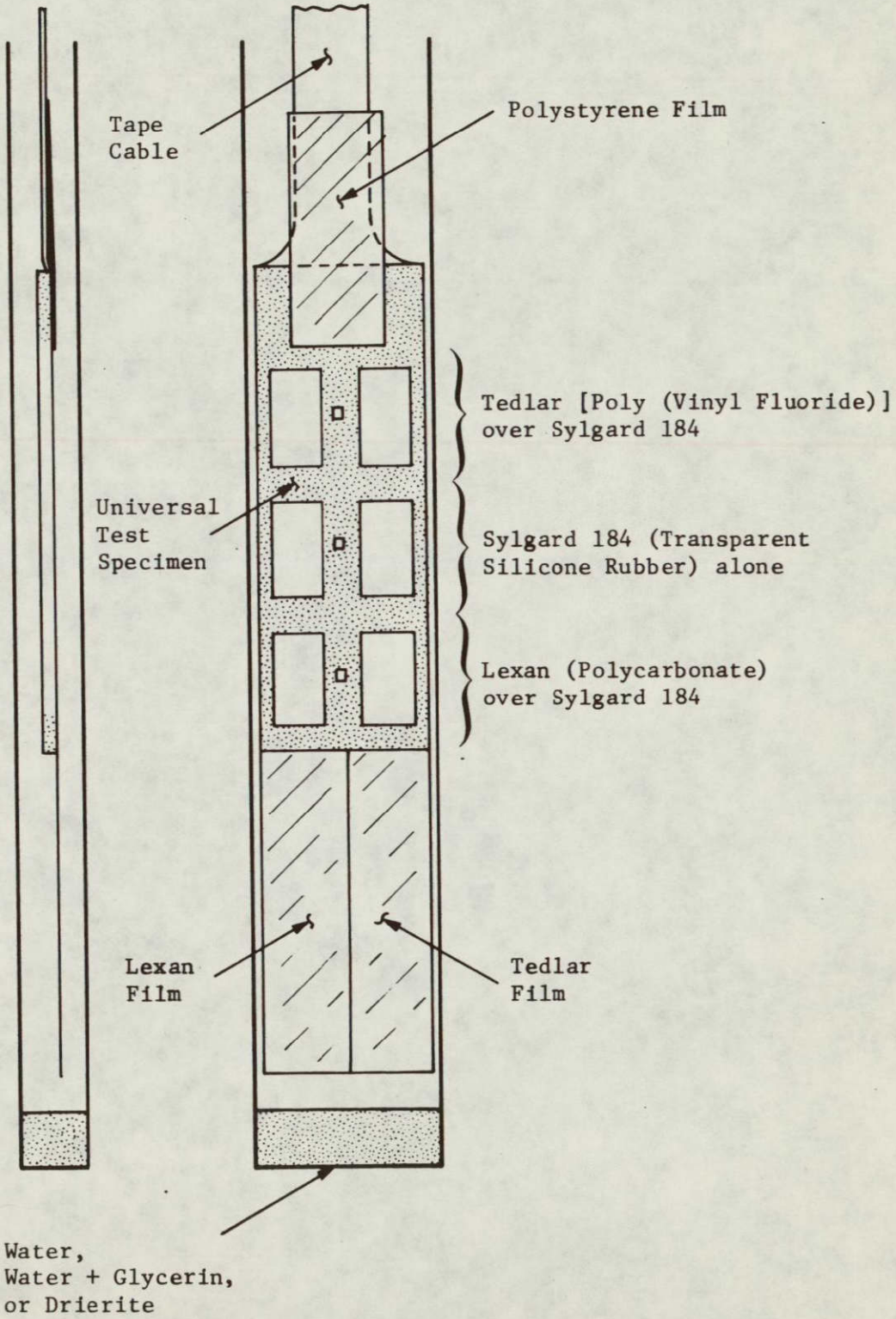

Fig A4. Diagram of UTS in Rectangular Tube

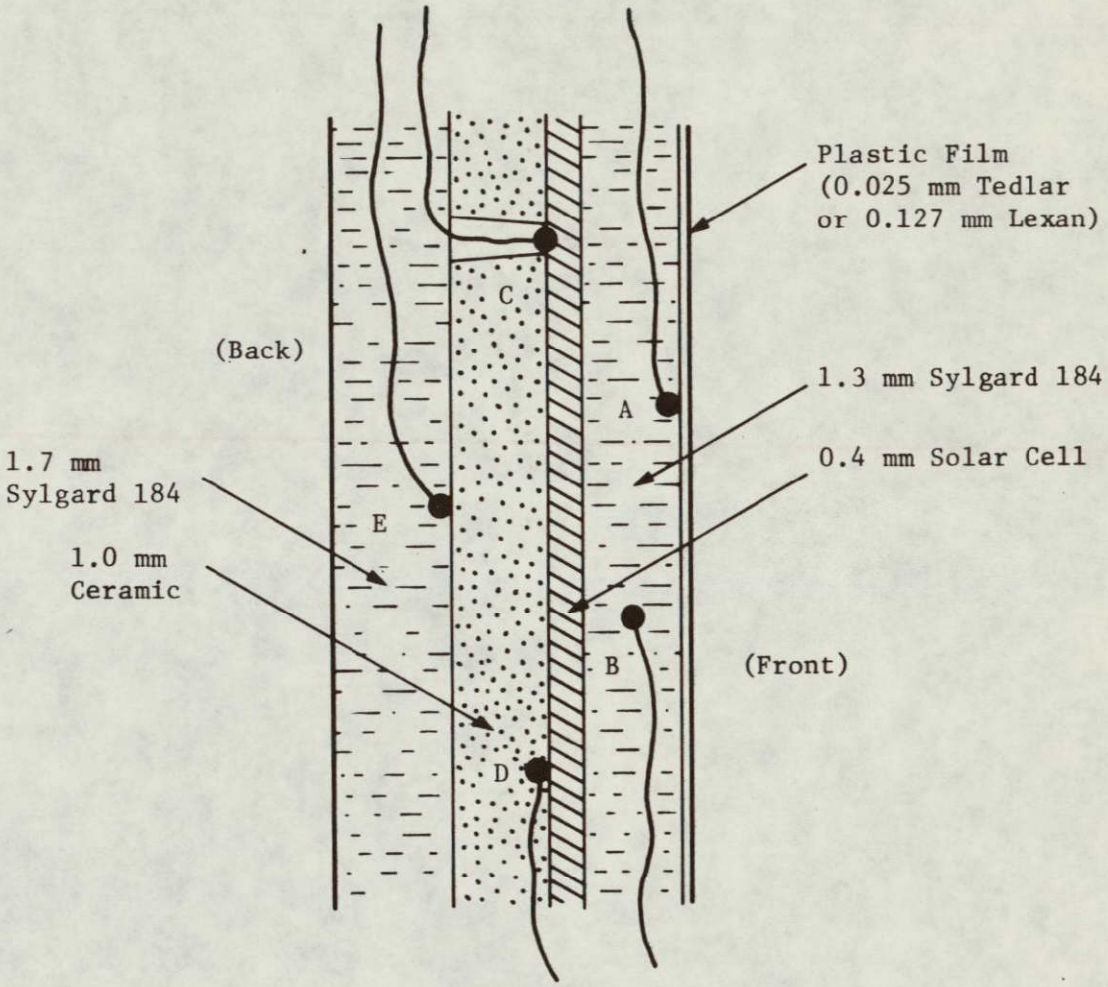

Position of fine-wire thermocouples:

A - just under plastic film cover

B - midway in Sylgard encapsulant layer

C - behind solar cell via hole in ceramic

D - forced under solar cell

E - at back surface of ceramic

Fig A5. Diagram of UTS with Fine-Wire Thermocouples, Cross-Section

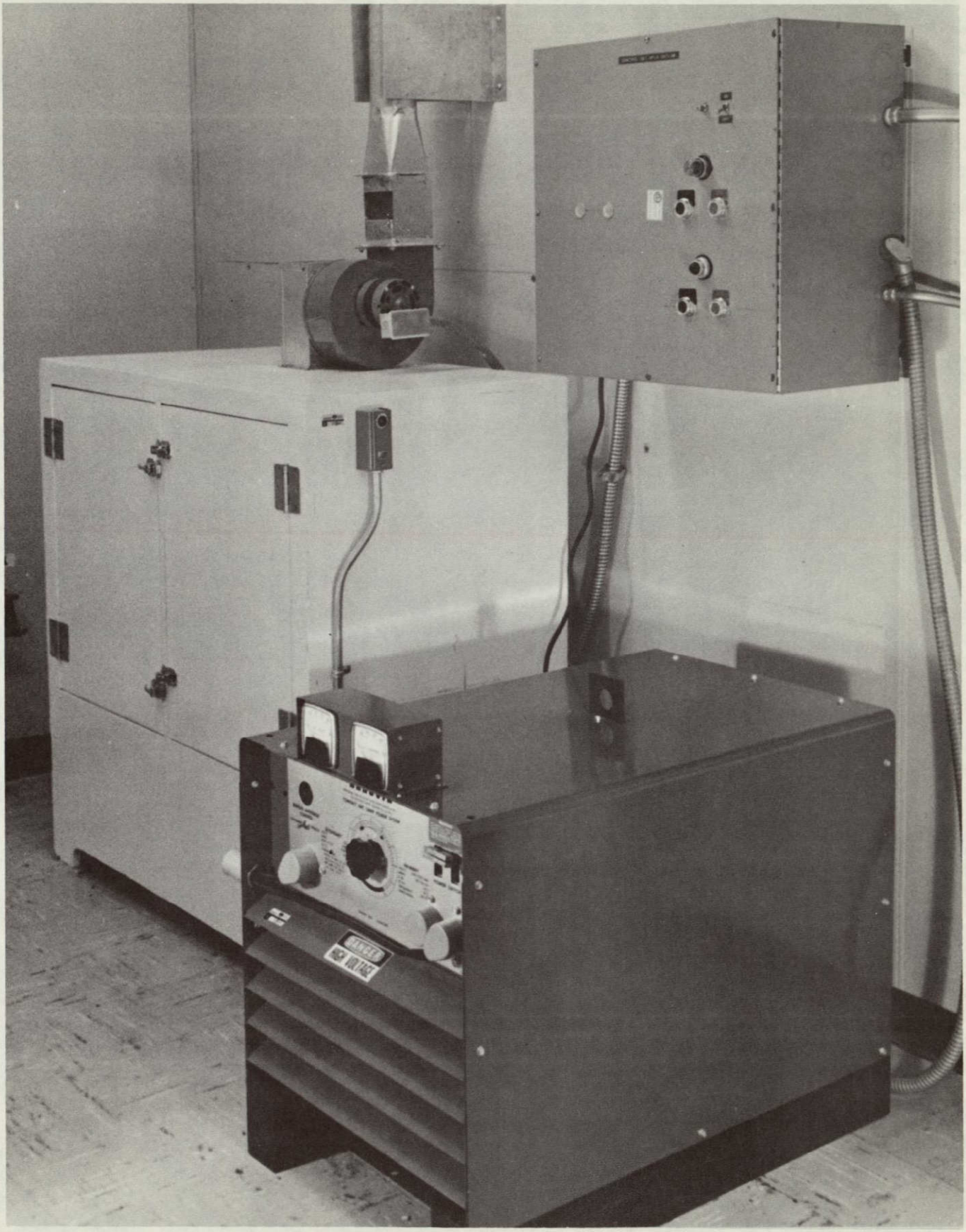

Fig A6. Artificial Weathering Chamber

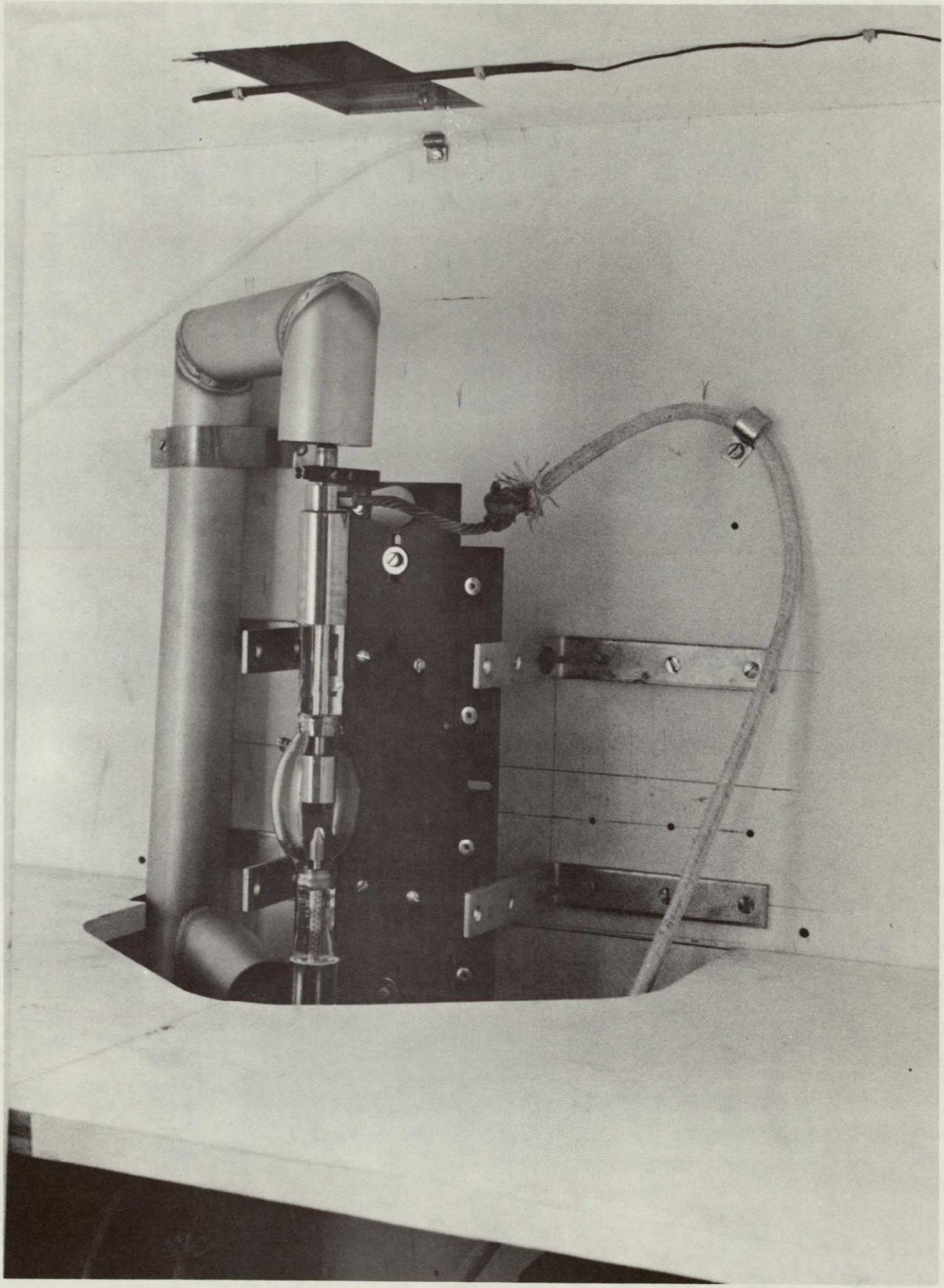

Fig A7. Interior of Chamber Showing Xenon Lamp

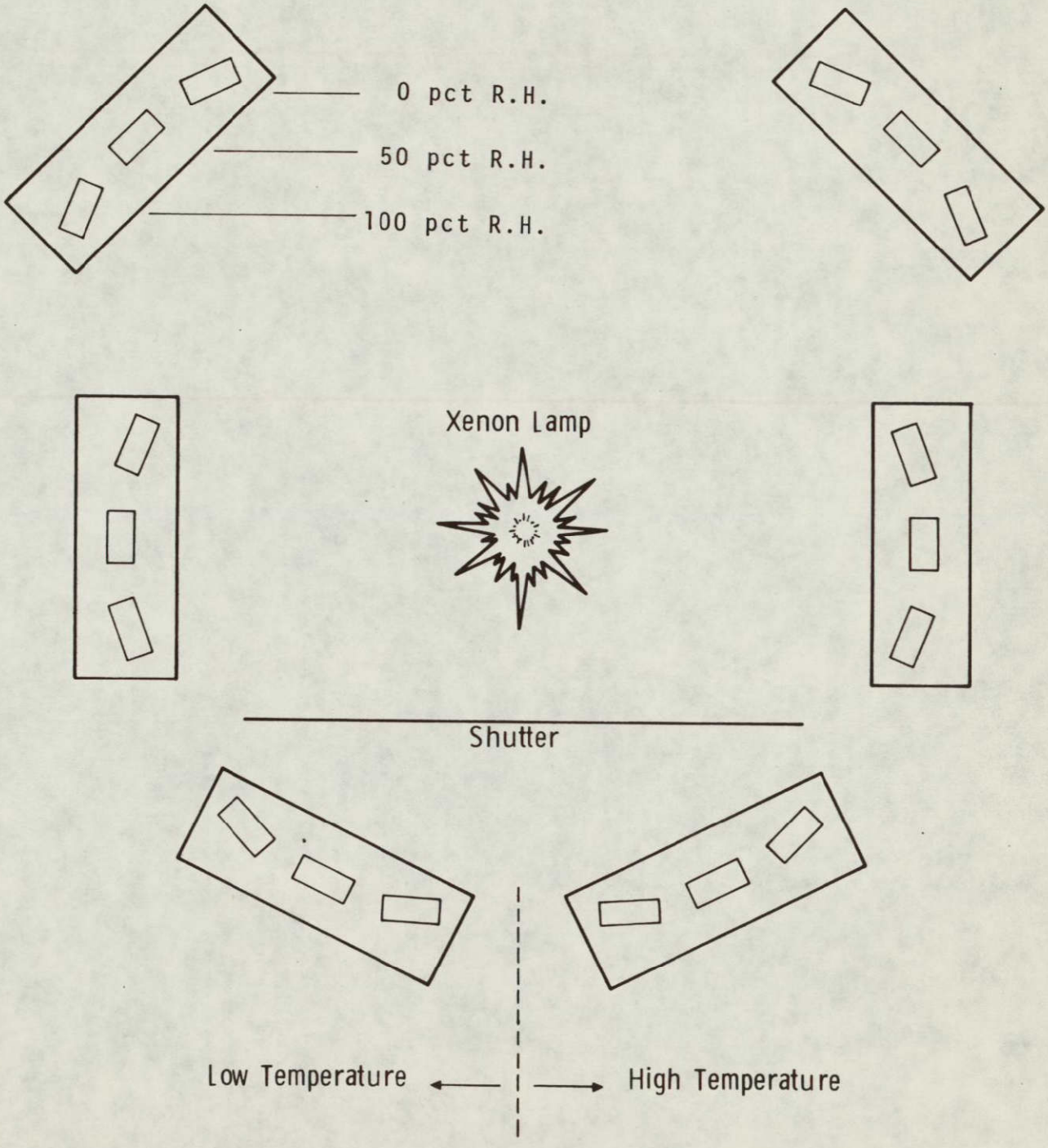

Fig A8. Diagram of Artificial Weathering Chamber, Top View

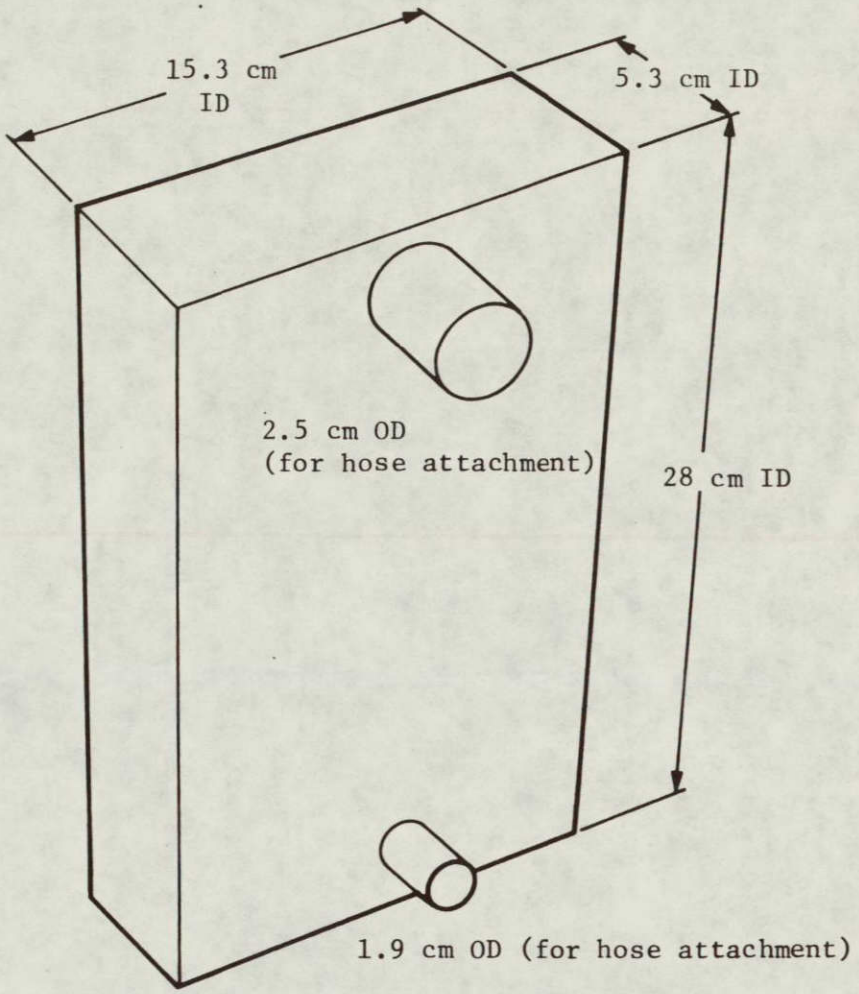

Fig A9. Quartz Tank Used in Accelerated Weathering Chamber

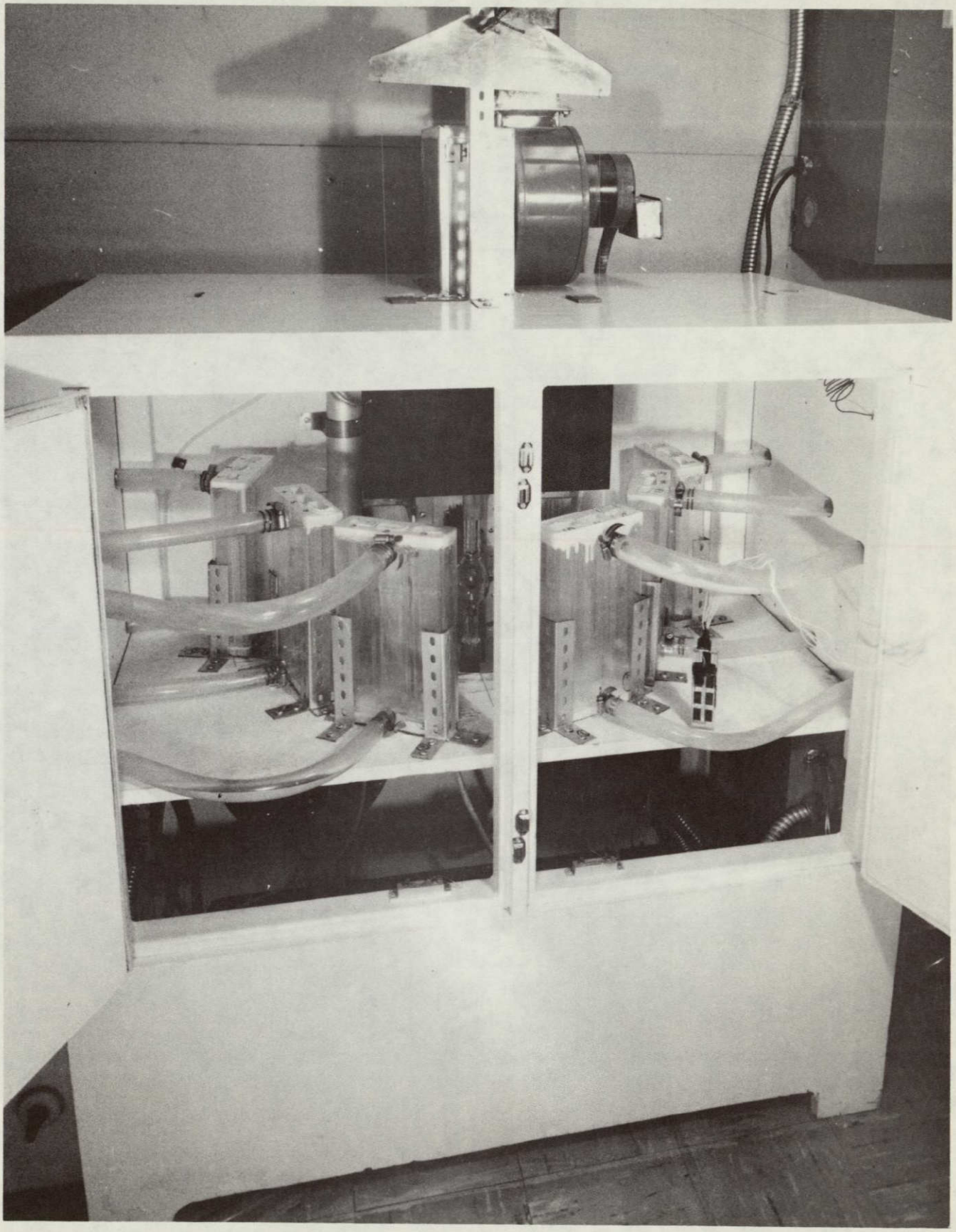

Fig A10. Interior of Accelerated Weathering Chamber Showing Quartz Tanks

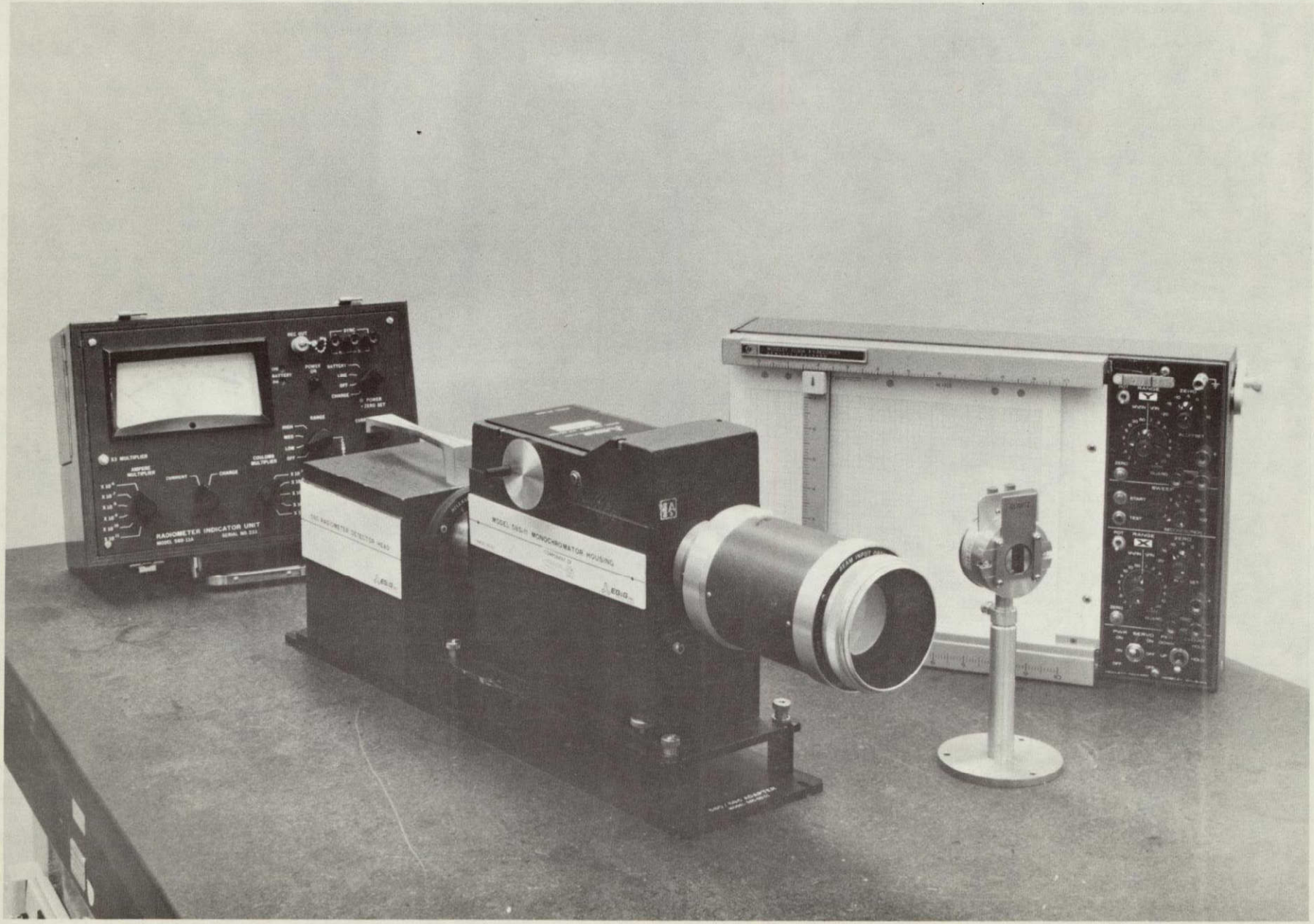

Fig A11. Spectroradiometer and Thermopile

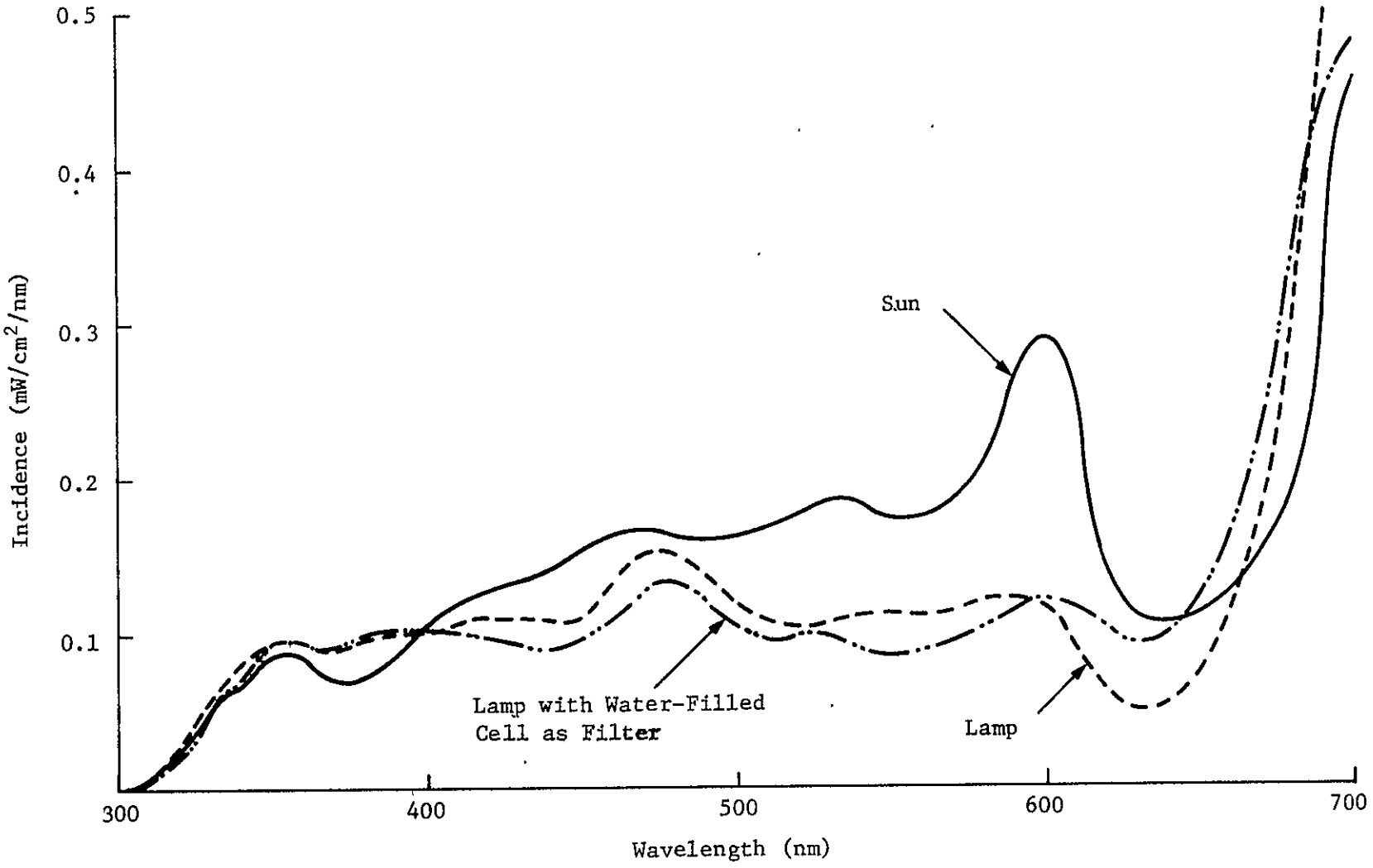

Fig A13. Incident Radiation of Sun vs 2500 W Xenon Lamp at 25 cm

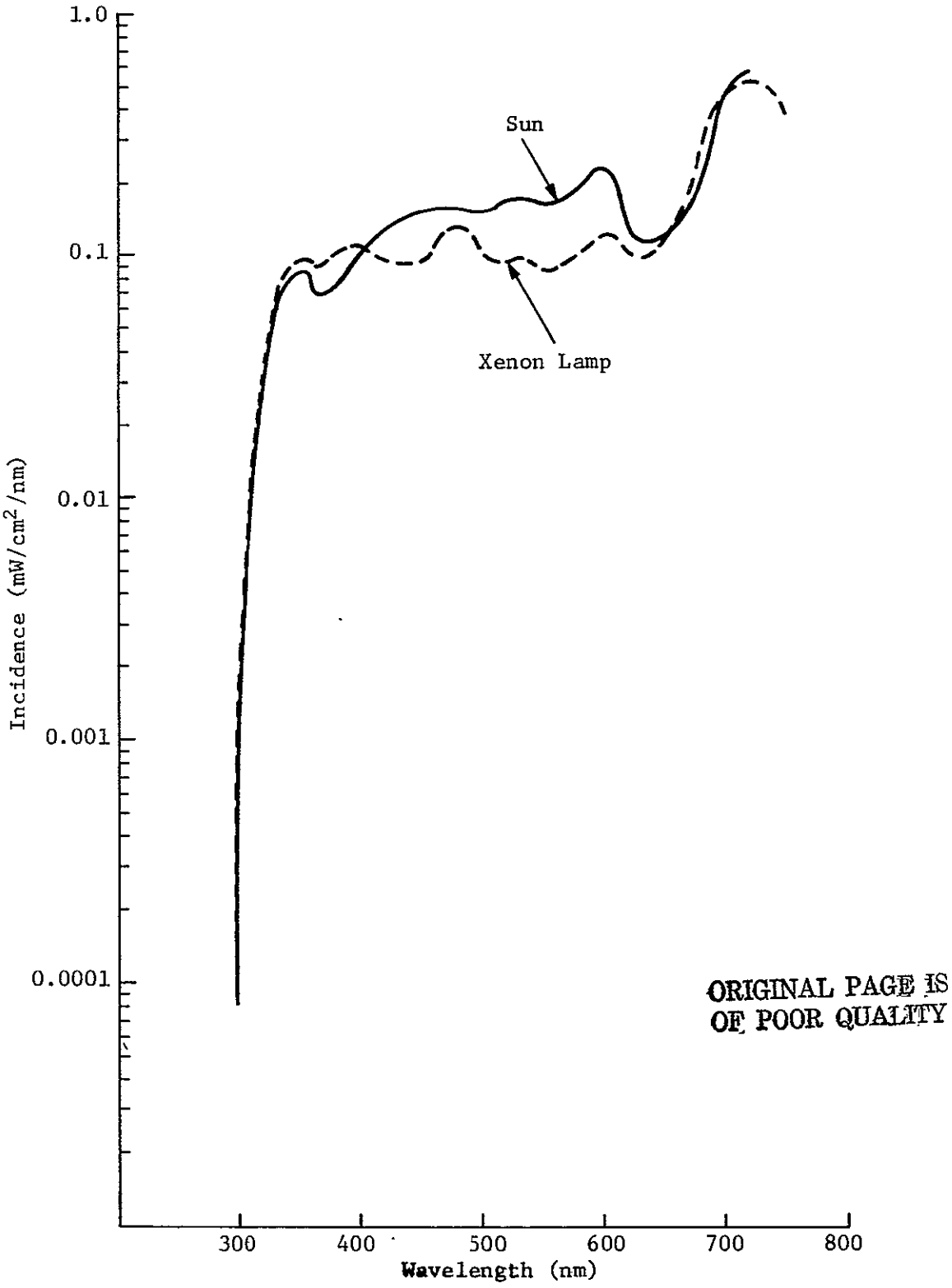

Fig A14. Incident Radiation of Sun vs 2500 W Xenon Lamp through Water-Filled Cell at 25 cm

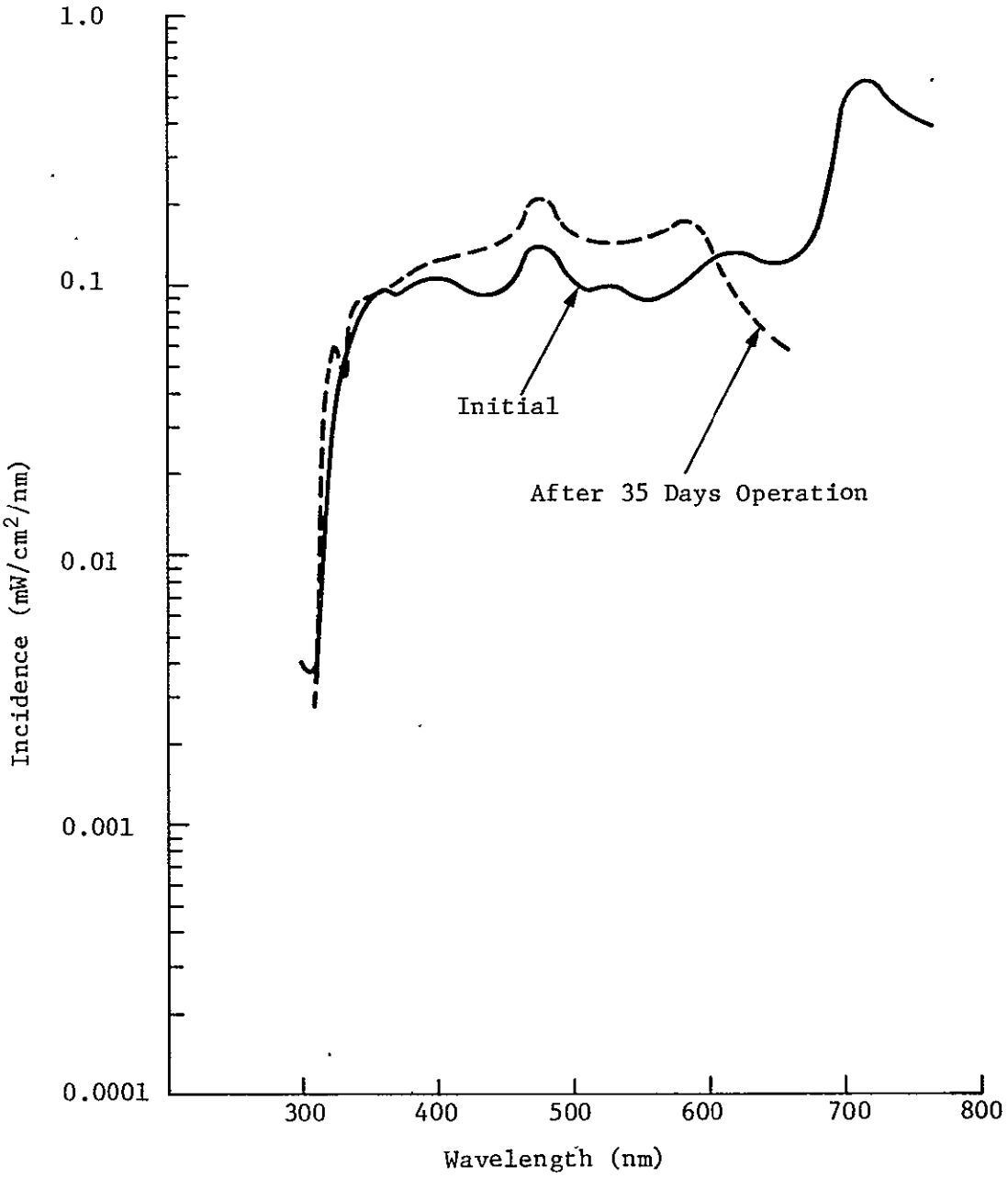

Fig A15. Incident Radiation of Xenon Lamp Through Water-Filled Cell (25 cm from Lamp)

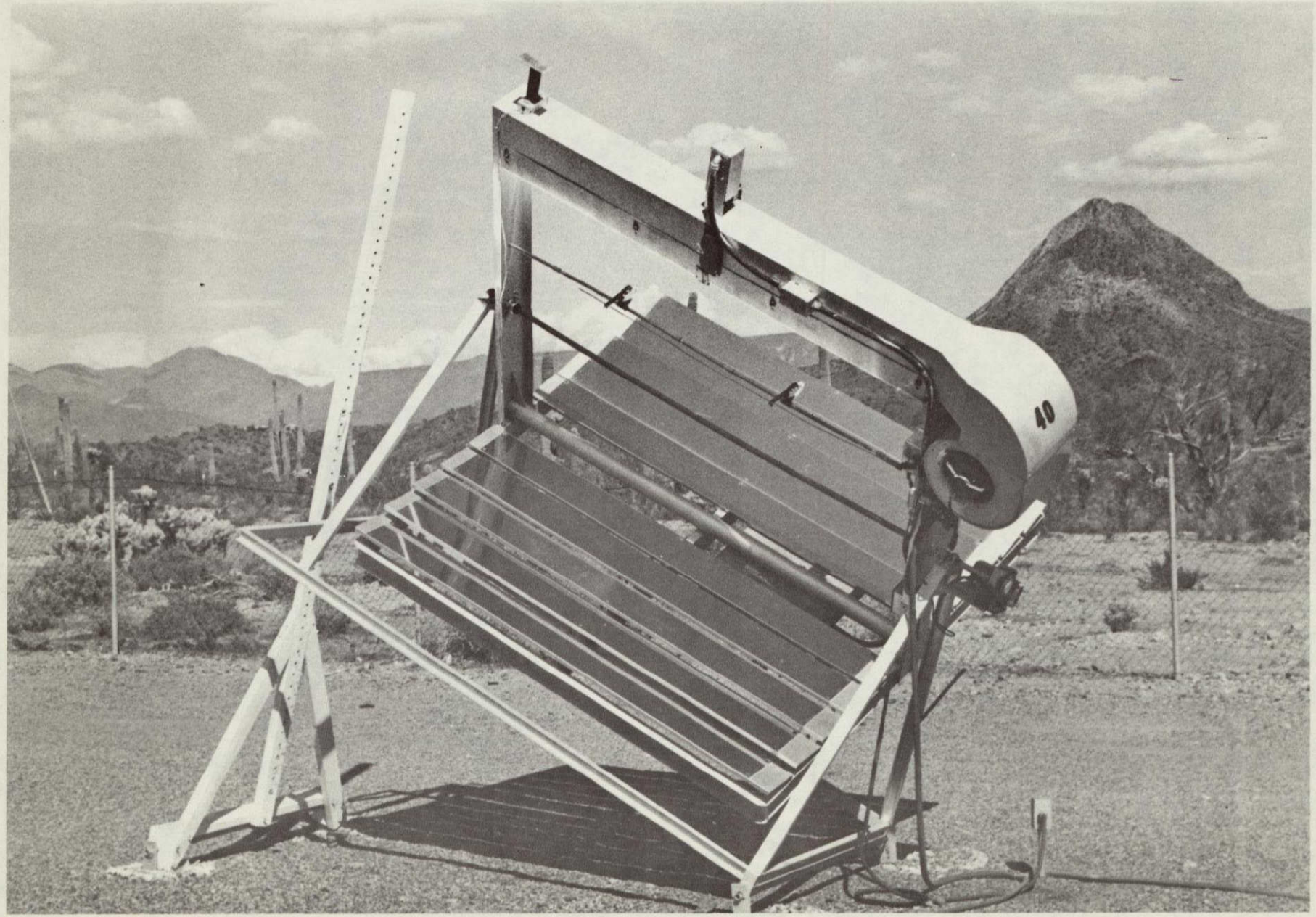

Fig A16. EMMAQUA, on the Desert Sunshine Test Site

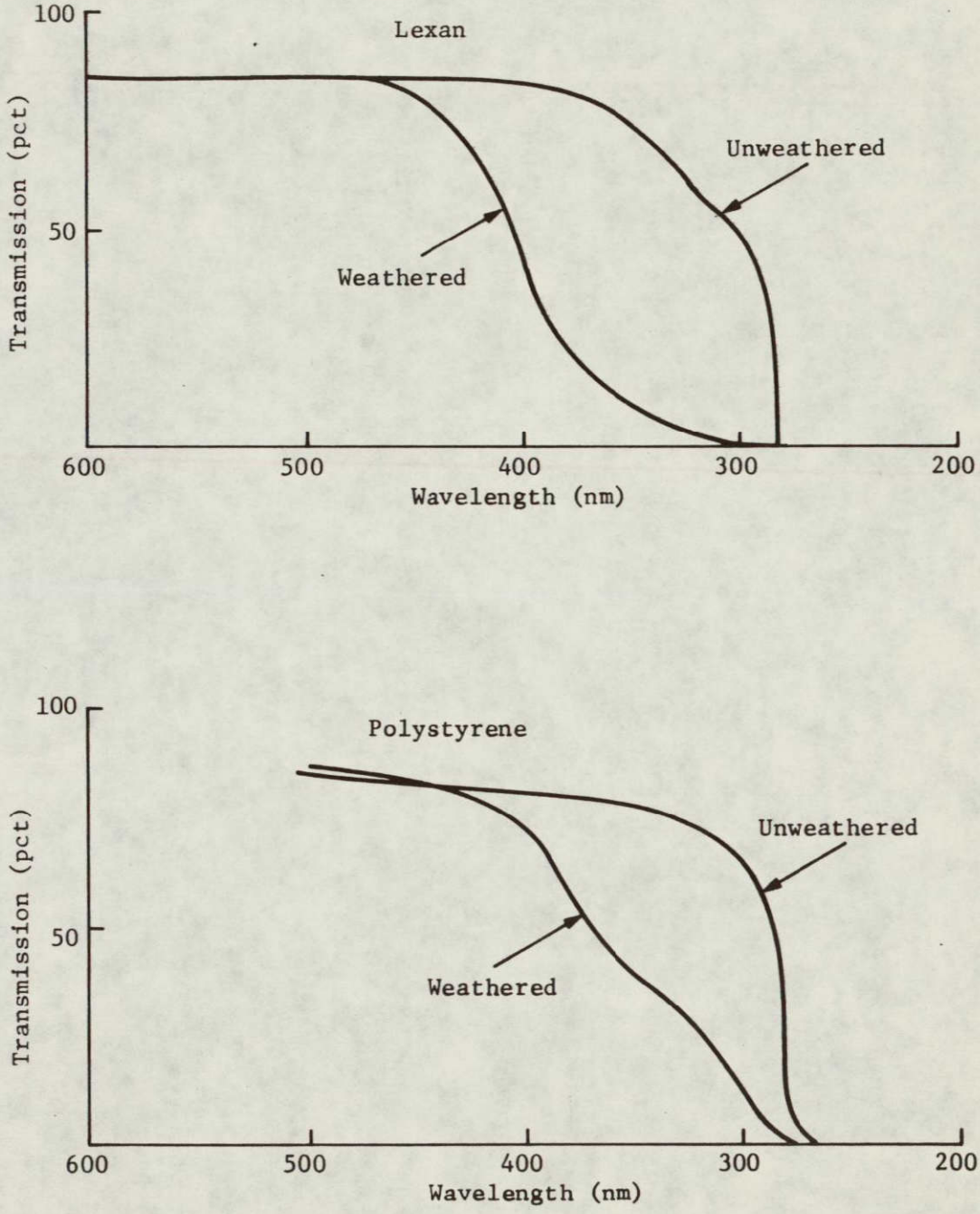

Fig A17. Spectra of Films Before and After Artificial Weathering for 5 Days

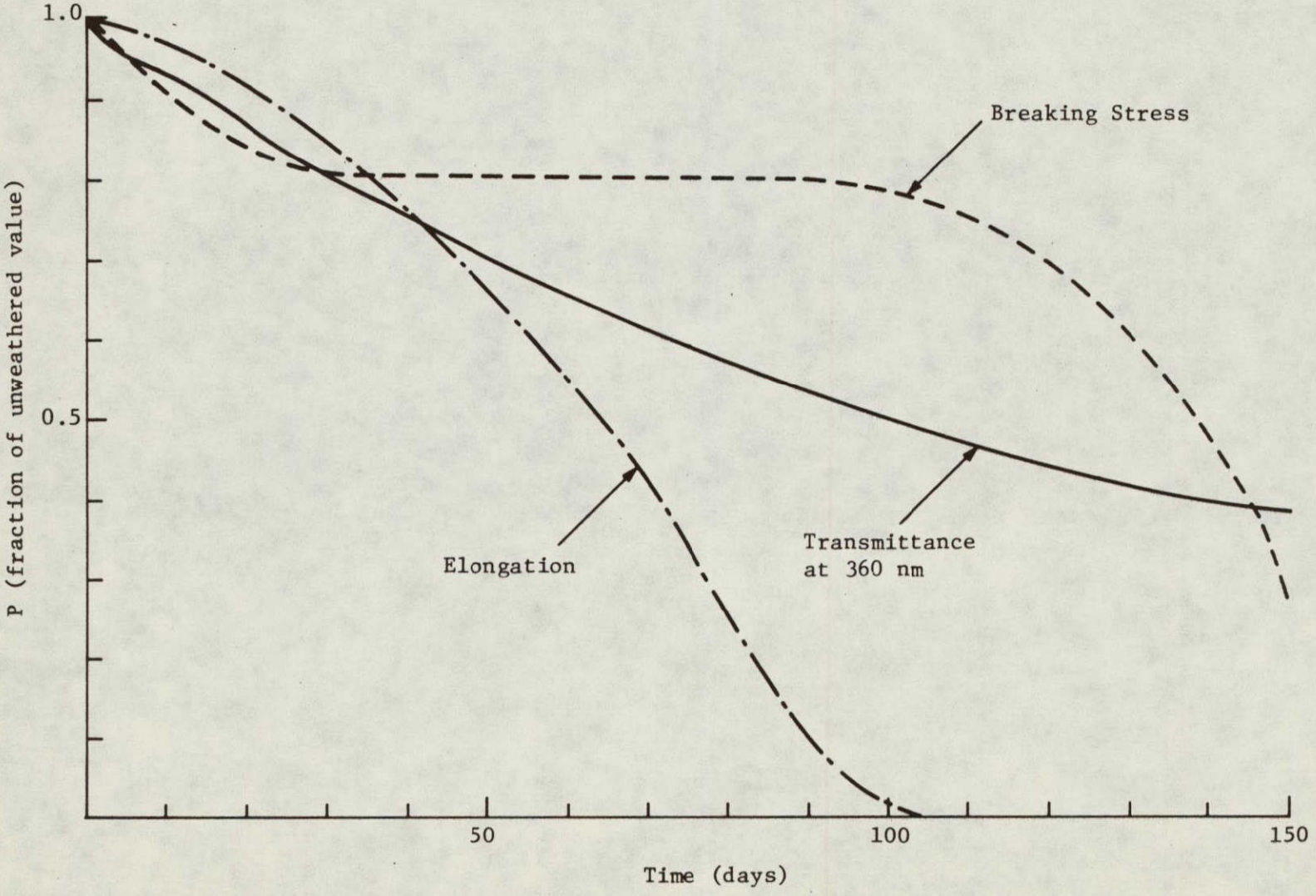

Fig A18. Lexan, EMMA Exposure -- Variation of Three Properties with Time

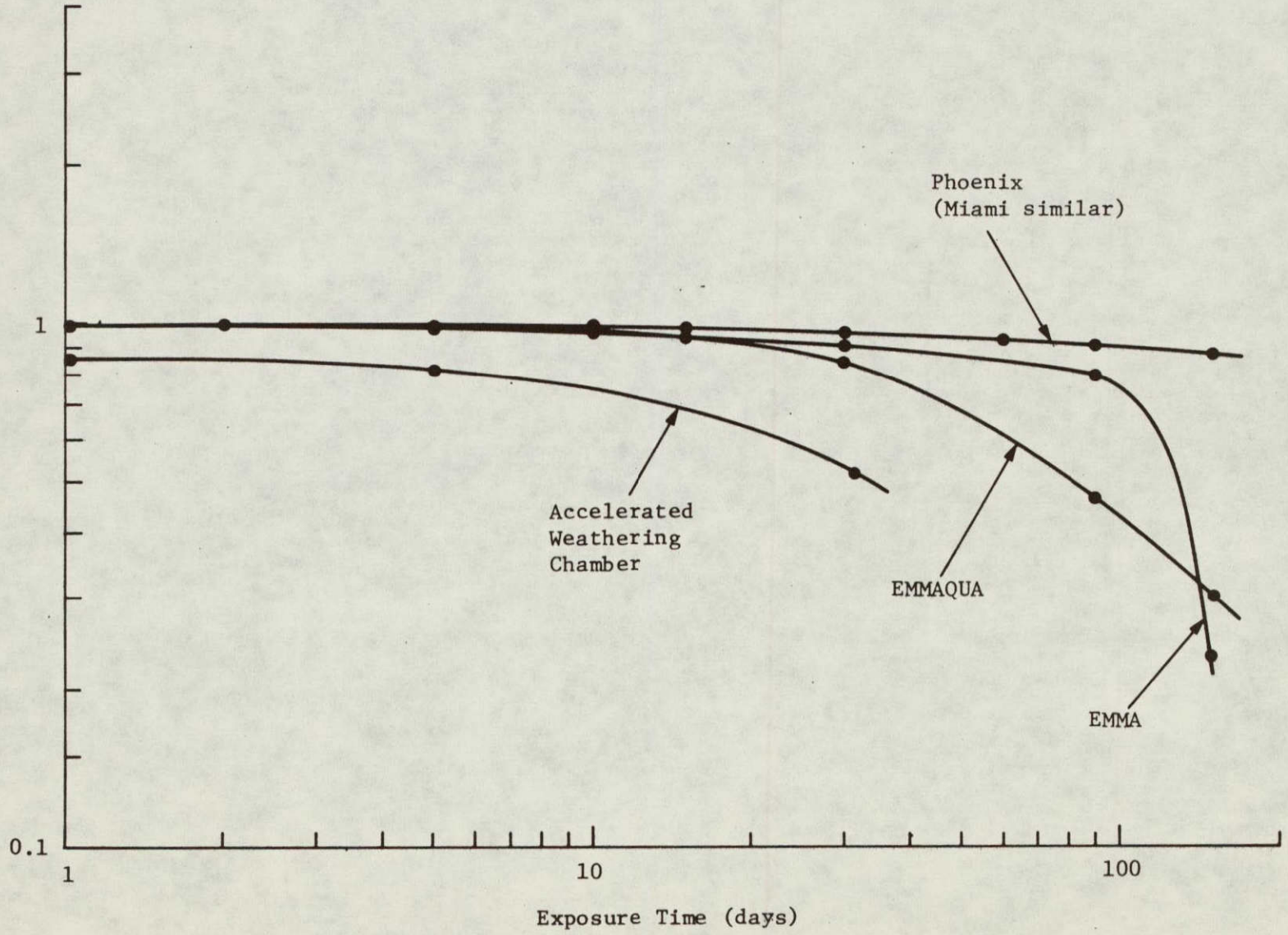

Fig A19. Retention of Tensile Strength by Weathered Lexan

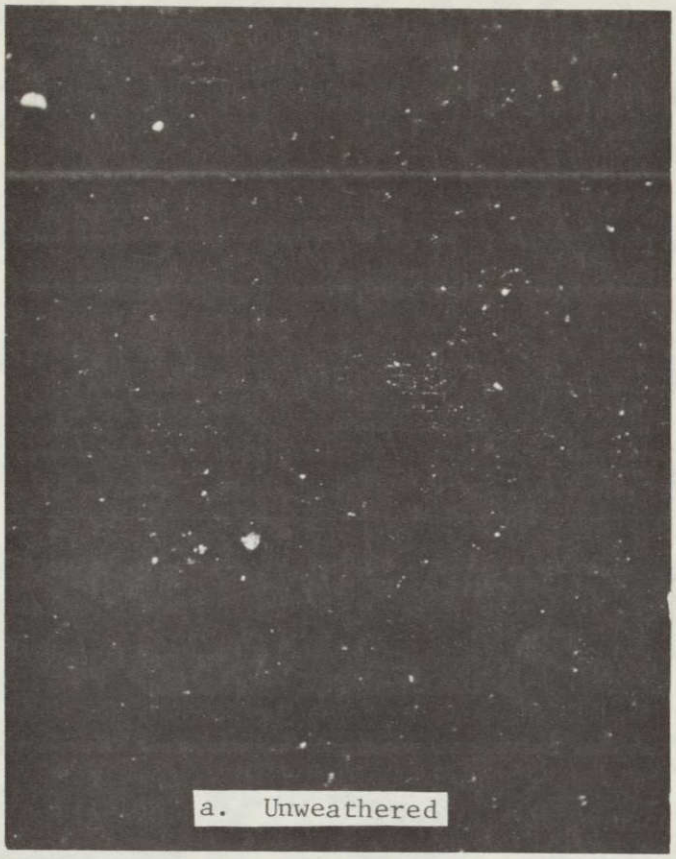

a. Unweathered

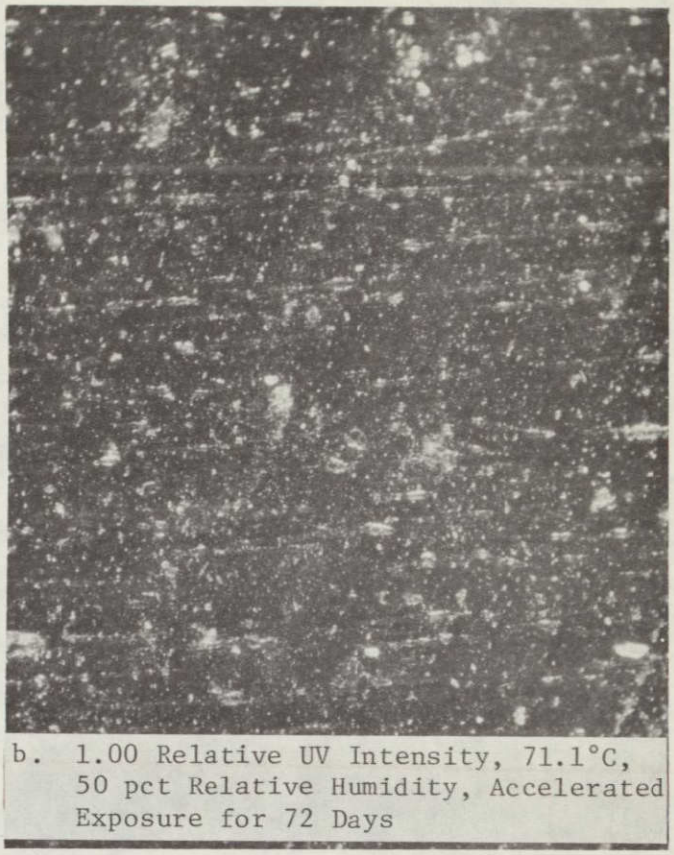

b. 1.00 Relative UV Intensity, 71.1°C, 50 pct Relative Humidity, Accelerated Exposure for 72 Days

c. EMMA for 150 Days

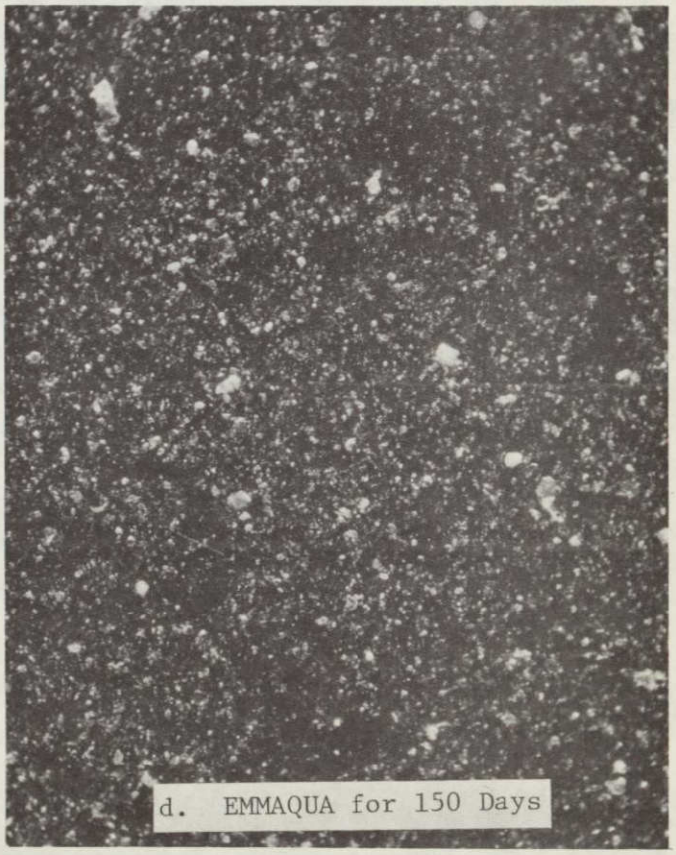

d. EMMAQUA for 150 Days

Fig A20. Particle Accumulation on Uncovered Sylgard on UTS, Magnification X200

a. Tedlar Cover, EMMAQUA for 150 Days, X50

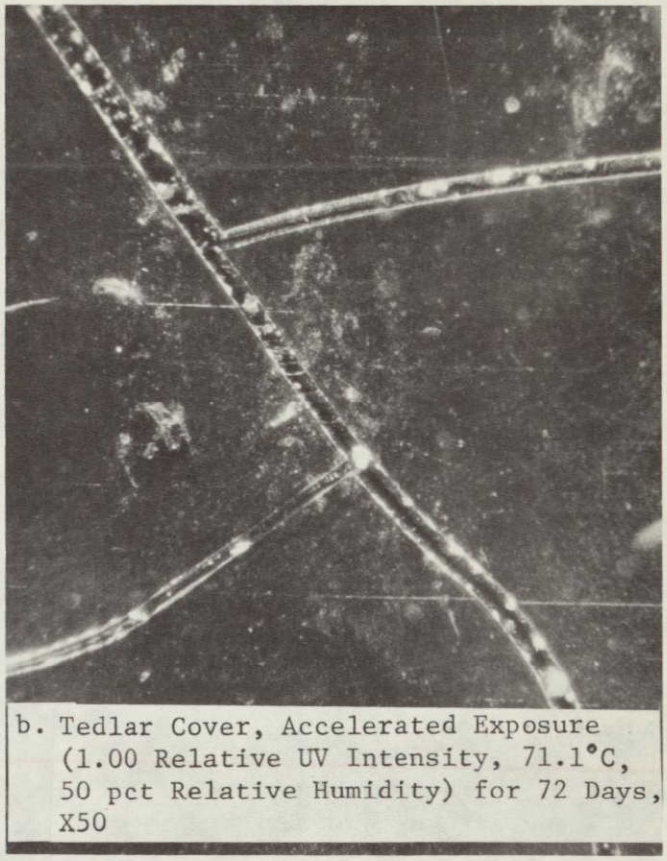

b. Tedlar Cover, Accelerated Exposure (1.00 Relative UV Intensity, 71.1°C, 50 pct Relative Humidity) for 72 Days, X50

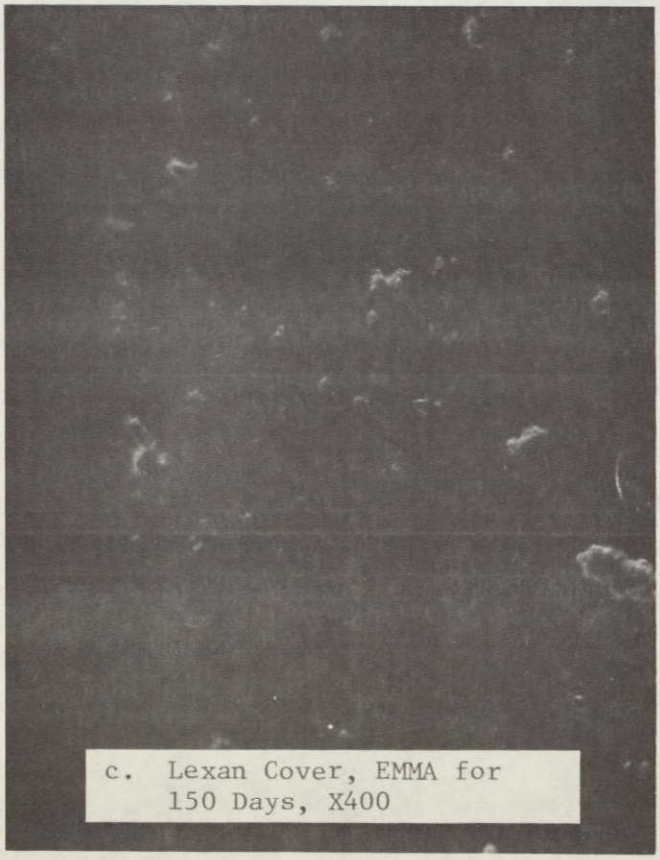

c. Lexan Cover, EMMA for 150 Days, X400

d. Lexan Cover, EMMAQUA for 150 Days, X400

Fig A21. UTS Plastic Covers After Exposure

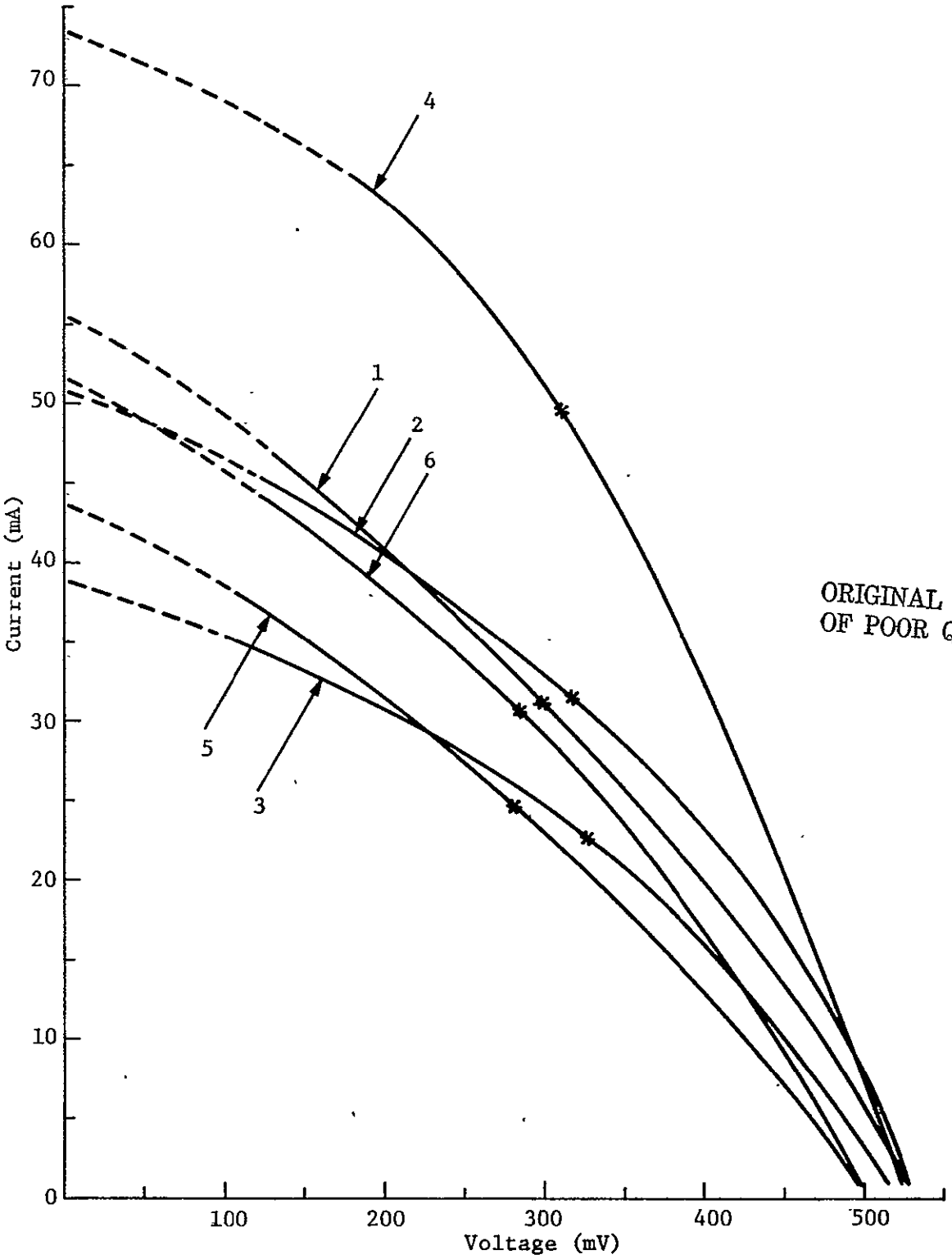

*Asterisks indicate power points

Fig A23. I vs E Curves for the Solar Cells in the UTS After Exposure to 80°C and 100 pct Relative Humidity in the Dark for 72 Days

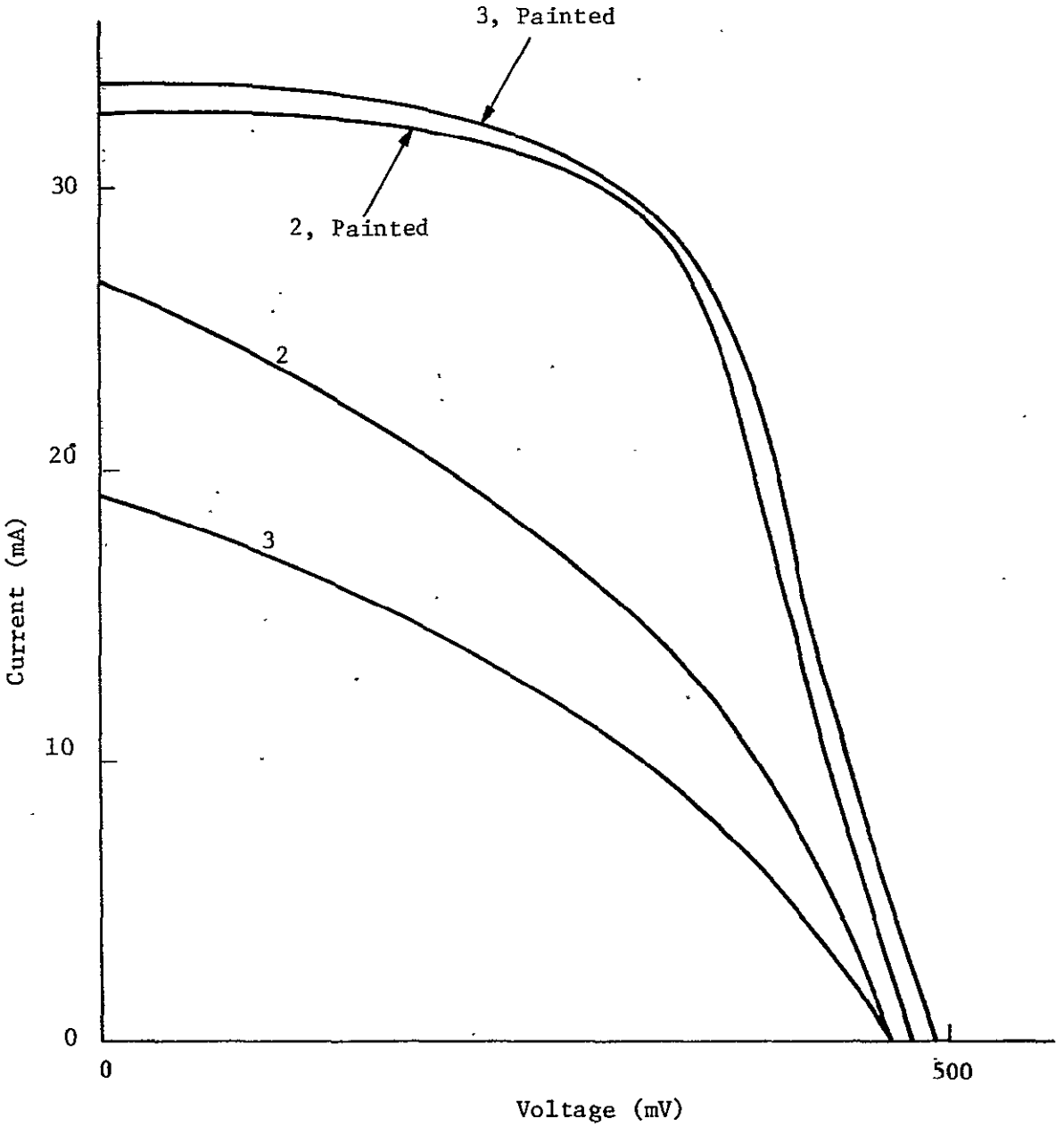

Note: Different illumination than used in Fig A22 and A23.

Fig A24. Restoration of Power of Moisture-Degraded Solar Cells by Application of Conductive Paint to Contacts

Table A1. UTS Temperatures Recorded at the Phoenix Test Site

Date	45° S				
	Solar Time	Total Radiation at 45° S, (Langleys/min*)	Temperature (Shaded Thermocouple) (°C)		
			Ambient Air	Air Next to UTS	Sylgard 184 over Solar Cell
3-18-77	11 AM	1.48	20	20	32
	1 PM	1.52	21	21	31

Date	EMMA					
	Radiation, Normal Incidence, (Langleys/min)			Temperature (Shaded Thermocouple) (°C)		
	Solar Time	Direct**	Total*	Ambient Air	Air Next to UTS	Sylgard 184 over Solar Cell
3-16-77	1 PM	1.44	1.64	23	27	48
3-17-77	11 AM	1.46	1.64	15	18	42
	1 PM	1.46	1.58	20	21	44

*Hemispherical measurement of direct plus sky radiation with Eppley 8-48 pyranometer.

**Radiation in a 6° solid angle centered upon the sun with an Eppley pyrheliometer.

Table A2. Temperatures of UTS in Accelerated Weathering Chamber

UV Intensity (300-400 nm) Relative to Typical Noon Sunlight (6.07 mW/cm^2)	Temperature (Shaded Thermocouple with 1 mm bead) (°C)	
	Air	Sylgard 184 over Solar Cell
1.00	26.1	42.2
1.00	60.3	72.8
0.66	18.3	29.4
0.66	55.3	62.8
0	40	40
0	80	80
Alternating (1.00 and 0) 12-h periods	26.1 (light) 6.7 (shade)	42.2 (light) 6.7 (shade)
Alternating (1.00 and 0) 12-h periods	60.3 (light) 43.9 (shade)	72.8 (light) 43.9 (shade)

Table A3. Temperatures of UTS in Accelerated Weathering Chamber, Using Fine-Wire Thermocouples

UV Intensity (300-400 nm) Relative to Typical Noon Summer Sunlight (6.07 mW/cm^2)	Temperature (°C)					
	Air	Thermocouple Position*				
		A	B	C	D	E
1.00	26.1	46.1 (42.2 shaded)	47.2 (42.8 shaded)	47.8	45.0	47.8
1.00	60.3	72.2 (71.1 shaded)	73.8 (71.7 shaded)	73.3	73.6	73.3
0.66	18.3	28.9 (26.7 shaded)	28.9 (28.0 shaded)	29.4	30.6	29.4
0.66	55.3	65.6 (64.1 shaded)	64.7 (63.6 shaded)	65.8	64.4	65.6

*See Fig A5

Table A4. Accelerated Weathering Results, 1536 h Exposure, 0 pct Relative Humidity

UV Intensity	Air Temperature, °C	Absorbance, Means			
		Lexan		Polystyrene	
		360 nm	600 nm	360 nm	600 nm
1.00	26.1	1.117	0.0661	1.204	0.0937
1.00	60.3	1.339	0.0589	1.447	0.1431
0.66	18.3	0.8506	0.0615	1.115	0.2465
0.66	55.3	1.059	0.0567	1.155	0.1096
		Absorbance, Replicates			
1.00	26.1	1.134	0.0661	1.254	0.1091
		1.087	0.0684	1.215	0.0882
		1.105	0.0618	1.182	0.0915
		1.120	0.0708	1.191	0.0937
		1.140	0.0630	1.178	0.0862
1.00	60.3	1.357	0.0633	1.450	0.1546
		1.359	0.0587	1.430	0.1411
		1.334	0.0589	1.436	0.1420
		1.337	0.0582	1.460	0.1409
		1.308	0.0552	1.460	0.1367
0.66	18.3	0.8603	0.0618	1.045	0.1872
		0.8580	0.0618	1.142	0.2711
		0.8600	0.0613	1.168	0.2813
		0.8446	0.0617	1.133	0.2569
		0.8301	0.0608	1.089	0.2361
0.66	55.3	1.103	0.0558	1.240	0.1345
		1.080	0.0572	1.176	0.1027
		1.070	0.0520	1.132	0.0896
		1.048	0.0562	1.129	0.1105
		0.993	0.0624	1.096	0.1108

Table A5. UTS Short Circuit Current, Percent of Original after 29 Days in Accelerated Weathering Chamber (in Situ Data)

UV Intensity (300-400 nm) Relative to Noon Sunshine (6.07 mW/cm^2)	Temperature of Sylgard 184 over Solar Cell (°C)	Relative Humidity (pct)	Short Circuit Current (Percent of Original)		
			Tedlar Cover	No Cover	Lexan Cover
1.00	42.2	0	104, 108	116, 109	112, 114
		50	110, 112	118, 114	111, 108
		100	109, 104	112, 105	106, 108
	72.8	0	105, 100	109, 100	84, 105
		50	95, 93	103, 98	104, 101
		100	64, 97	55, 85	103, 88
0.66	29.4	0	98, 90	95, 94	100, 97
		50	102, 102	102, 114	106, 106
		100	81, 92	98, 100	101, 103
	62.8	0	98, 97	100, 97	99, 98
		50	86, 92	83, 86	96, 90
		100	92, 92	97, 92	98, 94
Alternating (1.00 for 12 h, 0 for 12 h)	42.2 (light) 6.7 (shade)	0	106, 108	114, 98	108, 108
		50	98, 97	103, 100	107, 106
		100	99, 105	104, 105	109, 106
	72.8 (light) 43.9 (shade)	0	108, 95	107, 102	105, 106
		50	100, 92	107, 102	112, 110
		100	51, 64	73, 89	107, 100

Table A6. Absorbance at 360 nm and 600 nm for Lexan Weathered at Phoenix, 45°S

Exposure Time days	Start 9-12-76		Start 12-22-76		Start 6-21-77	
	360 nm	600 nm	360 nm	600 nm	360 nm	600 nm
5	0.0902	0.0547	0.0799	0.0545	0.1032	0.0683
10	0.1011	0.0586	0.0860	0.0570	0.0963	0.0572
15	0.1074	0.0596	0.0882	0.0563	0.1152	0.0648
30	0.1208	0.0628	0.0944	0.0587	0.1352	0.0704
60	0.1342	0.0631	0.1360	0.0827	0.1681	0.0706
90	0.1588	0.0678	0.1402	0.0699	0.2450	0.0730
150	0.1759	0.0678	0.2212	0.0745		
210	0.2610	0.0724	0.4377	0.0921		
300	0.5991	0.0869				

Table A7. Absorbance at 360 nm and 600 nm for Lexan Weathered at Miami, 45°S

Exposure Time, days	Start 9-1-76		Start 12-22-76		Start 6-21-77	
	360 nm	600 nm	360 nm	600 nm	360 nm	600 nm
0	0.0947	0.0638	-	-	-	-
5	0.0922	0.0568	0.0820	0.0561	0.1102	0.0720
10	0.0990	0.0582	0.0934	0.0619	0.1230	0.0820
15	0.1142	0.0613	0.1105	0.0723	0.1112	0.0655
30	0.1202	0.0624	0.1261	0.0783	0.1262	0.0651
60	-	-	0.1486	0.0837	0.1681	0.0706
90	0.1710	0.0749	0.1668	0.0775	0.1906	0.0640
150	0.2003	0.0712	0.2432	0.0781		
210	0.3014	0.1009	0.3852	0.0713		
300	0.5209	0.0916				
379	0.8895*	0.1593				

* Sample embrittled; test ended.

Table A8. Absorbance at 360 nm and 600 nm for Lexan Weathered on the EMMA and EMMAQUA

Start 9-12-76				
	EMMA		EMMAQUA	
Exposure time, days	360 nm	600 nm	360 nm	600 nm
1	0.0900	0.0539	0.0940	0.0614
2	0.1063	0.0603	0.0912	0.0565
5	0.1043	0.0561	0.1031	0.0622
10	0.1522	0.0842	0.1334	0.0747
30	0.2128	0.0803	0.2352	0.0854
90	0.4622	0.1234	0.6341	0.1791
150	0.6359	0.1513	0.9084	0.2417
210	1.3240	0.2458	1.9190	0.6512
300	2.3380	0.5331	2.6780	1.5230

Table A9. Absorbance at 360 nm and 600 nm for Polystyrene Weathered at Miami, 45°S

Exposure time, days	Start 10-20-76	
	360 nm	600 nm
0	0.0679	0.0540
5	0.1351	0.1096
10	0.1228	0.0978
15	0.0934	0.0659
30	0.1179	0.0771
60	0.1525	0.0873
90	0.1669	0.0734
150	0.3656	0.0919
210	0.9381	0.1286
300	1.2842	0.1376

C-2

Table A10. Absorbance Values for Exposed Tedlar

Exposure Conditions	A_{360}	A_{600}
Unexposed	0.1297	0.0807
Miami, 45°S, 300 days, start 9-1-76	0.1501	0.0926
Phoenix, 45°S, 300 days start 9-12-76	0.1501	0.0921
EMMA, 300 days start 9-12-76	0.1501	0.0914
EMMAQUA, 300 days start 9-12-76	0.2048	0.1143
Accelerated test, 1.00 rel. UV, 60.3°C air, 0 pct rel. hum., 32 days	0.1161	0.0715
Same, but 100 pct, relative humidity	0.1375	0.0734

Table A11. Increase in Yellowness of Samples Stored in Darkness After Weathering

Plastic	Exposure Condition (Exposed 210 Days)	Days From End of Exposure When Measured	A_{360}	A_{600}
Polystyrene	Miami, 45°S (start 10-20-76)	5	0.9381	0.1286
		111	1.0507	0.1316
Lexan	Phoenix, 45°S (start 9-12-76)	9	0.2610	0.0724
		116	0.2876	0.0757
Lexan	EMMA (start 9-12-76)	9	1.324	0.2458
		116	1.424	0.2435

Note: Readings are means of 5 to 10 replicates.

Table A12. Accelerated Weathering Results, Lexan (Unstabilized), A_{360}

Lexan (unstabilized)			A_{360}					
			Exposure Time (h)					
Relative UV Intensity	Air Temperature °C	Relative Humidity (pct)	3	6	12	24	120	768
1.00	26.1	0	0.1160	0.1498	0.2474	0.3522	0.6316	1.002
		50	0.1208	0.1553	0.2651	0.3868	0.6237	1.023
		100	0.1208	0.1714	0.2972	0.4045	0.6975	1.139
	60.3	0	0.1319	0.1539	0.3835	0.5228	0.8229	1.196
		50	0.1283	0.1664	0.3826	0.5385	0.7741	1.127
		100	0.1173	0.1812	0.3410	0.5169	0.8851	1.701
0.66	18.3	0		0.1127		0.2694	0.4511	0.7655
		50		0.1408		0.3204	0.5387	0.7608
		100		0.1257		0.3008	0.5198	0.9541
	55.3	0		0.1174		0.3590	0.6165	0.9930
		50		0.1469		0.4288	0.6585	1.232
		100		0.1460		0.4755	0.6962	1.250
0	40	0				0.0850	0.0701	0.0693
		50				0.0791	0.0730	0.0679
		100				0.0800	0.0711	0.0685
	80	0				0.0761	0.0674	0.0599
		50				0.0777	0.0698	0.0682
		100				0.0723	0.0729	0.0808
Alternating (1.0 for 12h, 0 for 12 h)	26.1(light) 6.7(shade)	0					0.4653	0.8102
		50					0.4838	0.8544
		100					0.5281	1.010
	60.3(light) 43.9(shade)	0					0.6711	1.042
		50					0.6286	0.9414
		100					0.5972	1.058

Table A13. Accelerated Weathering Results, Lexan (Unstabilized), A_{600}

Lexan (Unstabilized)			A_{600}					
			Exposure Time (h)					
Relative UV Intensity	Air Temperature °C	Relative Humidity (pct)	3	6	12	24	120	768
1.00	26.1	0	0.0543	0.0537	0.0526	0.0520	0.0540	0.0562
		50	0.0504	0.0545	0.0541	0.0544	0.0550	0.0552
		100	0.0497	0.0535	0.0505	0.0565	0.0569	0.0854
	60.3	0	0.0509	0.0518	0.0530	0.0572	0.0559	0.0516
		50	0.0498	0.0513	0.0522	0.0518	0.0510	0.0979
		100	0.0489	0.0508	0.0502	0.0477	0.0545	0.3567
0.66	18.3	0		0.0540		0.0572	0.0505	0.0634
		50		0.0566		0.0538	0.0512	0.0586
		100		0.0530		0.0512	0.0512	0.0584
	55.3	0		0.0513		0.0586	0.0496	0.0530
		50		0.0585		0.0507	0.0491	0.0756
		100		0.0509		0.0551	0.0536	0.1825
0	40	0				0.0590	0.0491	0.0501
		50				0.0534	0.0527	0.0494
		100				0.0588	0.0515	0.0497
	80	0				0.0539	0.0485	0.0437
		50				0.0537	0.0503	0.0501
		100				0.0518	0.0527	0.0550
Alternating (1.0 for 12 h, 0 for 12 h)	26.1(light) 6.7(shade)	0					0.0489	0.0514
		50					0.0505	0.0856
		100					0.0514	0.0735
	60.3(light) 43.9(shade)	0					0.0509	0.0533
		50					0.0533	0.0641
		100					0.0502	0.1189

Table A14. Accelerated Weathering Results, Polystyrene, A_{360}

Polystyrene			A_{360}					
			Exposure Time (h)					
Relative UV Intensity	Air Temperature °C	Relative Humidity (pct)	3	6	12	120	768	
1.00	26.1	0	0.0813	0.0778	0.0867	0.0975	0.1606	0.7458
		50	0.0711	0.0769	0.0839	0.0956	0.2454	0.7494
		100	0.0714	0.0805	0.0839	0.1034	0.2402	0.7093
	60.3	0	0.0764	0.0747	0.0874	0.1108	0.3850	1.030
		50	0.0739	0.0746	0.0964	0.1925	0.3547	1.087
		100	0.0723	0.0757	0.0984	0.1281	0.3308	1.070
0.66	18.3	0		0.0829		0.0863	0.1272	0.7353
		50		0.0823		0.0889	0.1143	0.5713
		100		0.0864		0.1053	0.1527	0.6021
	55.3	0		0.0757		0.0963	0.2182	0.9564
		50		0.0742		0.1028	0.1808	0.9822
		100		0.0719		0.1040	0.2497	0.9578
0	40	0				0.0743	0.0695	0.0692
		50				0.0716	0.0712	0.0671
		100				0.0807	0.0708	0.0703
	80	0				0.0711	0.0885	0.0674
		50				0.0756	0.0986	0.0682
		100				0.0682	0.0980	0.0797
Alternating (1.0 for 12 h, 0 for 12 h)	26.1(light) 6.7(shade)	0					0.1077	0.6238
		50					0.1156	0.5790
		100					0.1291	0.5825
	60.3(light) 43.9(shade)	0					0.1275	0.8253
		50					0.1532	0.8490
		100					0.1444	0.8998

Table A15. Accelerated Weathering Results, Polystyrene, A_{600}

Polystyrene			A_{600}					
Relative UV Intensity	Air Temperature °C	Relative Humidity (pct)	Exposure Time (h)					
			3	6	12	24	120	768
1.00	26.1	0	0.0589	0.0545	0.0565	0.0572	0.0513	0.0642
		50	0.0517	0.0537	0.0542	0.0534	0.0575	0.0943
		100	0.0511	0.0564	0.0544	0.0589	0.0546	0.0819
	60.3	0	0.0558	0.0529	0.0560	0.0555	0.0557	0.0750
		50	0.0519	0.0526	0.0592	0.1005	0.0578	0.0807
		100	0.0525	0.0519	0.0592	0.0672	0.0533	0.1447
0.66	18.3	0		0.0602		0.0539	0.0503	0.1612
		50		0.0580		0.0582	0.0502	0.0851
		100		0.0627		0.0621	0.0527	0.0719
	55.3	0		0.0585		0.0548	0.0541	0.0658
		50		0.0522		0.0557	0.0571	0.1304
		100		0.0511		0.0532	0.0503	0.1190
0	40	0				0.0573	0.0526	0.0544
		50				0.0536	0.0548	0.0525
		100				0.0611	0.0550	0.0547
	80	0				0.0542	0.0638	0.0536
		50				0.0566	0.0764	0.0524
		100				0.0523	0.0688	0.0609
Alternating 1.0 for 12 h, 0 for 12 h)	26.1(light) 6.7(shade)	0					0.0509	0.0559
		50					0.0506	0.0771
		100					0.0570	0.0606
	60.3(light) 43.9(shade)	0					0.0539	0.0609
		50					0.0589	0.0843
		100					0.0522	0.0739

Table A16. Accelerated Weathering Results (Lexan)

PLASTIC: Lexan

$\log (\frac{1}{P}) \times 10^4$, where P = fraction of original transmittance at 600 nm

UV Intensity (300-400 nm) Relative to Noon Sunshine (6.07 mW/cm^2)	Air Temperature (°C)	Relative Humidity (pct)	Exposure Time (h)					
			3	6	12	24	120	768
1.00	26.1	0				-27	31	34
		50				-3	41	24
		100				18	60	326
	60.3	0				25	59	-12
		50				-29	1	279
		100				-70	36	3039
0.66	18.3	0				25	-4	106
		50				-9	3	58
		100				-35	3	56
	55.3	0				39	-13	2
		50				-40	-18	228
		100				4	27	1297
0	40	0				43	-18	-27
		50				-13	18	-34
		100				41	6	-31
	80	0				-8	-24	-91
		50				-10	-6	-27
		100				-29	18	22
Alternating (1.0 for 12 h, 0 for 12 h)	26.1 (light) 6.7 (shade)	0				-21	-20	-14
		50				-6	-4	328
		100				-42	5	207
	60.3 (light) 43.9 (shade)	0				-17	0	5
		50				-25	24	113
		100				-45	-7	661

Table A17. Accelerated Weathering Results (Polystyrene)

PLASTIC: Polystyrene

$\log (\frac{1}{P}) \times 10^4$, where P = fraction of original transmittance at 600 nm

UV Intensity (300-400 nm) Relative to Noon Sunshine (6.07 mW/cm^2)	Air Temperature (°C)	Relative Humidity (pct)	Exposure Time (h)					
			3	6	12	24	120	768
1.00	26.1	0				32	-17	102
		50				-6	35	403
		100				49	6	279
	60.3	0				15	17	210
		50					38	439
		100				132	-7	907
0.66	18.3	0				-1	-37	
		50				42	-38	312
		100				81	-13	179
	55.3	0				8	1	118
		50				17	31	764
		100				-8	23	650
0	40	0				33	-14	4
		50				-4	8	-15
		100				71	10	7
	80	0				2	98	-4
		50				26	224	-16
		100				-17	148	69
Alternating (1.0 for 12 h, 0 for 12 h)	26.1 (light) 6.7 (shade)	0				25	-31	19
		50				2	-34	231
		100				4	30	66
	60.3 (light) 43.9 (shade)	0				20	0	69
		50				52	49	303
		100				52	-18	199

Table A18. Effect of Lamp Age on Lexan Yellowing

UV Intensity, Rel to Noon Summer Sunlight	Temperature	Lamp Operated, Days					
		0		40		69	
		A_{360}	A_{600}	A_{360}	A_{600}	A_{360}	A_{600}
0.66	18.3	0.2694	0.0572	0.1460	0.0503	0.1362	0.0514
1.00	26.1	0.3522	0.0520	0.1989	0.0498	0.1814	0.0529
1.00	60.3	0.5228	0.0572	0.2277	0.0515	0.1882	0.0532
0.66	55.3	0.3590	0.0586	0.1492	0.0489	0.1409	0.0515
Means:		0.3759	0.0563	0.1805	0.0501	0.1617	0.0523

Lamp Age, Days	$A_{360} - A_{600} - 0.0309$	Efficiency, pct
0	0.2887	100
40	0.0995	34
69	0.0785	27

Note: Samples were exposed 24 hours at 0 pct relative humidity.

Table A19. Effect of Lamp Age on Polystyrene Yellowing

UV Intensity, Rel to Noon Summer Sunlight	Temperature	Relative Humidity (pct)	Lamp Operated, days			
			8 to 40		40 to 72	
			A_{360}	A_{600}	A_{360}	A_{600}
1.00	26.1	0	0.7458	0.0642	0.8051	0.0614
		50	0.7494	0.0943	0.7930	0.0926
		100	0.7093	0.0819	0.8742	0.1451
1.00	60.3	0	1.030	0.0750	0.9438	0.0673
		50	1.087	0.0807	1.082	0.0840
		100	1.070	0.1447	1.039	0.0998
0.66	18.3	0	0.7353	0.1612	0.5914	0.0625
		50	0.5713	0.0851	0.5682	0.0558
		100	0.6021	0.0719	0.6659	0.0578
0.66	55.3	0	0.9564	0.0658	0.8816	0.0784
		50	0.9822	0.1304	0.9239	0.1306
		100	0.9578	0.1190	0.9120	0.0798
0 to 1.00, (alternating)	6.7 to 26.1 (alternating)	0	0.6238	0.0559	0.6259	0.0593
		50	0.5790	0.0771	0.5459	0.1074
		100	0.5825	0.0606	0.5046	0.0582
0 to 1.00, (alternating)	43.9 to 60.3 (alternating)	0	0.8253	0.0609	0.6628	0.0636
		50	0.8490	0.0843	0.8025	0.0853
		100	0.8998	0.0739	0.7991	0.0705
		Means:	0.8087	0.0882	0.7789	0.0811

Lamp Operated, Days	$A_{360} - A_{600} - 0.0139$	Efficiency, pct
8 to 40	0.7066	100
40 to 72	0.6839	97

Table A20. Accelerated Weathering Results

PLASTIC: Polystyrene

Carbonyl Peak Height (about 5.9 microns) as Percent of Aromatic Peak Height (about 6.7 microns)

UV Intensity (300-400 nm) Relative to Noon Sunshine (6.07 mW/cm^2)	Air Temperature (°C)	Relative Humidity (pct)	Exposure Time (h)					
			3	6	12	24	120	768
1.00	26.1	0				4	8	380
		50				5	50	415*
		100	5	7	6	3	44	431
	60.3	0				7	63	280
		50				3	48	434
		100	7	5	9	8	28	729
0.66	18.3	0				5	2	344
		50				3	4	287
		100				1	8	358
	55.3	0				—1	9	552
		50				3	9	1246
		100				6	17	613
0	40	0						3
		50						3
		100						1
	80	0						1
		50						1
		100						7
Alternating (1.0 for 12 h, 0 for 12 h)	26.1 (light) 6.7 (shade)	0						355
		50						204
		100						349
	60.3 (light) 43.9 (shade)	0						298
		50						248
		100						286

*19 on unweathered side

Table A21. Tensile Test Results on Lexan After Outdoor Exposure

Sample	Days	Yield Stress (psi)	Breaking Stress (psi)	Ultimate Elongation (pct)	Fraction of Original Breaking Stress	Fraction of Original Ultimate Elongation
Control for samples marked with asterisk(*)	0	7951	8861	86	1.00	1.00
Control for other samples	0	8672	9525	81	1.00	1.00
Phoenix 45° S (start 9-12-76)	5*	7682	8666	87	0.98	1.01
	10*	8372	9008	82	1.02	0.95
	15*	8305	8181	79	0.92	0.92
	30*	8076	8048	80	0.91	0.93
	60*	8112	8042	79	0.91	0.92
	90*	7879	7667	79	0.87	0.92
	150*	7770	7411	75	0.84	0.87
	210	7981	7651	74	0.80	0.91
	300	--	2585	0	0.27	0
Phoenix 45° S (start 12-22-76)	30	8226	8822	78	0.93	0.96
	60	8127	8897	85	0.93	1.05
	90	8163	9082	82	0.95	1.01
	150	8127	7865	78	0.83	0.96
	210	8336	7419	57	0.78	0.70
Phoenix 45° S (start 6-21-77)	30	8295	9105	85	0.96	1.05
	60	8034	8103	76	0.85	0.94
Miami 45° S (start 9-1-76)	5*	7961	8458	85	0.95	0.99
	10*	8130	8482	82	0.96	0.96
	15*	8209	8363	80	0.94	0.93
	30*	7977	7678	81	0.87	0.94
	90*	7850	7088	74	0.80	0.87
	150*	7762	7041	75	0.79	0.87
	210	8229	7599	73	0.80	0.90
	300	--	2297	0	0.24	0

Table A21. (continued)

Sample	Days	Yield Stress (psi)	Breaking Stress (psi)	Ultimate Elongation (pct)	Fraction of Original Breaking Stress	Fraction of Original Ultimate Elongation
Miami 45° S (start 12-22-76)	30	8867	10,042	87	1.05	1.07
	60	8484	8,969	84	0.94	1.04
	90	8382	8,398	72	0.88	0.89
	150	8255	7,720	74	0.81	0.91
	210	8781	8,058	43	0.85	0.53
Miami 45° S (start 6-21-77)	30	8049	8,265	73	0.87	0.90
	60	8220	8,005	79	0.84	0.98
EMMA (start 9-12-76)	1*	7932	8,557	85	0.97	0.99
	2*	8114	8,827	85	1.00	0.99
	5*	8027	8,524	84	0.96	0.97
	10*	8048	8,181	77	0.92	0.89
	30*	7807	7,016	73	0.79	0.85
	90*	-	7,181	7.7	0.81	0.09
	150*	-	2,402	0	0.27	0
	210	-	644	0	0.068	0
	300	(too brittle to test)				
EMMAQUA (start 9-12-76)	1*	7753	8,284	83	0.93	0.97
	2*	7894	8,757	87	0.99	1.01
	5*	7721	8,252	83	0.93	0.96
	10*	7950	8,404	81	0.95	0.94
	30*	7749	6,945	70	0.78	0.81
	90*	-	4,174	0	0.47	0
	150*	-	2,732	0	0.31	0
	210	-	728	0	0.076	0
	300	(too brittle to test)				

Note: To convert to megapascals, the values in psi are multiplied by 0.00689476. For example, the control breaking stress of 8861 psi is 61.1 megapascals.

Table A22. Tensile Test Results on Tedlar After Outdoor Exposure

Condition	Time (Days)	Yield Stress (psi)	Breaking Stress (psi)	Ultimate Elongation (pct)	Fraction of Original Breaking Stress	Fraction of Original Ultimate Elongation
Control, for 150 days	0	4939	11,741	47	1.00	1.00
Control, for 210 and 300 days	0	3855	8,937	60	1.00	1.00
Phoenix, 45° S (start 9-12-76)	150	4924	12,520	49	1.07	1.04
	210	3677	8,961	49	1.00	0.82
	300	3546	7,277	45	0.81	0.75
Miami, 45° S (start 9-1-76)	150	5364	10,041	42	0.86	0.89
	210	3660	7,721	59	0.86	0.98
	300	3943	8,277	51	0.93	0.85
EMMA (start 9-12-76)	150	4899	12,470	63	1.06	1.34
	210	3243	7,125	41	0.80	0.68
	300	3538	7,599	51	0.85	0.85
EMMAQUA (start 9-12-76)	150	4841	10,414	38	0.89	0.81
	210	3280	7,419	51	0.83	0.85
	300	3312	6,408	42	0.72	0.70

Table A23. Tensile Test Results for Polystyrene After Weathering in Miami (45°S)

Exposure Time (Days)	Breaking Stress (psi)	Fraction of Original Breaking Stress
0 (Control)	10,244	1.00
5	8,878	0.87
10	8,903	0.87
15	9,069	0.89
30	8,851	0.86
60	8,842	0.86
90	9,050	0.88
150	8,636	0.84
210	4,037	0.39
300	2,284	0.22

Table A24. Tensile Test Results on Lexan After Accelerated Weathering

Conditions: 1.00 UV Intensity (see Table A3), 26.1°C

Exposure Time (h)	Relative Humidity (pct)	Yield Stress (psi)	Breaking Stress (psi)	Ultimate Elongation (pct)	Fraction of Original Breaking Stress	Fraction of Original Ultimate Elongation
0 (Control)		8779	9728	84	1.00	1.00
3	0	8384	9255	83	0.95	0.99
3	100	8145	9082	85	0.93	1.01
6	0	8425	9658	87	0.99	1.03
6	100	8525	9292	77	0.96	0.92
12	0	8418	8881	78	0.91	0.93
12	100	8082	8487	76	0.87	0.90
24	0	8381	7296	66	0.75	0.79
24	100	-	8079	0	0.83	0
120	0	-	7988	0	0.82	0
120	100	-	8192	0	0.84	0
768	100	-	5101	0	0.52	0
1536	0	-	6553	0	0.67	0

Note: The control breaking stress is 9728 psi or 67.1 megapascals.

Table A25. Tensile Test Results on Tedlar after 768 Hours Accelerated Weathering

Conditions: 1.00 UV Intensity (see Table A3)

Temperature (°C)	Relative Humidity (pct)	Yield Stress (psi)	Breaking Stress (psi)	Ultimate Elongation (pct)
Control	-	6145	12,618	40
60.3	0	6705	11,205	45
26.1	100	5591	12,624	38

Note: The control breaking stress is 12,618 psi or 87.0 megapascals

Table A26. Tensile Test Results on Polystyrene After Accelerated Weathering

Conditions: 1.00 UV Intensity (see Table A3), 26.1°C

Exposure Time (h)	Relative Humidity (pct)	Breaking Stress (psi)	Fraction of Original Breaking Stress
0 (Control)		11,318	1.00
3	0	11,017	0.97
3	100	9,943	0.88
6	0	11,625	1.03
6	100	8,960	0.79
12	0	10,927	0.97
12	100	9,563	0.84
24	0	10,167	0.90
24	100	9,897	0.87
120	0	10,293	0.91
120	100	8,607	0.76
768	100	5,665	0.50
1536	0	3,647	0.32

Note: The elongation was too low to measure readily. The control breaking stress is 11,318 psi or 78.0 megapascals.

Table A27. TGA Data on Lexan and Tedlar

Conditions: 1.00 simulated noon sunshine, 60.3°C, 100 pct relative humidity

Temperature (°C)	Cumulative Weight Loss (pct)			
	Lexan		Tedlar	
	Unexposed	Exposed 768 h	Unexposed	Exposed 768 h
30	0	0	0	0
50	0	0	0	0
70	0	0	0	0
90	0	0.02	0.03	0.04
110	0.03	0.03	0.07	0.07
130	0.03	0.04	0.07	0.09
150	0.09	0.09	0.10	0.13
170	0.13	0.16	0.14	0.18
190	0.22	0.24	0.17	0.22
210	0.29	0.32	0.21	0.26
230	0.36	0.41	0.28	0.31
250	0.47	0.48	0.31	0.35
270	0.56	0.57	0.34	0.44
290	0.67	0.69	0.38	0.53
310	0.84	0.85	0.41	0.64
330	1.04	1.10	0.48	0.75
350	1.29	1.38	0.55	0.92
370	1.56	1.83	0.66	1.08
390	1.80	2.52	1.38	1.36
398				
410	2.09	3.37	3.93	2.02
420			5.0	
430	2.49	4.43	7.0	5.28
431				7.0
435				8.8
450	3.42	5.73		
470	5.47	8.12		
480	8.89			

Table A28. TGA Data on Polystyrene

Conditions: 1.00 simulated noon sunshine, 60.3°C, 100 pct relative humidity

Temperature (°C)	Cumulative Weight Loss (pct)					
	Unexposed	Exposed 6 h	Exposed 12 h	Exposed 24 h	Exposed 120 h	Exposed 768 h
30	0	0	0	0	0	0
50	0	0	0	0	0	0
70	0	0	0	0	0	0
90	0	0.07	0.07	0.04	0.04	0.06
110	0	0.11	0.10	0.08	0.08	0.08
130	0	0.15	0.13	0.12	0.08	0.14
150	0	0.15	0.17	0.21	0.15	0.25
170	0	0.18	0.20	0.25	0.23	0.39
190	0.04	0.19	0.26	0.29	0.34	0.56
210	0.09	0.22	0.33	0.33	0.46	0.73
230	0.18	0.30	0.36	0.41	0.61	0.95
250	0.22	0.37	0.43	0.46	0.72	1.40
270	0.31	0.41	0.46	0.54	0.88	1.62
290	0.36	0.48	0.56	0.58	1.03	2.01
310	0.44	0.55	0.66	0.70	1.22	2.40
330	0.60	0.66	0.73	0.87	1.45	2.91
350	0.85	0.85	0.86	1.12	2.06	3.91
370	1.27	1.26	1.26	1.70	3.59	6.43
390	2.80	2.44	1.98	4.22	5.64	11.19
398	7.0					
406					15.26	
410		8.71	5.42	14.40		

Table A29. Glass Transition Temperature by DSC and TMA

Conditions: 1.00 simulated noon sunshine, 60.3°C, 100 pct relative humidity

Material	Exposure Time (h)	T_g (Glass Transition Temperature) (°C)	
		By TMA	By DSC
Lexan	0	151.3	152.5
	6	149.2	
	12	148.2	
	24	147.0	
	120	145.6	
	768	144.2	144.8
Polystyrene	0	100	109
	768	96	104
Tedlar*	0	52	57
	768	57	

*Heat of Fusion: 7.24 cal/g for control
7.50 cal/g for sample exposed 768 h

Table A30. Short Circuit Current of Solar Cells in Weathered UTS's

Exposure Condition	Time (days)	Percent of Original Short Circuit Current		
		Lexan Cover	No Cover	Tedlar Cover
EMMA (start 9-12-76)	1	102, 100	88, 99	100, 99
	2	97, 99	96, 96	97, 97
	5	99, 99	98, 96	101, 97
	10	100, 101	98, 96	100, 100
	30	101, 102	98, 99	96, 101
	90	95, 105	96, 114	96, 101
	150	100, 98	95, 95	96, 101
	210	96, 103	90, 95	96, 100
	300	98, 107	95, 95	83, 96
EMMAQUA (start 9-12-76)	1	102, 101	100, 100	100, 99
	2	101, 100	99, 99	99, 100
	5	96, 97	94, 96	97, 97
	10	103, 102	101, 101	101, 101
	30	101, 97	99, 97	98, 96
	90	99, 102	92, 95	111, 99
	150	98, 100	91, 96	94, 99
	210	98, 101	92, 94	96, 97
	300	101, 103	93, 94	94, 96
45° S, Phoenix (start 9-12-76)	5	99, 99	98, 99	96, 97
	10	98, 97	101, 96	99, 97
	15	100, 100	99, 98	100, 98
	30	98, 98	94, 94	99, 96
	60	95, 98	94, 92	89, 104
	90	97, 100	78, 82	96, 102
	150	95, 98	95, 95	96, 101
	210	100, 102	75, 92	83, 95
	300	103, 104	91, 93	96, 96

Table A30. (continued)

Exposure Condition	Time (days)	Percent of Original Short Circuit Current		
		Lexan Cover	No Cover	Tedlar Cover
45° S, Florida (start 9-1-76)	5	99, 98	98, 98	99, 98
	10	100, 99	99, 97	99, 100
	15	100, 99	98, 97	90, 97
	30	99, 97	98, 96	98, 97
	60	96, 99	91, 96	92, 98
	90	96, 96	94, 95	94, 100
	150	97, 99	91, 97	90, 98
	210	99, 101	89, 90	94, 95
	300	92, 94	92, 93	92, 92

Table A31. Short Circuit Current of Solar Cells in UTS's After 72 Days Accelerated Weathering

UV Intensity (300-400 nm) Relative to Noon Sunshine (6.07 mW/cm^2)	Air Temperature (°C)	Relative Humidity (pct)	Short Circuit Current, Percent of Original		
			Lexan Cover	No Cover	Tedlar Cover
1.00	26.1	0	100, 99	95, 102	95, 101
		50	99, 100	97, 85	94, 101
		100	102, 102	89, 102	95, 101
	60.3	0	99, 92	95, 103	94, 104
		50	96, 99	95, 98	94, 100
		100	89, 98	96, 47	93, 57
0.66	18.3	0	98, 101	96, 102	94, 100
		50	98, 100	95, 100	93, 100
		100	101, 101	97, 101	95, 96
	55.3	0	99, 103	97, 102	95, 102
		50	97, 102	76, 70	94, 80
		100	98, 98	76, 101	95, 101
0	40	0	96, 104	101, 105	100, 102
		50	101, 105	100, 105	98, 105
		100	101, 103	97, 54	96, 102
	80	0	94, 104	98, 103	100, 104
		50	99, 103	97, 101	98, 100
		100	85, 105	80, 65	70, 93
Alternating (1.0 for 12 h, 0 for 12 h)	26.1 (light) 6.7 (shade)	0	98, 95	96, 104	95, 102
		50	98, 101	95, 98	96, 105
		100	97, 100	98, 100	98, 102
	60.3 (light) 43.9 (shade)	0	95, 100	98, 100	95, 100
		50	101, 102	96, 99	96, 101
		100	97, 112	92, 60	93, 49

Table A32. Maximum Power of Solar Cells in Weathered UTS's

Exposure Condition	Time (days)	Percent of Original Power (Watts) at Power Point on IV Curve		
		Lexan Cover	No Cover	Tedlar Cover
EMMA	1	95, 99	81, 98	97, 101
(start 9-12-76)	2	100, 103	101, 106	93, 101
	5	94, 104	97, 101	104, 105
	10	100, 102	101, 88	103, 101
	30	97, 102	96, 101	71, 100
	90	96, 105	91, 98	102, 107
	150	98, 88	91, 100	100, 106
	210	87, 94	65, 93	95, 96
	300	77, 95	86, 88	59, 94
EMMAQUA	1	100, 104	98, 104	101, 101
(start 9-12-76)	2	98, 101	99, 105	99, 99
	5	101, 98	98, 92	98, 96
	10	101, 99	101, 101	103, 101
	30	103, 101	96, 100	101, 100
	90	99, 102	92, 97	93, 101
	150	99, 104	86, 101	100, 105
	210	95, 103	84, 97	96, 98
	300	93, 96	88, 91	91, 94
45° S, Phoenix	5	100, 105	100, 112	96, 105
(start 9-12-76)	10	107, 107	111, 106	107, 108
	15	102, 103	101, 101	104, 103
	30	107, 106	91, 107	101, 105
	60	89, 86	86, 75	92, 94
	90	93, 99	55, 99	92, 102
	150	101, 90	93, 78	98, 101
	210	97, 101	76, 97	66, 100
	300	96, 99	94, 99	79, 103

Table A32. (continued)

Exposure Condition	Time (days)	Percent of Original Power (Watts) at Power Point on IV Curve		
		Lexan Cover	No Cover	Tedlar Cover
45° S, Miami	5	97, 94	98, 118	96, 98
(start 9-1-76)	10	99, 102	101, 104	102, 92
	15	99, 100	99, 102	84, 99
	30	96, 91	98, 99	99, 102
	60	96, 97	84, 93	92, 98
	90	100, 99	97, 94	98, 104
	150	103, 105	94, 97	93, 101
	210	84, 102	82, 91	76, 77
	300	58, 69	82, 89	84, 86

Table A33. Maximum Power of Solar Cells in UTS's After 72 Days Accelerated Weathering

UV Intensity (300-400 nm) Relative to Noon Sunshine (6.07 mW/cm^2)	Air Temperature (°C)	Relative Humidity (pct)	Percent of Original Power (Watts) at Power Point on IV Curve		
			Lexan Cover	No Cover	Tedlar Cover
1.00	26.1	0	97, 96	94, 99	94, 101
		50	103, 102	100, 88	96, 95
		100	103, 104	90, 100	99, 104
	60.3	0	104, 63	85, 101	99, 104
		50	116, 114	101, 93	106, 109
		100	74, 82	70, 39	95, 37
0.66	18.3	0	93, 102	97, 104	98, 102
		50	98, 102	93, 95	95, 102
		100	103, 104	95, 105	100, 79
	55.3	0	100, 100	98, 99	94, 102
		50	109, 103	60, 74	81, 68
		100	95, 83	66, 88	76, 99
0	40	0	100, 102	100, 101	101, 99
		50	101, 102	98, 98	95, 101
		100	85, 74	95, 33	56, 83
	80	0	100, 99	99, 101	98, 108
		50	98, 93	93, 89	89, 98
		100	52, 87	58, 47	50, 50
Alternating (1.0 for 12 h, 0 for 12 h)	26.1 (light) 6.7 (shade)	0	105, 105	101, 103	99, 105
		50	104, 104	99, 106	101, 110
		100	102, 105	98, 102	100, 107
	60.3 (light) 43.9 (shade)	0	103, 105	102, 105	96, 105
		50	102, 107	98, 96	88, 104
		100	87, 82	73, 57	45, 31

Table A34. Field Effect Transistor (FET) Leakage Current Ratios After Outdoor Exposure of UTS's

Exposure Condition	Time (days)	Ratio of Final to Initial Leakage Current (measured at 20 V)		
		Tedlar Cover	No Cover	Lexan Cover
Phoenix, 45°S	60	0.4	1.0	0.8
	90	1.1	1.3	1.0
	150	0.6	0.1	0.2
	210	>4000	0.7	0.7
	300	0.6	1.7	0.9
Miami, 45° S	60	0.7	0.6	1.3
	90	0.3	0.8	1.0
	150	0.5	1.0	0.5
	210	0.05	0.2	0.3
	300	0.2	0.4	1.4
EMMA	90	1.2	1.7	1.0
	150	0.7	0.4	0.3
	210	0.08	0.4	0.3
	300	0.05	0.1	0.1
EMMAQUA	90	0.5	0.5	0.5
	150	1.0	1.3	1.2
	210	0.2	0.3	0.3
	300	0.1	0.1	0.1

Table A35. Field Effect Transistor (FET) Leakage Current Ratios After 72 Days Accelerated Weathering of UTS's

UV Intensity (300-400 nm) Relative to Noon Sunshine (6.07 mW/cm^2)	Air Temperature (°C)	Relative Humidity (pct)	Ratio of Final to Initial Leakage Current (measured at 20 V)		
			Tedlar Cover	No Cover	Lexan Cover
1.00	26.1	0	0.5	1.2	1.5
		50	0.6	1.0	1.0
		100	0.7	1.8	0.7
	60.3	0	0.6	0.6	0.6
		50	0.4	0.5	0.4
		100	1.2	4.7	3.3
0.66	18.3	0	0.8	0.2	0.2
		50	3.7	4.4	2.4
		100	2.8	11.5	4.3
	55.3	0	0.7	0.6	1.7
		50	2.7	3.0	2.5
		100	0.9	3.0	4.0
0	40	0	0.6	0.8	0.8
		50	0.3	1.7	1.5
		100	0.8	1.5	1.0
	80	0	0.1	0.2	0.8
		50	2.0	1.7	2.5
		100	0.2	0.2	0.3
Alternating (1.0 for 12 h, 0 for 12 h)	26.1 (light) 6.7 (shade)	0	0.8	1.0	1.0
		50	0.4	2.5	3.0
		100	1.5	7.0	4.0
	60.3 (light) 43.9 (shade)	0	-	0.7	0.2
		50	0.9	1.0	0.3
		100	1.0	4.2	4.0

Table A36. Peel Strength of Plastic Covers on Weathered UTS's

Exposure Conditions	Time (days)	Tedlar		Lexan	
		Mean Force* (lb)	Fraction of Control	Mean Force* (lb)	Fraction of Control
Control	0	0.30	1.00	0.10, 0.35**	1.00
Accelerated test, 1.00 noon sunshine UV light intensity, 26.1°C, 100 pct relative humidity	72	0.25	0.83	0.36	1.03
Accelerated test, 1.00 noon sunshine UV light intensity, 60.3°C, 100 pct relative humidity	72	(too brittle to pull strips; adhesion seemed good)		0.14	1.4
Phoenix, 45° S	90	0.27	0.90	0.35	1.00
Miami, 45° S	90	0.30	1.00	0.38	1.09
EMMA	90	0.30	1.00	0.38	1.09
EMMAQUA	90	0.29	0.97	0.39	1.11

*To peel a 5 mm wide strip at 90° angle at 2 inches/min, mean of 5 replicates.

**The control failed sometimes adhesively (0.10 lb), sometimes cohesively (0.35 lb).

The only adhesive failure on weathered samples was for Lexan from the 60.3°C accelerated test. All other Lexan failures and all Tedlar failures were cohesive.

Table A37. Temperature and Moisture Effects in Accelerated Exposure

UV Intensity (300-400 nm) Relative to Noon Sunshine (6.07 mW/cm^2)	Air Temp. (°C)	Rel. Hum. (pct)	72 Days Exposure				32 Days Exposure	
			Tedlar Embrittlement (on UTS)	Solar Cells with Power <75 pct of Original	Solar Cells with Short Circuit Current <85 pct of Original	FET's with Leakage Current >2.0 × Original	Severe Loss of Gloss for Lexan (Film)	Severe Loss of Gloss for Polystyrene
1.00	26.1	0						X
		50						X
		100					X	X
	60.3	0	X	1				X
		50	X				X	X
		100	X	4	2	2	X	X
0.66	18.3	0						(not available)
		50				3		X
		100				3		X
	55.3	0						X
		50		3	3	3	X	X
		100		1	1	2	X	X

Table A37. (Continued)

UV Intensity (300-400 nm) Relative to Noon Sunshine (6.07 nW/cm^2)	Air Temp. (°C)	Rel. Hum. (pct)	72 Days Exposure				32 Days Exposure	
			Tedlar Embrittlement (on UTS)	Solar Cells with Power <75 pct of Original	Solar Cells with Short Circuit Current <85 pct of Original	FET's with Leakage Current >2.0 × Original	Severe Loss of Gloss for Lexan (Film)	Severe Loss of Gloss for Polystyrene
0	40	0						
		50						
		100		3	1			
	80	0						
		50				2		
		100		5	3			
Alternating (1.0 for 12 h, 0 for 12 h)	26.1 (light) 6.7 (shade)	0						
		50				2	X	X
		100				2	X	
	60.3 (light) 43.9 (shade)	0	X					
		50	X*					
		100**		4	2	2	X	X

*Slightly embrittled
**Tube flooded with water accidentally

REFERENCES

A1. Proceedings of the Second Project Integration Meeting, LSSA Project, ERDA/JPL-1012-76/4, April 1976, p 130.

A2. Atlas Xenon Arc Light Systems, Bulletin No. 1183, January 1975, Atlas Electric Devices Co., Chicago, IL.

A3. Catalog, Oriel Corporation of America, Stamford, CT, 1975, p 75.

A4. Kinmonth, R. A., and Norton, J. E., "Controlling UV Irradiance from Xenon Arc Lamps," ISWPR, pp B 3.1 - B 3.8.

A5. Kolyer, J. M., "Stability of Materials Under Worldwide Climatic Conditions," Conference on Aerospace Transparent Materials and Enclosures, Atlanta, GA, November 18-21, 1975, Technical Report AFML-TR-76-54, pp 405-432.

A6. "Standard Recommended Practice for Maintaining Constant Relative Humidity by Means of Aqueous Solutions," E104-51, 1974 Annual Book of ASTM Standards, pp 846-852.

A7. Kingsnorth, D. J., and Wood, D. G. M., "The Effect of Antioxidants on the UV Stability of Polypropylene. Correlations between Natural and Artificial Light Aging." ISWPR, pp E 2.1 - 2.10.

A8. DESERT-ation Newsletter, Volume 23, No. 7, February 1977, from Desert Sunshine Exposure Tests, Inc.

A9. Kay, E.; Davis, A.; and Palmer, G. L., "Recommended Procedures for the Effective Study of the Natural Weathering Behavior of Plastics." ISWPR, pp C 2.0 - C 2.12.

A10. Schmitz, O., Pigment and Resin Technology, Volume 1, May 1972, p 29.

A11. Butlers, G., and Marks, G. C., "Techniques for Predicting the Weathering Performance of Rigid PVC," ISWPR, pp D 6.1 - D 6.9.

A12. George, G. A.; Sacher, R. E.; and Sprouse, J. G., "Novel Techniques for Studying the Weathering Degradation of a Glass Fiber Epoxy Composite," ISWPR, pp D 4.1 - D 4.12.

A13. Mark, H., Editor, Encyclopedia of Polymer Science, Volume 13, 1970, p 239.

A14. Hanras, J., "Aging of Low Density Polyethylene Films for Agricultural Use," ISWPR, pp F 4.1 - F 4.9.

A15. Brandrup, J., and Immergut, E. H., Editors, Polymer Handbook, 2nd Edition, 1975, John Wiley and Sons, N.Y., p III-150.

A16. Mirtich, M. J., and Bozek, J. M., "FEP Encapsulated N/P Solar Cells After Simulated Micrometeoroid Exposure," Journal of Spacecraft, Volume 8, No. 11, November 1971, pp 1164-1165.

A17. Carmichael, D. C.; Gaines, G. B.; Sliemers, F. A.; Kistler, C. W.; and Igou, R. D.; "Review of World Experience and Properties of Materials for Encapsulation of Terrestrial Photovoltaic Arrays, Final Report," ERDA/JPL-954328-76/4, by Battelle, Columbus Laboratories, July 21, 1976, p 5.

954439 Avco Lycoming Corp. - Interim Report, August 26, 1977

954442 Motorola Inc. - Seventh Quarterly Progress Report, October 26, 1977

954458 Rockwell International - Final Report, October 24, 1977

954471 Stanford Research Corp. - Quarterly Progress Report, September, 1977

954475 Texas Institute - Final Report, March, 1977

954527 Springborn Laboratories - Fifth Quarterly Progress Report, August, 1977

954559 Dow Corning - Fifth Quarterly Report, August. 1977

954589 Westinghouse - Fourth Quarterly Report, June 1977

954605 Sensor Tech.. Inc. - Third Quarterly Progress Report, September, 1977

954607 General Electric Corp. - First Quarterly Progress Report, October 5, 1977

954653 Lockheed Missiles and Space Co., Inc. - Final Report, October, 1977

954694 Spectrolab - Third Quarterly Report, November 15, 1977

954700 954720 ILC Dover - Final Report and Supplement to the Final Report, July 4, 1977

954721 Sheldahl - Final Report, June 22, 1977

954807 Exotech Research Inc. - Final Report, August 31, 1977

Very truly yours,

George A. Wynecoop

for Joseph A. Wynecoop, Manager
Information Support Section
Technical Information and
Documentation Division

cc: Jerry Waldo, Acquisitions

* Including 954700 AEC-ABLE Engineering Company, Inc.
Final Report, October 20, 1977